The role of the organic matter for hydrophobicity in urban soils

Dissertation
zur Erlangung des akademischen Grades eines
Doktors der Naturwissenschaften
Fachbereich 7: Natur- und Umweltwissenschaften

Universität Koblenz-Landau

vorgelegt von
Dipl.-Ing.
Dörte Diehl

1. Gutachter: Prof. Dr. Gabriele Schaumann (Universität Koblenz-Landau, Germany)
2. Gutachter: Dr. Stefan Doerr (Swansea University, United Kingdom)

Promotionsausschuss:
Vorsitzender: Prof. Dr. Wieland Müller
Berichter: Prof. Dr. Ralf Schulz
Berichter: Prof. Dr. Andreas Müller

Tag der wissenschaftlichen Aussprache: 03.09.2009

Landau 2009

Declaration

I herewith declare that I autonomously carried out the PhD-thesis entitled “The role of the organic matter for hydrophobicity in urban soils”. All used assistances are declared and parts of involved contributors and other authors are clearly indicated.

This or another thesis has never been submitted elsewhere for an exam, as thesis or for evaluation in a similar context; neither to any department of this university nor to any other scientific institution.

_____

Place, date signature

The following parts of this thesis are published or submitted for publication:

Chapter 3 and the subsections 2.2.4 (par. 1-2), 2.3.1, 2.3.2 (par. 1-5), 2.2.4 and 2.5 (par. 2-4) are published:

Diehl, D. & G.E. Schaumann. (2007). Wetting mechanism assessed from time dependent sessile drop shape. Hydrological Processes, 21, 2255 - 2265.

Chapter 4 is published as:

Diehl, D., R.H. Ellerbrock & G.E. Schaumann. (2009). Influence of drying conditions on wettability and DRIFT spectroscopic C-H band of soil samples. European Journal of Soil Science, 60, 557-566.

I had the opportunity to conduct the DRIFT measurements at “ZALF” in Müncheberg by courtesy of Dr. Ruth H. Ellerbrock, who supported the evaluation of the spectra. My own contribution to Chapter 4 consists of > 90%.

Chapter 5 is submitted to the journal “Geoderma” as:

Diehl, D., J.V. Bayer, S.K. Woche, R. Bryant, S.H. Doerr & G.E. Schaumann. (subm.). Reaction of soil water repellency on artificially induced changes in soil pH. Geoderma.

Beside my own results, Chapter 5 comprises additional results of investigations carried out by Julia Bayer with samples from Netherlands, the UK and Australia, which were supervised by Prof. Dr. R. Bryant and Dr. S.H. Doerr from the University Swansea. Julia Bayer developed the method to artificially increase soil pH by addition of gaseous ammonia and I developed the method to artificially decrease soil pH by addition of gaseous hydrochloric acid. The measurements of titrable surface charges were carried out by Dr. Susanne Woche from the Institut of Soil Science at the University of Hannover. Some data of a long-term study of Buch and Tiergarten site were provided by the subproject SOIL from the Interurban research group by courtesy of Prof. Dr. Gerd Wessolek (Department of Soil Protection, TU-Berlin). My own contribution to Chapter 5 consists therefore of ~ 75%.

Additionally, this thesis benefited from the supervision by Prof. Dr. Gabriele Schaumann as well as from numerous discussions within the research group which helped me by suggestions, advices and ideas and which cannot be numeralized.

Achkowledgements

The present work is part of the subproject HUMUS of the interdisciplinary research project Interurban. I am grateful for the financial support granted from the German Research Foundation (DFG SCHA 849/4-3).
This work would not have been possible without the contribution of many people.

First of all I wish to express my sincere appreciation and gratitude to my supervisor Prof. Dr. Gabriele Schaumann for her confidence shown to me with the provision of this topic and the opportunity of working in her research group. Without her inspirational guidance, her enthusiasm, her encouragements and her unselfish help, I could never have finished my doctoral work. She always created a stimulating atmosphere that made me enjoy my work very much. I did not only find an excellent scientific advisor, but also a dear friend in her.

The present work started in Berlin at the department of Environmental Chemistry of the TU-Berlin. I would like to thank all the people who created a pleasant working atmosphere: My special thank goes to Julia Bayer, who introduced me to the contact angle tensiometer and the DRIFT measurement. She finished her diploma thesis in this time, which was, together with the PhD thesis of Julia Hurrass, a valuable base for my own work. My thanks go to the laboratory technicians Jeanette Regnéry and Katharina Knobel, as well as the student assistants Jenni Frank and Nils Meyer, who helped me measuring countless Wilhelmy plate contact angles, cared for the right humidity in the dessicators, fitted ellipses and evaluated DRIFT spectra. I also want to thank secretary Herta Klein who managed the project account and always knew what was going on in the department and of course my colleagues Daniela Gildemeister and Fabian Jäger who encouraged me to accompany Prof. Dr. Gabriele Schaumann to her new place of activity in Koblenz. A thank you also goes to all members of the research group Interurban and especially of the working group HUMUS for lively discussions and constructive teamwork. My thanks also goes to Dr. Ruth Ellerbrock from ZALF Müncheberg, where I measured DRIFT spectra, to Prof. Dr. Gerd Wessolek from the department of Soil Protection of the TU-Berlin for providing data from a long-term sampling in Tiergarten and Buch and to Dr. Susanne Woche from the institute of Soil Science of the University Hannover who measured particle charge.

I am grateful for the time with my collegue Daniela and her children as flatmates in Koblenz. The shared organisation of the daily routine as well as the trips with our children made the new beginning in Koblenz, without the former circle of friends, much easier. I also like to thank for the help which I got at the University in Koblenz from the technical assistants Andrea Schwarz, Claudia Stolze and Reimo Hagner, from the secretary Silvia Schuller as well as from my student assistant Lidiya Shemotyuk who measured numerous soil sample pH values. Although far too short, I enjoyed the time together with my colleagues Jenny Langbein and Irene Kamprad who left a gap in our working group when they parted.

I like to thank my current collegues at the University in Landau Lars Düster, Jette Schwarz, Nicole Bandow, Sina Egerer and again Juliua Bayer for their cooperative teamwork. My thanks also goes to Dr. Rob Bryant and Dr. Stefan Doerr from Swansea University who enabled a joint publication with Julia Bayer with data obtained in their institutes.

I also want to thank my parents who I could always rely on, even with a second move within 3 years. Finally, I am deeply indebted to my daughter Saïda who voluntarily made the sacrifice of changing school twice and leaving behind her circle of friends. Without her patience and love, particularly in those many days in which I spent more time with my computer than with her, this work would not have been possible.

Table of contents

1 GENERAL INTRODUCTION 5

1.1 ENVIRONMENTAL RELEVANCE OF SOIL WATER REPELLENCY 5
1.2 FACTORS AFFECTING SOIL WATER REPELLENCY 5
1.3 OBJECTIVES 10
1.4 SAMPLE SITES 13

2 THEORETICAL BACKGROUND 16

2.1 WATER REPELLENCY 16
2.2 DETERMINATION OF REPELLENCY 18
2.3 INFLUENCE OF GRAVITY, SURFACE ROUGHNESS AND CHEMICAL HETEROGENEITY ON CONTACT ANGLE DETERMINATION OF SOIL SAMPLES 22
2.4 WETTING KINETICS BY TIME DEPENDENT SESSILE DROP METHOD 26
2.5 SINKING AND SPREADING 27

3 THE NATURE OF WETTING ON URBAN SOIL SAMPLES - WETTING KINETICS AND EVAPORATION ASSESSED FROM SESSILE DROP SHAPE ..28

3.1 ABSTRACT 28
3.2 INTRODUCTION 28
3.3 MATERIAL AND METHODS 29
3.4 RESULTS AND DISCUSSION 33
3.5 CONCLUSIONS 40

4 INFLUENCE OF DRYING CONDITIONS ON WETTABILITY AND DRIFT SPECTROSCOPIC C-H BAND OF SOIL SAMPLES 42

4.1 SUMMARY 42
4.2 INTRODUCTION 42
4.3 MATERIALS AND METHODS 44
4.4 RESULTS & DISCUSSION 47
4.5 CONCLUSIONS 55

5 REACTION OF SOIL WATER REPELLENCY ON ARTIFICIALLY INDUCED CHANGES IN SOIL *PH* 57

5.1 ABSTRACT 57
5.2 INTRODUCTION 57
5.3 MATERIAL AND METHODS 60
5.4 RESULTS 66
5.5 DISCUSSION 73
5.6 CONCLUSIONS 78
5.7 ACKNOWLEDGMENTS 79

6 SYNTHESIS AND GENERAL CONCLUSIONS 80

6.1 SUMMARY OF OBSERVATIONS 80
6.2 CHEMICAL NATURE OF REPELLENCY IN BUCH SAMPLES 82
6.3 PHYSICOCHEMICAL NATURE OF REPELLENCY IN TIERGARTEN 84
6.4 SITE DEPENDENT CAUSES FOR THE NATURE OF SWR 87
6.5 FINAL CONCLUSION 88
6.6 OUTLOOK 90

7 REFERENCES 92

8 ANNEX 103

8.1 LIST OF ABREVIATIONS 103
8.2 LIST OF FIGURES 105
8.3 LIST OF TABLES 108
8.4 CURRICULUM VITAE 110
8.5 PUBLICATIONS 111

Abstract

The present work investigates the wetting characteristics of soils with regard to their dependence on environmental parameters such as water content (*WC*), *pH*, drying temperature and wetting temperature of wettable and repellent soils from two contrasting anthropogenic sites, the former sewage disposal field Berlin-Buch and the inner-city park Berlin-Tiergarten. The aim of this thesis is to deepen the understanding of processes and mechanisms leading to changes in soil water repellency. This helps to gain further insight into the behaviour of soil organic matter (SOM) and identifying ways to prevent or reduce the negative effects of soil water repellency (SWR).

The first focus of this work is to determine whether chemical reactions are required for wetting repellent samples. This hypothesis was tested by time and temperature dependence of sessile drop spreading on wettable and repellent samples. Additionally, diffuse reflectance infrared Fourier transform (DRIFT) spectroscopy was used to determine whether various drying regimes cause changes in the relative abundance of hydrophobic and hydrophilic functional groups in the outer layer of soil particles and whether these changes can be correlated with water content and the degree of SWR. Finally, by artificially altering the pH in dried samples applying acidic and alkaline reagents in a gaseous state, the influence of only pH on the degree of SWR was investigated separately from the influence of changes in moisture status.

The investigation of the two locations Buch and Tiergarten, each exceptionally different in the nature of their respective wetting properties, leads to new insights in the variety of appearance of SWR. The results of temperature, water content and *pH* dependency of SWR on the two contrasting sites resulted in one respective hypothetical model of nature of repellency for each site which provides an explanation for most of the observations made in this and earlier studies:

At the Tiergarten site, wetting characteristics are most likely determined by micelle-like arrangement of amphiphiles which depends on the concentration of water soluble amphiphilic substances, *pH* and ionic strength in soil solution. At low *pH* and at high ionic strength, repulsion forces between hydrophilic charged groups are minimized allowing their aggregation with outward orientated hydrophobic molecule moieties. At high *pH* and low ionic strength, higher repulsion forces between hydrophilic functional groups lead to an aggregation of hydrophobic groups during drying, which results in a layer with outward oriented hydrophilic moieties on soil organic matter surface leading to enhanced wettability.

For samples from the Buch site, chemical reactions are necessary for the wetting process. The strong dependence of SWR on water content indicates that hydrolysis-condensation reactions are the controlling mechanisms. Since acid catalyzed hydrolysis is an equilibrium reaction dependent on water content, an excess of water favours hydrolysis leading to an increasing number of hydrophilic functional groups. In contrast, water deficiency favours condensation reactions leading to a reduction of hydrophilic functional groups and thus a reduction of wettability.

The results of the present investigation and its comparison with earlier investigations clearly show that SWR is subject to numerous antagonistically and synergistically interacting environmental factors. The degree of influence, which a single factor exerts on SWR, is site-specific, e.g., it is dependent on special characteristics of mineral constituents and SOM which underlies the influence of climate, soil texture, topography, vegetation and the former and current use of the respective site.

Zusammenfassung

In der vorliegenden Arbeit wurden Benetzungseigenschaften zweier stark anthropogen beeinflusster Böden in Abhängigkeit von Einflussfaktoren wie Wassergehalt, pH, Trocknungs- und Benetzungstemperatur untersucht. Ziel war es die Prozesse und Mechanismen, die zu Veränderungen der Benetzungseigenschaften von Böden führen, besser zu verstehen. Erkenntnisse über diese Prozesse und Mechanismen lassen zum einen Rückschlüsse auf das generelle Verhalten von organischer Bodensubstanz zu, können zum anderen aber auch helfen, vorsorgliche Maßnahmen zu ergreifen um Bodenhydrophobie zu verhindern oder deren negative Effekte zu reduzieren.

Anhand der Zeit- und Temperaturabhängigkeit der Spreitung von liegenden Tropfen (TISED) auf hydrophoben und benetzbaren Bodenproben beider Standorte wurde die Hypothese getestet, dass der Benetzungsprozess durch chemische Reaktionen kontrolliert wird. Mithilfe von DRIFT (Diffuse Reflectance Infrared Fourier Transform) Spektren wurde überprüft, ob unterschiedliche Trocknungsbedingungen (Temperatur, Dauer, Luftfeuchte) zu Unterschieden in der Anzahl hydrophober und hydrophiler funktioneller Gruppen in den äußeren Molekülschichten führen die sich im Grad der Benetzungshemmung widerspiegeln. Durch künstliche pH-Wert Änderung über die Gasphase konnte die pH-Wert Abhängigkeit der Benetzungshemmung unabhängig vom Wassergehaltseinfluss beider Standorte verglichen werden.

Die beiden Standorte weisen extreme Unterschiede in der Art der Benetzungshemmung auf und sind dadurch beispielhaft für die Bandbreite der möglichen Ursachen und Mechanismen der Benetzungshemmung in Böden. Die Ergebnisse der Untersuchungen zur Temperatur- Wassergehalts- und pH-Abhängigkeit der Benetzungshemmung aus dieser Arbeit im Vergleich mit Ergebnissen vorhergehender Arbeiten lassen sich am besten mit jeweils einem konzeptionellen Modell pro Standort zur Natur der Benetzungshemmung erklären:

Am Standort Tiergarten werden die Benetzungseigenschaften vermutlich durch mizellartige Anordnung amphiphiler Substanzen an der Oberfläche der organischen Bodensubstanz bestimmt, die abhängig vom Gehalt wasserlöslicher amphiphiler Substanzen, dem pH-Wert und der Ionenstärke in der Bodenlösung im Verlaufe der Trocknung zu einer unterschiedlichen Orientierung der hydrophilen funktionellen Gruppen führt. Bei niedrigen pH-Werten und hoher Ionenstärke herrschen schwache Abstoßungskräfte zwischen den hydrophilen Gruppen, diese können aggregieren und hydrophobe Molekülketten sind nach außen gerichtet. Bei höheren pH-Werten und niedrigerer Ionenstärke sind die abstoßenden Kräfte zwischen den hydrophilen Gruppen groß und führen zu einer Aggregation hydrophober Gruppen, wobei die hydrophilen Gruppen nach der Trocknung nach außen gerichtet sind und für eine bessere Benetzbarkeit sorgen.

Am Standort Buch sind chemische Reaktionen zur Benetzung nötig. Aufgrund der starken Wassergehaltsabhängigkeit der Benetzungshemmung könnte es sich dabei um Hydrolysereaktionen handeln, die säurekatalysiert reversible wassegehaltsabhängige Gleichgewichtsreaktionen und im Basischen irreversibel sind.

Die beiden Modelle können eine Vielzahl von Beobachtungen erklären, die im Verlaufe dieser Untersuchung aber auch in vorhergehenden Untersuchungen gemacht wurden. Die Ergebnisse dieser Untersuchungen und ihr Vergleich mit vorherigen Untersuchungen auf denselben Standorten zeigten, dass Benetzungshemmung in Böden durch eine Vielzahl von Faktoren und Prozessen beeinflusst ist, die sowohl synergistisch als auch antagonistisch wirken können. Welche Faktoren den größten Einfluss ausüben bzw. welche Prozesse die vorherrschenden sind, hängt von lokalen Größen wie der Art des Mineralbodens und der organischen Bodensubstanz ab, die wiederum dem Einfluss von Klima, Textur, Topografie, Vegetation und der Nutzungsgeschichte unterliegen.

1 General introduction

1.1 Environmental relevance of soil water repellency

Soil water repellency (SWR) is a surface property of soil particles which reduces or prevents water infiltration into the soil (Doerr & Ritsema, 2005). When it comes into contact with a wettable soil, water spontaneously penetrates. In contrast, water balls up into spherical droplets on a repellent soil. These surface properties of soil particles have a high impact on soil hydrology (Doerr *et al.*, 2000) and thereby on processes like mobilisation, transport and immobilisation of substances within a soil. The resistance against wetting of a repellent soil may last for periods between seconds and weeks. This reduced infiltration capacity leads to increased surface run off, increased erosion of top soil components (Shakesby *et al.*, 2000) and thus an increased risk of surface waters pollution. In contrast, the filter function may be significantly reduced in repellent soils by the development of uneven wetting patterns (Ritsema & Dekker, 1994). In this case, the vertical water flow is concentrated on a small part of the soil cross-section, such as cracks, macro pores or regions with discontinuities in texture or wettability. An increased water flux is channelled through these preferential flow paths. Thus, the travel time of soluble nutrients or pollutants - and also of colloids and substances adsorbed on them - is significantly shortened, and the risk of groundwater contamination increases (Nguyen *et al.*, 1999; Ritsema & Dekker, 2000). Additionally, soil moisture conditions affect sorption properties of soil organic matter and the pore size distribution of a soil and are therefore expected to have an impact on the availability of pollutants and nutrients within the soil (Schaumann *et al.*, 2005). Furthermore, microbial activity and agriculture production are strongly influenced by hydrological soil properties, i.e., by the availability, distribution and storage of soil water. Repercussions of SWR on crops are reduced seed emergence and plant growth caused by water deficiency in the root zone (Blackwell, 2000). In contrast, positive effects of SWR have been reported with regard to the stability of soil aggregates (Piccolo & Mbagwu, 1999; Mataix-Solera & Doerr, 2004; Goebel *et al.*, 2005) and sequestering organic carbon (Piccolo *et al.*, 1999; Spaccini *et al.*, 2002). Furthermore, SWR leads to a reduced loss of soil water by evaporation (Imeson *et al.*, 1992; Yang *et al.*, 1996).

1.2 Factors affecting soil water repellency

1.2.1 Nature of soil organic matter and humic substances

The understanding of the role of soil organic matter (SOM) for the appearance of SWR requires a general knowledge about composition and functionality of SOM. In addition to living biomass, SOM consists of undecayed plant and animal tissues and their partial decomposition and transformation products, or humus. Humus can be divided into non-humic substances (e.g. sugars, amino acids, fats, polysaccharides and proteins) and humic

substances (HS), which have a high molecular weight, are brown to black in colour and are formed by secondary synthesis reactions. HS are a heterogeneous mixture of compounds and cannot be described by one specific structural formula. They can be divided into typical humic-fractions according to their solubility under acidic or alkaline conditions: (i) the light yellow to yellow-brown fulvic acids (FA) which are soluble in water under all *pH* conditions, (ii) the dark brown to grey black humic acids (HA) which are not soluble in water under acidic conditions ($pH < 2$) but are soluble at higher *pH* values and (iii) the black humins (HU) which are not soluble in water at any *pH* value (Stevenson, 1994). These operationally based classes are characterised by heterogeneous molecular weight and structure but show a general tendency in chemical and physical properties from FA over HA to HU as follows: an increasing intensity of colour, degree of polymerisation, molecular weight and carbon content and a decreasing oxygen content, exchange acidity, and solubility (Stevenson, 1985). This includes a decreasing polarity and therefore an increasing hydrophobic character from FA over HA to HU. The composition of humus varies considerably among different soil types and vegetation. The humus of forest soils is characterized by high fulvic acid content, while the humus of peat and grassland soils is high in humic acids (Stevenson, 1985). The HA to FA ratio usually, but not always, decreases with increasing depth.

Formation and molecular structure of HS are far from being fully explained. Currently, three main pathways of humification, including several sub-pathways, are under debate. (i) The *lignin theory* views lignins as the source of HS, which are more or less modified by soil microbes (Akim *et al.*, 1998). Repolymerisation of lignin monomers or of larger lignin structures occurs (e.g., via demethylation of phenolic esters, oxidation of propanol side chains, cleavage of aromatic rings and condensation reactions with amino compounds and quinones (Waksman & Reuszer, 1932)) forming the relatively oxygen-poor polymeric HUs. During continuous oxidation they become enriched with functional groups and develop into HAs and ultimately into FAs. (ii) The *polyphenol theory* considers all biopolymers to be decomposed to their monomeric units before repolymerisation (Stevenson, 1994). In contrast to lignin theory, increasing humification leads to increasing complexity of HS, i.e. in the earlier stages FAs develop into HAs and upon further humification into HUs. (iii) A third theory, the *sugar-amine condensation theory*, suggests that sugar, amines and/or glycine may be abiotically converted into melanine or glycosylamine which may undergo a complex series of chemical processes including polymerisation and condensation reactions forming HSs (Abadi Ghadim, 2000). Since this theory does not require lignin, it is a probable pathway for humic matter formation in marine environments.

The described theories of humification end up in hypothesised macromolecular polymeric structures (e.g. Graber & Borisover, 1998; LeBoeuf & Weber, 2000; Pignatello, 2003) with numerous cross-linkages formed by condensation reactions involving strong covalent C-C and C-N bonds (Essington, 2003). Some aspects of SOM behaviour like swelling and gel-like properties (Schaumann *et al.*, 2000) as well as nonlinearity, competition and hysteresis effects of sorption are currently best explained by the polymeric model.

An alternative paradigm, the *self aggregation theory*, considers humic substances as supramolecular associations formed by relatively small molecules which are self-organising into relatively large entities (e.g. Schulten & Schnitzer, 1997; Wershaw, 1999; Piccolo, 2002). These molecules derive from enzymatic and oxidative depolymerisation of biopolymers into tannins, cutins and carboxyl groups and contain relatively unaltered hydrophobic portions like aromatic and aliphatic structures as well as hydrophilic portions with carboxylic and phenolic groups (Essington, 2003). The amphiphilic, surfactant-like molecules may be aggregated at mineral surfaces, dispersed in soil solution at low concentrations, or forming micelles if critical micelle concentration (cmc) is exceeded (Wershaw, 1986). The micelles are stabilised by weak non-covalent forces like van der Waals forces, hydrogen bonds, π–π interactions, electrostatic effects and/or hydrophobic interactions (Conte & Piccolo, 1999). The enormous flexibility of dissolved SOM in response to changes in environmental conditions and the cross-linking effects of multivalent cations or water molecules in dissolved and undissolved SOM can be best explained by supramolecular associations of SOM (Schaumann & Bertmer, 2008). Therefore, probably neither macromolecules nor smaller molecules forming supramolecular associations can be fully excluded in SOM, but SOM is suggested to be regarded as amorphous material with a wide range of molecular mass and microregions with various properties (Schaumann, 2006).

1.2.2 The role of soil organic matter composition for soil water repellency

Since most mineral compounds of soils are hydrophilic (Tschapek, 1984), it is generally accepted that SWR is mainly caused by organic compounds in the form of more or less continuous coatings on mineral surfaces (Ma'shum *et al.*, 1988; Bisdom *et al.*, 1993) or as interstitial particulate organic material (McGhie & Posner, 1981; Franco *et al.*, 2000).

Attempts to find correlations between SOM content and SWR have produced inconsistent results: some studies found positive correlations (McKissock *et al.*, 1998; Mataix-Solera & Doerr, 2004), others having a negative (Teramura, 1980) or no relationship (DeBano, 1992; Wallis *et al.*, 1993). This shows that rather the quality than the quantity of soil organic matter determines the degree of SWR (Wallis & Horne, 1992). Hydrophobic compounds in SOM relevant for inducing SWR may derive directly from the decomposition of organic matter (McGhie & Posner, 1981) via accumulation of hydrophobic organic acids released as root exudates (Stevenson, 1985) or by fungal or microbial by-products (Savage *et al.*, 1969; Jex *et al.*, 1985; Hallett & Young, 1999). SWR has been observed in almost every part of the world in various climates, with various types of vegetation and in soils with various textures (Jaramillo *et al.*, 2000; Doerr *et al.*, 2007). Specific vegetation types, like certain types of evergreen trees (Mataix-Solera & Doerr, 2004), trees with considerable amounts of resins, waxes or aromatic oils (Doerr *et al.*, 2000; Ferreira *et al.*, 2000) shrubs and chaparral vegetation (Scholl, 1975) as well as certain grass species (Holzhey, 1968; DeBano, 2000) seem to favour the development of repellency which in turn may be associated with a specific microbial community.

Compounds most suspected to cause SWR among others are alkanes (Savage *et al.*, 1972; Ma'shum *et al.*, 1988; Roy *et al.*, 1999), amphiphilic compounds, mainly long-chained fatty acids (Ma'shum *et al.*, 1988; Hudson *et al.*, 1994; Roy *et al.*, 1999; Franco *et al.*, 2000; Horne & McIntosh, 2000), insoluble Ca and Mg fatty acid salts (Wander, 1949; Graber & S. Taggera, 2009), waxes (Franco *et al.*, 2000; Horne & McIntosh, 2000), phytanes, phytones or sterols (Franco *et al.*, 2000). In order to identify chemical compounds causing water repellency, numerous investigations have been carried out (Ma'shum *et al.*, 1988; Horne & McIntosh, 2000; Doerr *et al.*, 2005b). Most of the various extraction procedures showed no differences in amount of hydrophobic extractable compounds between wettable and repellent samples (Hudson *et al.*, 1994; Horne & McIntosh, 2000; Mainwaring *et al.*, 2004; Doerr *et al.*, 2005b; Morley *et al.*, 2005). In contrast, Morley *et al.*(2005) and Mainwaring *et al.*(2004) found a greater abundance of high molecular mass polar compounds in the water repellent samples which were essentially absent in wettable samples. Wettability of acid washed sand was modified in the same manner by extracts of wettable as well as by extracts of repellent samples (Horne & McIntosh, 2000). Furthermore, alternating extraction with polar and non-polar solvents leads to marked fluctuations in repellency (Horne & McIntosh, 2000).

These and comparable results suggest that water repellency is determined by the composition and nature of the outermost layer of organic material rather than by the characteristics of the bulk of the organic matter (Horne & McIntosh, 2000). Suggested mechanisms for changes in the arrangement of molecules and functional groups may be conformational changes, hydration or spatial rearrangement of organic molecules in the surfaces of organic coatings as a result of contact with water (Tschapek, 1984; Ma'shum & Farmer, 1985; Horne & McIntosh, 2000; Doerr *et al.*, 2005b). An alternative mechanism for enhanced wettability that suggests the reduction of surface tension via dissolution of soil-borne surface active organic compounds into the wetting water (Chen & Schnitzer, 1978; Tschapek, 1984; Barrett & Slaymaker, 1989; Doerr *et al.*, 2000; Hurraß & Schaumann, 2006) was rejected by Graber *et al.* (2007).

1.2.3 Water content

The relation between SWR and water content (*WC*) has been investigated in many studies with some contradictory results. Under field conditions, sub-soils are subjected to short-term and seasonal moisture variations. Repellency is generally considered to increase with increasing dryness of soil (Berglund & Persson, 1996; Doerr & Thomas, 2000). Thus, Dekker & Ritsema (1994) measured actual SWR in field moist state and potential SWR after air drying or oven drying and defined a critical water content (WC_{crit}) above which a soil sample is wettable and below which it becomes repellent. Täumer *et al* (2005) found that SWR in the former sewage disposal field at the Buch site can be predicted with data of SOM content using a linear function to calculate WC_{crit}.

However, other studies investigating soil water repellency in dependency of *WC* found an apparently contradictory SWR-*WC* relation especially at *WCs* around and below the wilting point. Ziogas *et al* (2003) showed that oven drying might render samples fully wettable. Other studies found repellency maxima at intermediate to small water content

between air-dried states and wilting points (King, 1981; Goebel *et al.*, 2004; Bayer & Schaumann, 2007) and a decrease in repellency with further drying to lower *WCs*. Contrary to this, equilibration of dry soils at high relative humidity resulted in an increase of repellency (Hurraß & Schaumann, 2006; Wallach & Graber, 2007). As changes in repellency are not fully reversible after rewetting (Doerr & Thomas, 2000; Bayer & Schaumann, 2007) water content alone seems to be an inadequate characteristic to predict soil water repellency. Soil texture (de Jonge *et al.*, 1999) and SOM content and quality as well as additional factors such as drying duration and temperature (Bayer & Schaumann, 2007) together with equilibration time (Hurraß & Schaumann, 2006; Wallach & Graber, 2007) seem to influence changes in SWR.

1.2.4 Soil pH

Soil *pH* or better soil solution *pH* depends on various environmental factors, e.g., parent rock material, climate, organic matter composition, degree of degradation and vegetation. In turn, soil *pH* determines soil characteristics like charge of mineral and organic surfaces, exchange capacity, availability of nutrients and contaminants, plant growth, microbial activity as well as stability and structure of organic matter. Several studies found alkaline soils to be less prone to SWR compared to acidic soils (Dekker & Jungerius, 1990; Cerdà & Doerr, 2007; Mataix-Solera *et al.*, 2007). Furthermore, SWR has been successfully reduced in acidic soils by increasing soil *pH* via liming (van't Woudt, 1959; Karnok *et al.*, 1993; Roper, 2005). However, SWR has also been reported in calcareous soils in the Netherlands (Dekker & Jungerius, 1990), California, USA (Holzhey, 1968) and Spain (Mataix-Solera & Doerr, 2004).

This study focuses in particular on *pH* since the results of earlier studies point to a general difference in the nature of repellency between the two investigated sites, among others, regarding *pH* dependent SWR. Hurraß & Schaumann (2006) found that only for one of the two investigated sites, repellency of closely neighbouring wettable and repellent samples were interrelated with differences in *pH*. Bayer & Schaumann (2007) confirmed this assumption by artificially changing *pH* in samples from the same sample sites. However, in contrast to the expectation that increasing *pH* will improve the wettability and decreasing *pH* will intensify water repellency, they found a maximum in water repellency at a *pH* above the original *pH*.

1.2.5 Temperature

Temperature has an influence on many processes in soils. Changes in temperature are linked with changes in surface tension and viscosity of liquids, in solubility of salts and gases, in evaporation rates and rates of chemical reactions. Thus temperature may play an important role in appearance of SWR and changes in its degree.

Several studies investigated the influence of the drying temperature on potential SWR with contradictory results. Dekker et al (2001) found an increasing potential SWR with increasing drying temperature for 75 Dutch dune sand samples, whereas Ziogas et al. (2005) found the contrary relation in 35 Greek sandy soil samples. The importance of pre-treatment temperatures for SWR determination was also emphasised by de Jonge et

al.(1999) who compared freeze-dried and oven-dried samples and found a significantly higher degree of SWR in samples after oven drying. In contrast to that, Ziogas et al. (2003) showed that oven drying might render samples fully wettable. King (1981) investigated the temperature influence on $\log_{10}$ of infiltration rate and on contact angle at a temperature between 0 and 45°C. He found a positive linear relationship between temperature and SWR with a stronger temperature effect on samples with a higher degree of SWR and no significant temperature effect in ignited samples emphasising the major contribution of organic matter on the temperature dependency. Lichner et al. (2002) tested the re-establishment of SWR in model repellent sands after intermixing with kaolinite. When these samples are dried at 30 and 60°C most of them exhibit SWR again. Following drying at 120°C, SWR only reappears in a few samples which contained a high amount of humid acids. However, drying at 90, 150 and 270°C does not re-induce repellency. Bachmann et al. (2002) studied the temperature dependence of water retention curves and found a six times higher temperature dependence of capillary pressure than predicted by the temperature dependence of pure water only. They suggested 3 possible mechanisms: (i) temperature-induced changes in contact angle, (ii) changes in liquid-gas in interfacial tension because of solute effects and (iii) changes of the enthalpy of immersion with temperature or capillary pressure. By calculating the activation energy, temperature dependency of the rate of a depicted process may also give information about the nature of the rate limiting step of the respective process. Todoruk et al (2003a) used proton nuclear magnetic resonance spectroscopy (^{1}H-NMR) to measure the temperature dependence of pore-scale redistribution of water during wetting in repellent soils contaminated with crude oil and obtained an activation energy within the range of chemical reactions.

The influence of higher temperatures, which under field conditions may be expected only during wildland fires, are intensively investigated since burnt soils are especially prone to SWR (Scholl, 1975; Doerr, 1997; Robichaud, 2000; Shakesby *et al.*, 2003; Varela *et al.*, 2005). Suggested mechanisms are the volatilisation of hydrophobic organic substances and a concentrated condensation in cooler soil regions (Savage, 1974). Between 175 and 200°C SWR is intensified (DeBano, 1981), around 250°C hydrophobic substances are fixed on soil particles (Doerr *et al.*, 2000) and between 280 and 400°C SWR is destroyed (DeBano, 2000).

1.3 Objectives

Part of the experimental workings for this thesis originated from the interdisciplinary research project Interurban "Water and Organic Matter in Anthropogenic Soils: Dynamics and Processes". This project is aimed at a systematic understanding of water and matter cycles in soils of urban sites. In the first phase of the project, soil water repellency (SWR) turned out to be one of the most important controlling factors of these cycles in both of the investigated sites. Therefore, the second phase focused mainly on causes and effects of SWR at these sites. The objective of the present study is to clarify

the role of soil organic matter (SOM) for the appearance of SWR and its dynamics and dependency on environmental conditions in two anthropogenically influenced urban sites in Berlin, Germany. Earlier investigations showed that mechanisms controlling SWR may significantly differ from location to location and that drying conditions such as temperature and relative humidity, *WC* and *pH* are probably the influencing factors with the highest relevance for SWR at the investigated sites (Bayer, 2004; Hurraß, 2006).

Therefore, the following hypothesises should be tested:

(i) Wetting of water repellent soils is controlled by chemical processes.

(ii) The relative abundance of hydrophobic molecular parts in the outer layer of soil organic matter increases with water content and drying temperature dependent degree of repellency.

(iii) The degree of repellency decreases with increasing *pH* caused by increasing negative surface charge of deprotonated functional groups of SOM molecules.

In order to prevent measurement artefacts, methods for determination of contact angle had to be adapted to an application in soil science. In this context, special properties of soil samples like the surface roughness had to be considered in sessile drop and Wilhelmy plate contact angle measurement. A theoretical introduction into the measurements of surface characteristics of solids and an approach to approximate influence of distortion variables on repellency measurement at soil samples are presented in Chapter 2.

(i) Chapter 3 describes the investigation of the influence of temperature on the wetting process of soil samples. The wetting rate as a function of temperature may give information about the nature of the rate limiting step of this process. Therefore, the activation energy of wetting of repellent samples can describe the nature of repellency and distinguish between chemical reactions and physical processes as rate limiting steps. We tested the hypothesis previously suggested by Todoruk *et al.* (2003a) that wetting of repellent soil samples is controlled by chemical processes. Therefore, the spreading kinetics of sessile drops on wettable and water repellent sample pairs has been investigated. Under controlled conditions, which prevent evaporation and infiltration, the rate limiting step of wetting was assessed via the activation energy, which was obtained from the temperature dependence of spreading.

(ii) The studies described in Chapter 4 are aimed at the interaction of three influencing factors: SOM surface properties, *WC* and various drying regimes. Several authors suggested that changes in SWR may be caused by changes in the spatial arrangement of molecules or moieties in the outer-most layer of SOM (e.g., Tschapek, 1984; Horne & McIntosh, 2000; Doerr *et al.*, 2005b). Previous studies at the investigated sites showed that not only changes in *WC* but also the conditions of drying, like temperature and relative humidity, have an influence on the degree of SWR (Hurraß & Schaumann, 2006; Bayer & Schaumann, 2007). Therefore, the hypothesis that increased SWR caused by drying is related to an increase in the relative abundance of outward orientated hydrophobic organic moieties was tested. The relative abundance of functional groups in the SOM can be determined by diffuse reflectance infrared fourier transform spectroscopy (DRIFT) which, in contrast to infrared spectroscopy in transmission mode,

provides information about the outer layers of a sample and gives information about hydrophobicity of SOM (Capriel *et al.*, 1995). The DRIFT spectra were obtained from wettable and repellent samples treated by various drying procedures in order to verify the extent to which changes in water repellency are (a) related to changes in the relative abundance of hydrophobic molecular parts in the outer layer of soil organic matter and (b) caused solely by changes in water content.

(iii) The studies described in Chapter 5 aimed at the influence of *pH* on SWR. Hurraß & Schaumann (2006) found that at one of the two investigated sites repellency appears only at a *pH* below a certain value whereas wettable samples are not restricted to a special *pH* range. For the other site, no relation between *pH* and repellency could be observed. Bayer & Schaumann (2007) investigated the influence of addition of liquid acid and base solution with increasing concentration to wettable and repellent samples from both sites and found a strong *pH* dependency of SWR in samples from one site but no response on *pH* changes at the other site. However, all samples significantly changed in degree of repellency even when treated with pure water. This led to the conclusion that the results of this investigation were partly caused by changes in the moisture status of the samples and could not exclusively be related to changes in *pH*. Therefore, in collaboration with Julia Bayer who investigated wettable and repellent samples from UK, Netherlands and Australia at the University of Wales Swansea, an advanced experiment was developed and carried out contemporaneously. This experimental design was aimed at a further understanding of the direct influence of soil *pH* on SWR excluding the influence of soil moisture changes on SWR. The new method allows changing *pH* in soil samples without altering soil moisture by subjecting the samples to varying concentrations of gaseous hydrochloric acid or ammonia. Using three different methods of SWR determination, the hypothesis was tested that artificially increasing *pH* decreases the degree of repellency caused by increasing negative surface charge of deprotonated functional groups of SOM molecules. Furthermore, the results of the three applied methods of repellency determination i.e. sessile drop contact angle, Wilhelmy plate contact angle and water drop penetration time should be compared regarding their expressiveness and sensitivity in various repellency ranges.

Finally, the experimental results are summarized in Chapter 6 and a comprehensive interpretation is presented which includes nearly all observations of this study obtained from the two investigated sites. With special consideration for the differences in the nature of repellency between the two sites, a schematic concept is suggested as to how SWR may develop at these two sites and which environmental conditions may especially favour or impede its appearance. The final conclusion aimed at the transfer of results and new insights drawn from the investigations of the two Berlin sites into a more general comprehension of SWR and behaviour of SOM under various environmental conditions. Furthermore, open questions for which further research is needed and suggestions for approaching these questions are presented in the outlook.

1.4 Sample sites

1.4.1 Berlin-Tiergarten

The city park Tiergarten is located in the centre of Berlin and has been in use as a natural park since the 17th century. After the Second World War, between 1945 and 1950, it was totally deforested for firewood production. After 1950, the bomb and shell craters were filled with rubble and construction waste and covered by a top soil to start reforestation (Wendland, 1993). The area investigated by INTERURBAN is a highly frequented lawn for sunbathing with a light slope (Figure 1-1). In spring and summer, the grass is periodically cut, fertilized and irrigated. The soil is classified as *Cambisol* (Klitzke & Lang, 2007).

Figure 1-1 Sample site Berlin-Tiergarten (photo: K. Täumer, Department of Soil Protection, TU-Berlin)

The variety of anthropogenic influences leads to high small-scale heterogeneity of soil properties. E.g., water content and SWR reveal major differences even in closely adjacent sectors. In field moist state wettable and repellent samples were taken at a depth of 10 - 20 cm at distances of about 10 cm and named as TW for initially wettable samples with water drop penetration times (*WDPT*) < 10 s and TR for initially repellent samples with *WDPT* > 10 s.

Besides differences in *WC* and *WDPT*, 95% of the repellent samples appear only at $pH < 4.6$ whereas wettable samples appear at pH values above and below 4.6. Furthermore, 95% of the wettable samples only appear with electrical conductivity of soil solution $EC < 270$ µS/m, whereas repellent samples cover a range of $100 < EC < 1300$ µS/m. Loss on ignition (*LoI*) and C to N ratio (*C/N*) (Table 1-1) as well as soil texture with 85% sand, 11% silt and 5% clay (Schaumann *et al.*, 2005) is comparable for wettable and repellent samples.

Table 1-1 Water content (*WC*), loss on ignition (*LoI*), *pH*, electrical conductivity, C to N ratio (*C/N*) and water drop penetration time in field moist state ($WDPT_{fm}$) and in air dried state ($WDPT_{ad}$) of wettable and repellent samples from Tiergarten TW and TR, respectively.

		WC	*LoI*	*pH*	*EC*	*C/N*	$WDPT_{fm}$	$WDPT_{ad}$
		%	%	($CaCl_2$)	µS/m		h	h
TW	*N*	34	34	34	28	29	37	30
	mean (SD)	20 (8)	10 (4)	4.8 (0.6)	140 (130)	14 (2)	0 (0)	0 (0)
TR	*N*	24	23	23	20	18	25	20
	mean (SD)	17 (12)	10 (4)	4.1 (0.3)	480 (490)	14 (1)	6 (4)	6 (4)

1.4.2 Berlin-Buch

The sample site Berlin-Buch is located northeast of Berlin. The former sewage disposal field in Buch was irrigated with untreated waste water for almost 80 years, until, in 1985, application of waste water was stopped. Without consideration of soil characteristics and distribution of contamination the dams for flood irrigation were levelled and an afforestation was attempted (Hoffmann, 2002). Between 30 and 60 % of the planted trees died mainly because of nutrient and water deficiency as well as heavy metal contamination (Schlenther, 1996).

The termination of waste water application resulted in a lowering of the groundwater table and changed reducing into oxidising conditions. With increased microbial activity, this lead to a rapid turnover of organic matter resulting in a decrease in *pH* and an increased mobilisation of heavy metals and nitrates (Hoffmann, 2002).

Figure 1-2 Sample site Berlin-Buch: result of an attempt of afforrestation (left), small-scale differences in *WC* visible in dark wettable and light repellent patches at a depth of 5 cm during sampling in Berlin-Buch (Hurraß & Schaumann, 2006); (right); (photos: K. Täumer, Department of Soil Protection, TU-Berlin)

The sample site in Buch is now mainly covered by couch grass *(Agropyron repens)* and a few trees like ash *(Fraxinus)* and box elder *(Acer negundo)* (Figure 1-2, left). The surface (or ground surface) is uneven as a result of furrows created when trees were planted at this site. Since most of the trees died, today the surface has grooves approximately 1m wide. The 40–60 cm thick organic topsoil upon medium-sized sand shows a high and very heterogeneous organic matter content between 4 and 6 %, seldom reaching up to 30 % and reveals strong variation in thickness over the investigated area. The soil is classified as *Regosol* (Klitzke & Lang, 2007) with clay content in the noncalcareous fluvial sand of < 1 % (Täumer *et al.*, 2005).

Table 1-2 Water content (*WC*), loss on ignition (*LoI*), *pH*, electrical conductivity, C to N ratio (*C/N*) and water drop penetration time in field moist state ($WDPT_{fm}$) and in air dried state ($WDPT_{ad}$) of wettable and repellent samples from Buch BW and BR, respectively.

		WC	*LoI*	*pH*	*EC*	*C/N*	$WDPT_{fm}$	$WDPT_{ad}$
		%	%	($CaCl_2$)	µS/m		h	h
BW	*N*	82	76	75	76	61	82	71
	mean (SD)	23 (12)	11 (6)	4.6 (0.5)	160 (270)	10 (1)	0 (0)	1 (2)
BR	*N*	48	43	43	42	35	48	35
	mean (SD)	10 (3)	9 (2)	4.7 (0.5)	220 (170)	10 (1)	5 (3)	5 (3)

Comparable to the sampling from Tiergarten, wettable and repellent samples in a field moist state were taken at a depth of 10-20 cm at distances of about 10 cm apart and named as BW for initially wettable samples with water drop penetration times (*WDPT*) < 10 s and BR for initially repellent samples with *WDPT* > 10 s. Samples of each sampling differed significantly in field moist *WC* and *WDPT* (Figure 1-2, right) but revealed comparable values of *LoI*, *pH*, *EC* and *C/N*. In contrast to Tiergarten samples, which kept the differences in *WDPT*, initially wettable Buch samples lost their wettability and reached a degree of SWR comparable to that of initially repellent samples (Table 1-2).

2 Theoretical background

2.1 Water repellency

Water repellency is a surface property of a solid which impedes complete wetting, i.e. it prevents water from spreading on its surface and forming a continuous water layer. Instead, a water repellent surface causes partial wetting, i.e. the water is forced to ball up as droplets with a finite contact angle. To understand the physical background, the interfacial tensions of the three adjacent phases vapour (v), liquid (l) and solid (s) have to be considered. The surface tension of a substance (i.e., the interfacial tension between this substance and the surrounding vapour phase) is based on the difference in energetic state between molecules in the bulk phase and the molecules at the surface. The molecules at the surface are attracted by a reduced number of neighbours and therefore in an energetically unfavourable state. The creation of new surfaces is thus energetically costly, and a fluid system will act to minimize surface areas. Principally, the same is valid for solid surfaces although solid surfaces cannot react in minimizing surface areas like fluids. The interfacial tension γ^{ab} between the phases a and b can be described (a) by the energy E that is needed to increase the surface area A_s (Schwuger, 1996):

$$\gamma^{ab} = \left(\frac{\partial E}{\partial A_s^{ab}} \right)_{T,V,n_k} \tag{2-1}$$

or (b) by the force F that is needed to increase the length of the perimeter l_s of the respective surface area:

$$\gamma^{ab} = \left(\frac{\partial F}{\partial l_s^{ab}} \right)_{T,V,n_k} \tag{2-2}$$

Consequently interfacial tension has the dimension of [N m^{-1}] or [J m^{-2}].

If the system of the three phases vapour (v), liquid (l) and solid (s) is in a mechanical equilibrium at the three phase line (TPL) the Antonow equation is true (Schwuger, 1996):

$$\gamma^{sv} \leq \gamma^{sl} + \gamma^{lv} \tag{2-3}$$

When a liquid is in contact with a solid surface, the following cases are possible: If $\gamma^{sv} \geq \gamma^{sl} + \gamma^{lv}$, then the liquid spreads spontaneously and forms a continuous layer on the solid surface (Figure 2-1 A). No mechanical equilibrium is possible and no contact angle can be formed because no three phase line exists.

For $\gamma^{sv} < \gamma^{sl} + \gamma^{lv}$ the liquid forms a droplet on the solid. In mechanical equilibrium and for an ideal smooth surface, the contact angle Θ is defined by the Young equation (Young, 1855):

$$\cos\Theta = \frac{\gamma^{sv} - \gamma^{sl}}{\gamma^{lv}} \tag{2-4}$$

In this case,

if $\gamma^{sv} < \gamma^{sl}$ then $\cos\Theta < 0$, i.e., $\Theta < 90°$ (Figure 2-1 B),

if $\gamma^{sv} = \gamma^{sl}$ then $\cos\Theta = 0$, i.e., $\Theta = 90°$ (Figure 2-1 C),

if $\gamma^{sv} > \gamma^{sl}$ then $\cos\Theta > 0$, i.e., $\Theta > 90°$ (Figure 2-1 D).

If $\gamma^{sv} = \gamma^{sl} + \gamma^{lv}$ then, according to Equation (2-4), $\Theta = 0$ and the limit case between complete wetting (spontaneous spreading) and partial wetting is reached.

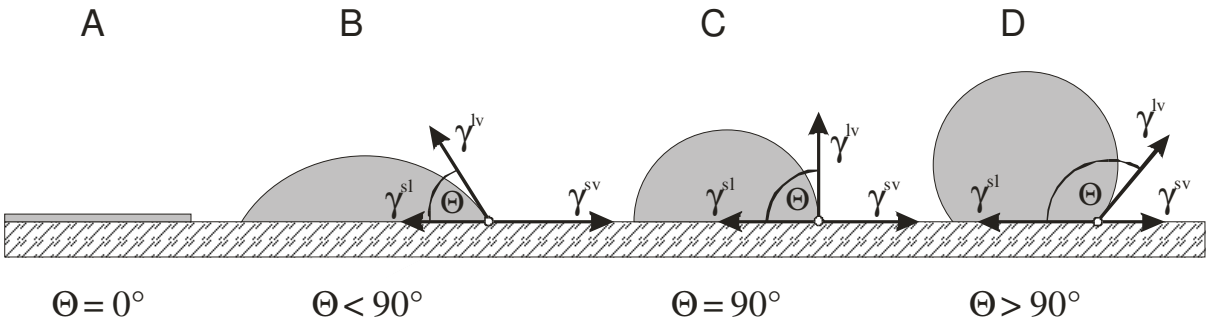

Figure 2-1 Interfacial tensions at the three phase line (TPL) of the adjacent liquid, solid and vapour phase for various contact angles Θ.

Although water is the most abundant molecule on Earth's surface, it is the most atypical liquid. The anomalous properties of water are caused by its high electronegativity. Water molecules are formed of two hydrogen atoms covalently bonded to one oxygen atom. Since oxygen attracts electrons much stronger than hydrogen, a dipole exisits within each water molecule with a positive charge $\delta+$ on the hydrogen atoms and negative charges $\delta-$ on the oxygen atom. Due to this dipole, water molecules are electrically attracted to each other forming clusters via so-called hydrogen bonds HB. Each water molecule may interact with up to four other water molecules via hydrogen bonds (Figure 2-2). This leads to a more compact structure and causes the anomalies of water. E.g., water has an exceptionally high surface tension which is 72.75 mN m^{-1} at 21.5°C (Adamson & Petry, 1997), the highest surface tension of non-metallic liquids and the highest polarity of all substances.

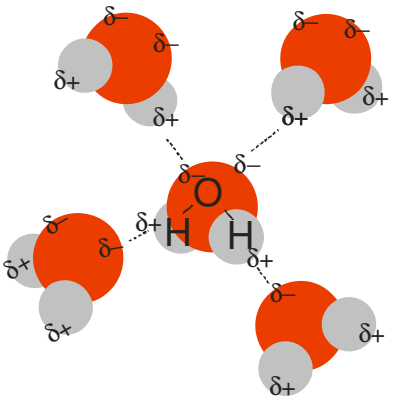

Figure 2-2 Schematic drawing of hydrogen bonds between water molecules

As shown in Figure 2-1, the higher the surface tension of a solid (for solid also called surface free energy) the better it is wettable by water. The condition for complete wetting (variations of Equation 2-3) shows that only solids with surface free energy γ^{sv} significantly higher than the surface tension of water with 72.75 mN m^{-1} are completely wettable and are therefore called hydrophilic.

Since the so-called high energy solids are substances which are held together by strong chemical bonds (e.g. covalent, ionic, or metallic bonds), they are very hard and have a high melting point like in metals, glass, ceramics or minerals. Low energy solids like non-polar organic substances are much softer, have a lower melting point and are held together by weaker non-covalent bonds (e.g. Van der Waals bonds). All of these partially wettable substances have a surface free energy lower than 72.75 mN m^{-1} and are therefore called hydrophobic.

2.2 Determination of repellency

2.2.1 Water drop penetration time (*WDPT*)

Water drop penetration time is a very simple and rapid method to obtain a measure of the resistance of repellency. A drop of water is placed on a flattened soil surface and the time needed for the drop to penetrate into the soil is recorded (Letey, 1969). For a better reproducibility, soil samples are sieved, placed on a dish, and the surface is smoothed to provide comparable conditions (Wallis & Horne, 1992) because surface roughness and pore geometry have an effect on the penetration process (Wessel, 1988). In many studies, the applied drop volume is not reported or varies, e.g, between 0.035 mL (Kostka, 2000) and 0.200 mL (Wallach & Graber, 2007). Drops of higher volumes underlie the influence of gravity and their penetration may be accelerated by hydrological pressure. At the same time, they are larger than the largest pores in the soil sample (Roy & McGill, 2002) and by covering a larger area they are better in considering the heterogeneity of soil material. Even the number of repetitions differs between several studies. Most often, however, three drops for each sample are applied and considered as sufficient for SWR determination (e.g. Dekker & Ritsema, 1994; Doerr *et al.*, 2006; Wallach & Graber, 2007). As temperature and ambient relative humidity affect the penetration time a constant defined temperature, e.g. between 18 and 23°C (Richardson, 1984), and a calibration to a defined ambient relative humidity (Bisdom *et al.*, 1993) enhance comparability of results.

Table 2-1 Repellency classes according to (Dekker & Jungerius, 1990).

classes	0	1	2	3	4	5	6
WDPT	< 5 s	5 – 60 s	1 - 10 min	10 – 60 min	1 – 3 h	3 – 6 h	> 6 h
notation	wettable	slightly repellent	strongly repellent	severely repellent	extremely repellent	extremely repellent	extremely repellent

The interpretation of *WDPT* is controversially discussed. Letey (1969) considers instantaneous penetration to indicate an initial contact angle (Θ) smaller 90°. Longer penetration times would indicate that the soil-water contact angle decreases and penetration occurs when $\Theta = 90°$ is reached. Therefore, *WDPT* is considered to be a measure of persistence of repellency rather than of actual wettability. However, several studies reported linear relationship between logarithm of *WDPT* and Θ (King, 1981;

Wessel, 1988; Buczko *et al.*, 2006). *WDPT* related to 90° of these studies, however, are ranging between < 1 s and several minutes. Therefore, the distinction between wettable and repellent soils using *WDPT* can be only arbitrary. A widely accepted practise is the interpretation of *WDPT* using repellency classes (Table 2-1) as suggested by (Dekker & Jungerius, 1990).

2.2.2 Contact angle by Capillary Rise Method

The capillary rise method (CRM) is a common method to determine wettability of porous material (e.g., Siebold *et al.*, 1997; Michel *et al.*, 2001; Goebel *et al.*, 2004) which is at least partially wettable, i.e., with $\Theta < 90°$. The measurement principle is based on the Washburn equation for rising flow in a vertical thin cylindrical capillary (Washburn, 1921):

$$h^2 = \frac{\cos\Theta_{adv}\ \gamma^{lv}}{2\eta}\ r\ t \tag{2-5}$$

By means of capillary forces, a liquid with a surface tension γ^{lv} and a viscosity η in a capillary with the advancing contact angle Θ_{adv} and the radius r reaches height h at the time t. In porous media the pores where liquid can penetrate are not ideally cylindrical. Thus r is substituted by a geometrical factor C reflecting porosity and tortuosity of the pores. This factor depends on particle size and packing density of the measured medium. Since in porous media the height h is difficult to measure it is substituted by:

$$h = \frac{w}{\rho\,\pi\,C} \tag{2-6}$$

where w is the weight of risen water, which can easily be detected by a balance, and ρ is the density of the liquid. The substitution of the height in Equation (2-5) by Equation (2-6) and solving for cos Θ_{adv} leads to:

$$\cos\Theta_{adv} = \frac{w^2}{t}\left(\frac{2\eta}{\gamma^{lv}\ C\ \pi^2\ \rho^2}\right) \tag{2-7}$$

For applications in soil science, the samples are filled in tubes with a liquid permeable bottom, e.g., a glass frit. In order to obtain reproducible results, the samples have to be compacted in a defined way and kept at a controlled temperature during measurement. The tubes are suspended from a balance and the glass frit bottom brought into contact to the surface of the wetting liquid. The rate of liquid rise can be measured by recording the increase in weight as a function of time. The geometry factor C has to be determined for each sample by additional measurements with an optimally wetting liquid, e.g., n-hexane, whose advancing angle is virtually 0°, i.e., cos $\Theta_{adv} = 1$. The factor C can be calculated in the range of linear increase of Δw^2 by the slope of w^2 as a function of t with the constant term in brackets of Equation (2-8), where η, γ^{lv} and ρ are the properties of the optimally wetting liquid, e.g., n-hexane.

$$C = \frac{w^2}{t}\left(\frac{2\eta}{\gamma^{lv}\ \pi^2\ \rho^2}\right) \tag{2-8}$$

The advancing contact angle is calculated based on Equation (2-7) in the range of linear increase of Δw^2 by multiplying the slope of w^2 as a function of t with the constant term in brackets of Equation (2-7). Measurements are generally carried out by a special device, a contact angle tensiometer, with sensitive balances, motor driven plates for the liquid vessel with precise programmable positions, temperature control and software which records weight changes in the sample, temperature and position of the liquid table and offers the calculation of the respective parameter.

However, besides restriction of this method to samples with $\Theta_{adv} < 90°$, many researchers recognized additional disadvantages of CRM. Marmur (1992) and Siebold *et al.* (2000) reported that Θ_{adv} measured by CRM is often overestimated in comparison with corresponding equilibrium contact angles. Furthermore, contact time of the sample with the testing liquid depends on Θ_{adv} and may lead to systematic errors, e.g., due to sorption kinetics of the vapour on the solid surface (Bachmann *et al.*, 2006).

2.2.3 Contact angle by Wilhelmy Plate Method

An additional method of contact angle determination is the Wilhelmy plate method. This method is based on the following principle (Wilhelmy, 1863): the weight of a solid plate immersed into a liquid is subjected to gravitational force acting vertically downwards; the buoyancy acting vertically upwards and the surface force acting along the liquid vapour interface directly at the three phase line (Figure 2-3). The acting gravitational force depends on weight w_p of the plate

$$F_g = m_p \; g \; = \; w_p \tag{2-9}$$

and the buoyancy on density ρ_l and volume V_l of the displaced liquid which can be expressed by the immersion depth of the plate z and the cross sectional area of the plate A_p:

$$F_b = \rho_l \; A_p \; z \; g \tag{2-10}$$

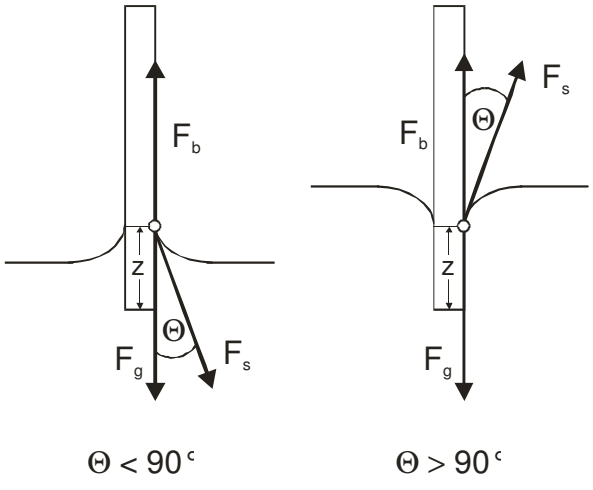

Figure 2-3 Gravitational force F_g, buoyancy F_b and surface force F_s acting at the three phase line of a Wilhelmy plate immersed into a liquid with liquid-solid contact angle below and above 90°.

The surface force depends on the surface tension of the liquid and the wetted length L_w, i.e., the perimeter of the plate, l_s. Since the surface force does not act in the same direction as gravitation and buoyancy, the resulting force is the surface force multiplied by cos Θ_{adv}.

$$F_s = \cos\Theta\ \gamma^{lv}\ L_w \tag{2-11}$$

When balanced, the sum of these forces (Equation (2-9), (2-10), and (2-11) is zero:

$$\cos\Theta_{adv}\ \gamma^{lv}\ L_w - \rho_l\ \ A_p\ \ z\ \ g + w_p = 0 \tag{2-12}$$

and can be expressed as the change of weight of the plate as a function of immersion depth z with F_s as the intercept:

$$\Delta\, w_p = \rho_l\ A_p\ g\ \ \ z\ -\ \cos\Theta_{adv}\ \ \gamma^{lv}\ L_w \tag{2-13}$$

In order to measure the advancing contact angle Θ_{adv} by a tensiometer, a plate of the sample material is suspended from a balance, the vessel with the respective liquid is lifted with a defined speed and the plate immerses while the balance records changes in weight Δw_p as a function of immersion depth z. The $\cos\Theta_{adv}$ can be calculated by dividing the intercept of this function, i.e., F_s, by $L_w\ \gamma^{lv}$. When maximum immersion depth is reached the vessel with the liquid is lowering and the plate emerges from the liquid. The receding contact angle is calculated in the same way with Δw_p as a function of z during emersion. An important advantage of the Wilhelmy Plate Method is that it theoretically covers the whole Θ range between 0 and 180° and that the measurement is comparably fast.

2.2.4 Sessile Drop Method

A water drop placed on a non- or only partially wettable solid surface, as depicted in Figure 2-4, forms a shape that depends on the interfacial tensions *(γ)* of the three adjacent surfaces: solid (*s*), liquid (*l*) and vapour (*v*). The angle at the three phase contact line between the solid-liquid *(sl)* and the liquid-vapour *(lv)* interface is called the contact angle, *Θ*. In equilibrium, the relation of the interfacial tensions at the three-phase line is given by the Young equation(Young, 1855):

$$\gamma^{sl} - \gamma^{sv} + \gamma^{lv}\cos\Theta_Y = 0 \tag{2-14}$$

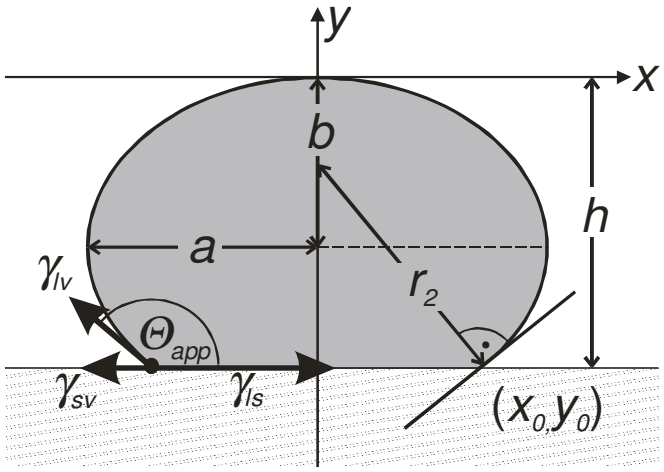

Figure 2-4 A sessile drop fitted as ellipsoidal cap showing the vectors of interfacial tensions, *γ*, at the drop edge, the observable contact angle Θ_{app} and elliptical parameters a, b, h necessary to calculate Θ_{app} and drop volume V according to Equation (2-20) and (2-21).

In order to compare the change of soil surface characteristics at different temperatures, a value is needed that is independent of the temperature effect on the liquid surface tension. The work of adhesion, W_{adh}, the energy necessary to separate the water-solid contact area, can be expressed according to Dupré (1869) by:

$$W_{adh} = \gamma^{lv} \left(1 + \cos\Theta_Y\right) \tag{2-15}$$

For determination of Θ for a sessile drop, various techniques are applied. Using the static method, equilibrium contact angle Θ is measured for a drop on a solid surface with a constant volume. Using the dynamic method the largest advancing contact angle Θ_{adv} and the smallest receding contact angle Θ_{rec} are determined by increasing or decreasing drop volume, respectively. In the simplest method, the user measures the contact angle visually by a microscope equipped with a goniometer scale. Currently available software-driven systems with high resolution cameras make it possible to automatically capture and analyse sessile drop contact angles under various environmental conditions.

A simplified method is used in this study; the soil samples are fixed by double sided adhesive tape on a glass slide (Bachmann *et al.*, 2000b). Pictures of droplets on soil samples taken by a digital camera are used for geometrical analysis of drop shape and calculation of the respective contact angles. In contrast to Bachmann *et al.* (2000b), who applied drop volumes of 2 – 10 µL and used a microscope for determination of sessile drop contact angle, in this study the drops contain a volume of 100 µL. The large area covered by one drop better considers the high inhomogeneity of the investigated humus sandy samples.

2.3 Influence of gravity, surface roughness and chemical heterogeneity on contact angle determination of soil samples

2.3.1 Influence of gravity on static sessile drop contact angle

Equation (2-14) and (2-15) are dealing with the Young´s law contact angle Θ_Y and are therefore only applicable for ideally smooth surfaces and drop sizes smaller than a tenth of the capillary length (κ^{-1})

$$\kappa^{-1} = \left(\frac{\gamma^{lv}}{\Delta\rho\ g}\right)^{\frac{1}{2}} \tag{2-16}$$

so that gravity can be neglected and the drop shape can be assumed as spherical cap (McHale *et al.*, 2001).

In order to consider the inhomogeneity of soil samples, this study deals with drop volumes of 100 µl. Initial drop heights up to 4 mm are significantly larger than $\kappa^{-1} \approx 2.7$ mm (for water). In this case, under consideration of the hydrostatic pressure, the Young – Laplace equation (Stenius, 1994):

$$\Delta p = \gamma^{lv}\left(\frac{1}{r_1} + \frac{1}{r_2}\right) \tag{2-17}$$

changes according to Schwuger (1996) to

$$\Delta p = \frac{2\,\gamma^{lv}}{r_0} + g\ \Delta\rho\ \ y_0 = \gamma^{lv}\left(\frac{1}{r_1} + \frac{1}{r_2}\right) \tag{2-18}$$

where r_0 is the radius of curvature at the drop apex at $y = 0$, where the hydrostatic pressure p is zero, and r_1 and r_2 are the radii of curvature of the drop surface at (x_0, y_0)

(Schwuger, 1996). A transformation into a set of three differential equations as formulated by Bashforth and Adams (1882) allows a numerical solution for the drop shape, as used by various authors in combination with image analysis software (Bashforth & Adams, 1883; Lin *et al.*, 1996; de Ruijter *et al.*, 1998; Spiros & Savvas, 1998).

In this study, we apply a simplifying approximation for the drop shape, assuming an axis symmetric ellipsoidal cap as a gravity-influenced drop shape model as suggested by McHale *et al.*(2001). Based on the general equation of an ellipse in Cartesian coordinates:

$$\frac{x^2}{a^2}+\frac{(b+y)^2}{b^2}=1 \tag{2-19}$$

the derivative dx/dy at the point $y_0 = -h$, provides the slope of the tangent at the contact line (Figure 2-4) and the apparent contact angle, Θ_{app}, as a function of drop height, h, and the semi-major and semi-minor axis, a and b, can be determined by:

$$\begin{aligned}\Theta_{app} &= 90° + \arctan\left(\frac{dx}{dy}(y=-h)\right)\\ &= 90° + \arctan\left(-\frac{a}{b^2}(b-h)\left(1-\frac{(b-h)^2}{b^2}\right)^{-\frac{1}{2}}\right)\end{aligned} \tag{2-20}$$

The drop volume as a volume of rotation is given by:

$$\begin{aligned}V_{drop} &= \pi\int_h^b f(y)^2 dy \qquad = \pi\int_h^b a^2\left(1-\frac{y^2}{b^2}\right) dy\\ &= \pi a^2\left[y-\frac{y^3}{3b^2}\right]_h^b = \pi a^2\left(\frac{2}{3}b-h+\frac{h^3}{3b^2}\right)\end{aligned} \tag{2-21}$$

The approximation of the drop shape by an ellipsoidal cap improves the determination of the gravity influenced contact angle, but it underestimates Θ_{app} especially in the range greater than 90°, where the surface curvature of an ellipsoid decreases with decreasing y_0, while in reality, the surface curvature at the drop bottom increases due to an increasing hydrostatic pressure with increasing drop height. Since all samples investigated in the present study were measured under exactly the same conditions, differences in Θ are unambiguously caused by differences in the degree of repellency and not by the influence of gravity, although the absolute values may not be compared with Θ obtained under differing method conditions, e.g., with lower drop volumes.

2.3.2 Influence of surface roughness and chemical heterogeneity on sessile drop

In addition to gravity, surface roughness and chemical heterogeneity of soil samples have an influence on Θ_{app} of a sessile drop and therefore on the observable wetting kinetics. As described by McHale and colleagues, there are two approaches to consider surface roughness and heterogeneity in contact angle measurement (McHale *et al.*, 2005).

The Cassie-Baxter equation(Adamson & Petry, 1997):

$$\cos\Theta_{sm} \equiv \sum \frac{A_i}{A_{tot}} \cos\Theta_{y,i} \qquad (2\text{-}22)$$

applies for the contact angle Θ_{sm} of a smooth chemically heterogeneous surface, which is composed by different materials with different respective Young´s law contact angles, $\Theta_{y,i}$, where A_i is the area of the material i and A_{tot} is the total area.

Wenzel's equation (Wenzel, 1949)

$$\cos\Theta_r = \frac{A_{act}}{A_{geo}} \cos\Theta_{sm} \qquad (2\text{-}23)$$

applies for the contact angle Θ_r of a rough surface of an chemical homogenous material, where the liquid follows the profile at any point of the contact area so that the actual contact area, A_{act}, is greater than its planar projection, the geometric area, A_{geo}. At the so-called *Wenzel state*, an increasing roughness results in an increase of Θ_r for materials with $\Theta_y > 90$ and in a decrease of Θ_r for materials with $\Theta_y < 90°$.

Gaps between dry particles smaller than a tenth of κ^{-1} may be bridged by the water, so that a fraction of the water-soil contact area is represented by the included air, which has the contact angle of 180° against water (McHale *et al.*, 2005). Simplifying a horizontal interface between included air and water with Equation (2-22) the effective contact angle Θ_{eff} can be expressed according to McHale and co-workers (McHale *et al.*, 2005) by:

$$\cos\Theta_{eff} = \frac{A_{geo,s}}{A_{tot}} \left(\cos\Theta_r\right) - \left(1 - \frac{A_{geo,s}}{A_{tot}}\right) \quad , \qquad (2\text{-}24)$$

where $A_{geo,s}$ is the water covered solid area. The state of a water-"rough solid" interface, where the effect of included air dominates the Wenzel effect on Θ_{eff}, is called *Cassie-Baxter state* (McHale *et al.*, 2005).

In natural soil samples, a combination of all the above described effects has to be assumed, and the observable effective contact angle, Θ_{eff}, can be expressed as a combination of Equations (2-22), (2-23) and (2-24)

$$\begin{aligned} \cos\Theta_{eff} &= \frac{A_{geo}}{A_{tot}} \frac{A_{act}}{A_{geo}} \cos\Theta_{sm} - 1 + \frac{A_{geo}}{A_{tot}} \\ &= \frac{A_{act}}{A_{tot}} \sum_i \frac{A_i}{A_{tot}} \cos\Theta_{Y,i} - 1 + \frac{A_{geo}}{A_{tot}} \end{aligned} \qquad (2\text{-}25)$$

A recent study (Bachmann & McHale, in press) approaches the influence of surface roughness on sessile drop contact angle by considering soil particles as ideally smooth spheres with a uniform radius r and a constant distance 2 ε r between each other. Then the planar projection of soil surface can be divided into identical subunits in the form of equilateral triangles with a side length of 2 (1 + ε) r and with the top point of one of three adjacent spheres at each angle (McHale *et al.*, 2007). By this model,

$$\frac{A_{geo}}{A_{tot}} = f\left(\Theta_Y, \varepsilon\right) = \frac{\pi \sin^2 \Theta_Y}{2\sqrt{3}\left(1+\varepsilon\right)^2} \qquad (2\text{-}26)$$

$$\frac{A_{act}}{A_{geo}} = f\left(\Theta_Y, \varepsilon\right) = \frac{2\left(1+\cos\Theta_Y\right)}{\sin^2\Theta_Y} \qquad (2\text{-}27)$$

and Equation (2-25) changes into:

$$\cos\Theta_{eff} = \frac{\pi\left(1+\cos\Theta_Y\right)}{\sqrt{3}\left(1+\varepsilon\right)^2}\cos\Theta_Y - 1 + \frac{\pi\sin^2\Theta_Y}{2\sqrt{3}\left(1+\varepsilon\right)^2} \qquad (2\text{-}28)$$

This model was tested with monodisperse spherical glass beads and irregular soil particles, treated with dichlorodimethylsilane (DCDMS) and compared with Young contact angles, obtained from smooth DCDMS treated glass surfaces. These tests produced reasonably accurate predictions of the contact angles for a range of liquid surface tensions with ε between 0.26 – 0.31. However, to adapt and establish the efficacy of these methods for naturally hydrophobic soils, further work has to be done (Bachmann & McHale, in press).

Thus, the contact angle data obtained in this study are not corrected with regard to the influence of surface roughness. Since all investigated samples consist of the same predominant grain size fraction of medium-sized sand, and samples were prepared in a comparable manner, i.e., resulting in a comparable grain density fixed on the glass slide, differences in Θ are unambiguously caused by differences in the degree of repellency and not by the influence of surface roughness, although the absolute values may not be compared with values obtained of samples of different grain size distribution or different grain density on the glass slide.

2.3.3 Influence of surface roughness on Wilhelmy Plate Method

For the Wilhelmy plate measurement, samples are fixed on a rectangular glass slide completely covered by double-sided adhesive tape. Comparable to sessile drop measurement, Θ_{eff} determined by Wilhelmy plate measurement is influenced by surface roughness. However, in contrast to sessile drop method, for this method it is not the water covered area but the wetted length, i.e., the three phase line at which the measured forces are acting. For ideal smooth plates, L_W is equal to the perimeter of the plare, l_s. The recent suggestion of approximating L_w by l_s (Bachmann & McHale, in press) leads to $\cos\Theta_{adv} < -1$ or to $\cos\Theta_{rec} > 1$ for several of the sandy samples of this study which can be only explained by an underestimation of L_w. Thus, for the relatively coarse sandy soil samples of this study, L_W has to be estimated. As a very rough estimation, we assumed that the effective surface of the soil covered plate is formed by close-packed solid hemispheres and is in Wenzel's state (no entrapped air) from the first moment of immersion. Under these assumptions, L_W is the sum of the arc lengths of semicircles, U_i in the intersecting planes of the hemisphere particles, while l_s is the sum of diameters d_i of these semicircles. L_W and l_s can be expressed as a function of d_i, and L_W is estimated as follows:

$$l_s = \sum_i d_i \qquad L_W = \sum_i l_{s,i} = \frac{\pi}{2}\sum_i d_i \qquad L_W = \frac{\pi}{2} l_s \qquad (2\text{-}29)$$

If L_W is larger than assumed by the hemispheric particle shape, Θ_{adv} is overestimated in the range larger than 90° and underestimated in the range smaller than 90°. If part of

the gaps between the soil particles remains air filled after immersion, what probably happens in the range > 90° is that Θ_{adv} is overestimated as well. J. Bachmann (personal communication, 2006) obtained a factor of 0.7-0.8 to reduce the $\cos\Theta_{adv}$ measured by Wilhelmy plate method and calculated the possible consequences for the wetted length and included air. The good accordance of Equation (2-29) with the estimation by J. Bachmann shows that our assumption is applicable, and therefore we corrected the geometric circumference l_s with the factor $\pi/2$ according to Equation (2-29). This leads invariably to reasonable results of cos Θ_{adv} and cos Θ_{rec}. In contrast to Bachmann & McHale (in press), who considered the mean of cos Θ_{adv} and cos Θ_{rec} as equilibrium contact angle, in this study, only Θ_{adv} is considered since it cannot be excluded that surface properties have been changed during the immersion and emersion time. With an immersion depth of 10 mm and an immersion speed of 0.2 mm s^{-1}, the samples are in contact with water for 100 s. The results of time dependent sessile drop measurement suggest that the strongest change in surface properties occur especially in the first minutes.

2.4 Wetting kinetics by time dependent sessile drop method

Thermodynamics and kinetics in chemistry are often confused. Thermodynamic, other than indicated by the word “dynamic”, describes how stable a system is in one state versus another state. In contrast, kinetics describes how quickly or slowly the system changes from one state to another state. Generally, systems are only spontaneously changing from a less stable state into a more stable state with a reduction in free energy (ΔG). But even if the products have a significantly lower free energy than the reactants, a reaction will not happen in practice if the reaction is too slow. This is for instance the case if an activated transition state during the reaction has a higher free energy than the reactants. Such an energy barrier which has to overcome by input of energy before a reaction occurs is called activation energy E_A. Kinetic investigations allow the determination of E_A.

To investigate wetting kinetics, a depicted parameter of surface characteristic is monitored as function of time and rate constants are extracted from the respective time law. The parameter of interest in this study is the Young contact angle and the work of adhesion (Equation (2-15)). According to the Arrhenius equation, the temperature dependence of the rate constant, k, of this time law allows the calculation of the activation energy, E_A, which is the minimum energy necessary for a specific process to occur (Wedler, 1987):

$$\ln k = \ln A - \frac{E_A}{RT} \qquad (2\text{-}30)$$

The activation energy gives information about nature of the rate limiting step of the investigated process. Chemical reactions are characterised by $E_A > 60$ kJ mol^{-1}, while physically controlled processes require $E_A < 42$ kJ mol^{-1} (Sparks, 1985).

2.5 Sinking and Spreading

The influencing factors on Θ_{eff} discussed above likewise have an effect on time dependent changes in Θ_{eff}. Thus, in the course of wetting by sessile drop, the drop water is moving into two directions:

Vertical: *Sinking* of the drop of water into the gaps between the particles accesses new *inner contact area* beneath the drop (Figure 2-5 (b) – (c) side view). The increase of the solid-liquid interface and decrease of the air-liquid interface, as well as the increase of the total interface (for $\Theta_y < 90°$, Figure 2-5 (b) – (c) plan view) and contact angle hysteresis effects due to apparent volume loss result in a observable Θ_{app} decreasing faster than the Θ_y of the soil material.

Horizontal: *Spreading* of the drop of water accesses new geometric *outer contact area* around the initial interface. The new accessed area is not influenced by water solid interactions yet, like the earlier wetted area, and has a higher fraction of air-liquid interface, so that the Θ_{app} decrease diminishes by spreading.

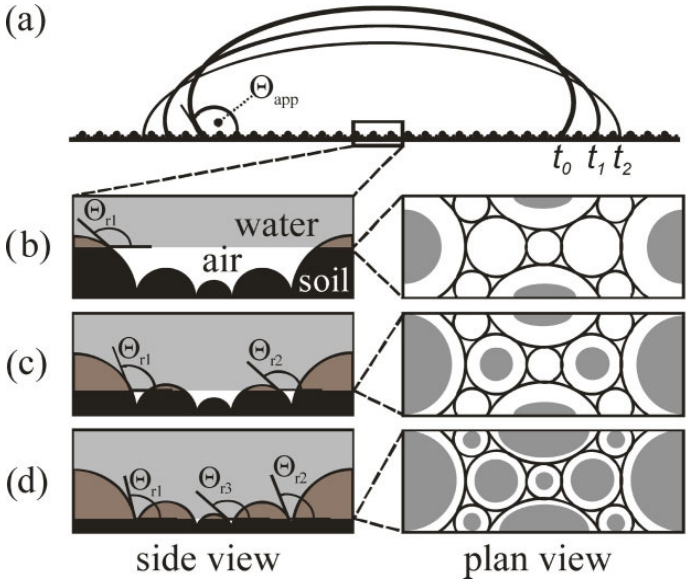

Figure 2-5 (a): Sessile drop on rough surface with decreasing apparent contact angle, Θ_{app}, and increasing total geometric contact area, A_{tot}, by *spreading* from time t_0 to t_2. (b – d): *sinking* of drop water into air filled gaps in a zoomed intersection of the water-solid contact area beneeth the drop. Side views: hemispheric particles partly covered by water in dark grey, entrapped air (white) between dry parts of particles (black) and from t_0 to t_2 sinking water level (light grey). Plan views: from t_0 to t_2 increasing geometric area, A_{geo}, (grey) of water covered particles and decreasing water-air interface (white)

The driving force for s*preading* as well as for *sinking* is the change of soil surface characteristics with water contact time. The centre of interest of this investigation is dedicated to the time and temperature dependent change of soil surface characteristics in the course of wetting. As shown above, due to the influence of gravity and roughness, the time dependence of the experimentally accessible Θ_{app} does not allow conclusions to be drawn with regard to the time dependence of the respective Θ_Y as a value of the actual soil surface characteristics. So, the time law determined from the apparent work of adhesion, $W_{app}(\Theta_{app})$, according to Equation (2-15) reflects the sum of different influences on wetting by sessile drop, and not solely the direct water-solid interaction. However, conversely, the activation energy, E_A, of the change of $W_{app}(\Theta_{app})$ directly reflects the activation energy of the change of $W_{adh}(\Theta_y)$, as long as the influence of roughness and gravity on the temperature dependence of the rate constants is negligible.

3 The nature of wetting on urban soil samples - Wetting kinetics and evaporation assessed from sessile drop shape

3.1 Abstract

The understanding of soil water repellency in its complexity requires knowledge of the mechanisms leading to changes in surface characteristics. Wetting kinetics may serve as means to investigate the origin of soil water repellency, but have been scarcely investigated yet. We observed the wetting kinetics of soil samples from two locations via the time-dependent shape of sessile drop (TISED) at three temperatures.

Our study showed that drop penetration may be exceeded by evaporation for high *WDPT*. The time-dependent change of drop shape and apparent contact angle was explained by surface hydrophilisation including the change from Cassie-Baxter into Wenzel's state. We identified principal differences in the nature of water repellency between the two investigated locations: Only the samples from the former sewage disposal field Buch lost most initial differences in wettability upon air drying and storage. Wetting of these samples required activation energy of 65-94 kJ mol^{-1}, indicating chemical reactions as rate-limiting step. In contrast, wetting of the samples from the inner city park Tiergarten required activation energy of 42 kJ mol^{-1} for the repellent and 8-20 kJ mol^{-1} for the wettable samples, which suggests physico-chemical and physical processes as rate-limiting steps.

Our study showed for the first time that the process of soil wetting can be monitored by TISED assessment, and that assessment of the temperature dependence of the wetting kinetics allows distinguishing between different natures of wetting and soil water repellency. It therefore represents a novel approach to investigate wetting processes. Combination of such approaches with spectroscopic investigations will help to deepen our understanding on possible causes of water repellency. They further help to understand the great variety of suggested causes of repellency and indicate locational material-specific effects rather than one general cause for water repellency.

3.2 Introduction

It is widely accepted that soil water repellency is, among others, caused by hydrophobic organic compounds as coating on mineral surfaces (Bisdom *et al.*, 1993; Doerr *et al.*, 2000) as well as organic interstitial material (Franco *et al.*, 2000). Numerous investigations in order to identify chemical compounds causing water repellency (Ma'shum *et al.*, 1988; Horne & McIntosh, 2000; Doerr *et al.*, 2005b) had been carried out. Many of these investigations suggest that rather the structural composition and the arrangement of molecules and functional groups than the amount of certain organic substances affect water repellency (Doerr *et al.*, 2005b). The factors, however, that establish the structural composition and arrangement of molecules on the outer side of

the organic coatings, and which lead to water repellency, are still poorly understood. Generally, repellent soils become wettable, if they stay long enough in contact with water (Doerr *et al.*, 2000). In consequence of this, it can be assumed that molecules at organic matter-water interfaces undergo conformational or structural rearrangement. Differences of wetting kinetics between wettable and water repellent soil samples may give information about processes, which break down the repellent character. They may therefore also allow conclusions about processes inducing water repellency in soils.

Despite the high potential, wetting kinetics of soils has been scarcely investigated yet. Todoruk and co-workers and Schaumann and co-workers used ^{1}H-NMR Relaxometry to monitor wetting and swelling kinetics of soil samples (Todoruk *et al.*, 2003a; Schaumann *et al.*, 2005). The results indicate a pore-scale redistribution of water in the soil samples, which is, most probably, due to changes in the wettability of pore. Todoruk and co-workers suggested ester hydrolysis as rate limiting step of water redistribution (Todoruk *et al.*, 2003a). In contrast to this, Hurraß and Schaumann (2006) suggest, from drying-remoistening experiments, slow conformational changes as dominating process in the course of wetting. The results obtained by ^{1}H-NMR Relaxometry do not allow distinguishing between the processes of water redistribution and changes in surface characteristics. For a deeper understanding of the wetting process, it is necessary to directly assess the change in surface characteristics induced by soil-water contact.

We tested the hypothesis, previously suggested by Todoruk and co-workers, that the process of wetting is controlled by chemical processes like ester hydrolysis. Based on the assumption, that the contact angle of sessile drops on a soil sample surface reflects the respective surface characteristics, we compared the spreading kinetics of sessile drops on wettable and water repellent sample pairs of two highly anthropogenically influenced urban sites. Under controlled conditions, which prevent evaporation and infiltration, we assessed the rate limiting step of wetting via the activation energy, obtained from the temperature dependence of spreading.

3.3 Material and Methods

3.3.1 Sample sites

The research group Interurban has been investigating two strongly anthropogenically influenced locations on the former sewage disposal fields Buch in the north east of Berlin and on the inner city park Tiergarten.

The sewage disposal fields in Buch had been irrigated with untreated waste water for about 80 years, until, in 1985, they stopped to run. Without consideration of soil characteristics and distribution of contamination the dams were levelled and trees were planted(Hoffmann, 2002). Between 30 and 60 % of the planted trees died because of nutrient and water deficiency as well as heavy metal contamination (Schlenther, 1996). The sample site in Buch is now mainly covered by couch grass *(Agropyron repens)* and a few trees like ash *(Fraxinus)* and box elder *(Acer negundo)*. The surface is slightly wavy due to the furrows of plantation. The top soil consists of medium sized sand and is

characterized by high and very heterogeneous organic content. It reveals a strong variation in thickness over the investigated area. The soil is classified as *hortic anthrosol* (Täumer *et al.*, 2005).

The Tiergarten has been in use as a natural park since the 17th century. Between 1945 and 1950, it was totally deforested for firewood production. After 1950, the bomb and shell craters were filled by rubble and covered by a top soil to start a reforestation (Wendland, 1993). The area investigated by Interurban is a high frequented meadow with a light slope. In spring and summer, the grass is periodically cut, fertilized and irrigated.

3.3.2 Sample preparation and characterization

In the present study, one sample pair of each site was taken in a depth of 15-20 cm. It consists of two neighboured samples (maximal 20 cm of distance), which differ strongly in actual wettability and actual field moisture, while soil characteristics like texture and organic content were comparable within each sample pair (see Table 3-1).

Table 3-1 Characteristics of the field moist and air-dried initially water repellent (B1, T1) and initially wettable samples (B2, T2) from Buch and Tiergarten (a - by Wilhelmy Plate Method, b - by Capillary Rise Method)

sample	B1	B2	T1	T2
pH	5.1	5.2	4.6	5.3
ignition loss / % dry mass	11	18	6	7
water content / % field moist	13	33	7	13
WDPT / h field moist	3	0	5	0
Θ_{adv} / ° field moist	121[a]	85[b]	124[a]	87[b]
Θ_{sess} / ° field moist	110	85	103	67
water content / % dried	2	3	1	1
WDPT / h dried	6	5	2,3	0,1
Θ_{adv} / ° dried	132[a]	118[a]	126[a]	122[a]
Θ_{sess} / ° dried	123	117	112	86

We used field samples which were air dried and stored at room temperature over saturated $CaCl_2$ solution in desiccators (31-35 % *RH*). The water content was determined gravimetrically by drying at 105°C, and the organic content was assessed by ashing for 5 h at 550°C. All measurements of this study were performed with samples sieved < 1 mm.

Between the two sample sites the following differences could be observed (Table 3-1): The sample pair from Buch had a higher organic and water content than the pair from Tiergarten. As shown in Table 3-1, contact angle and *WDPT* of the field moist sample B2 from Buch increased by air drying and storage and the sample became as water repellent as its repellent neighboured sample B1. In contrast, contact angle and *WDPT* of the repellent sample T1 from Tiergarten decreased only slightly, so that the sample pair from Tiergarten kept its differences in wettability after drying. In order to consider the effect of drying and storage conditions on the wetting characteristics, in the

following, the dried samples, which were wettable in field moist state, are named "initially wettable", and dried samples, which were water repellent in field moist state, are named "initially repellent" samples.

3.3.3 Determination of repellency

Water drop penetration time (WDPT)

The wetting resistance of the soil samples was determined by the water drop penetration time *(WDPT).* The samples were filled in small containers, the surface smoothed without pressure by a spatula and the containers posed in a temperature regulated incubator at 20°C. Three drops containing 100 µl of distilled water were placed on each sample. For *WDPT* > 1 min, the points of time, when the droplets penetrate into the soil samples, were observed by magnified digital photographs automatically taken in increasing time intervals from 12 s up to 10 min, so that the relative error of *WDPT* did not exceed 5 %.

Advancing contact angle by Wilhelmy Plate Method

The initial contact angle was measured as advancing contact angle, Θ_{adv}, with the Dynamic Contact Angle Meter and Tensiometer (DCAT 21, DataPhysics, Filderstadt, Germany). Field moist repellent ($\Theta_{adv} > 90°$) and air dried samples were measured by the dynamic Wilhelmy Plate Method (WPM) (Wilhelmy, 1863). The soil samples were fixed on a rectangular glass slide (76 x 26 x 1 mm) completely covered by double sided adhesive tape and suspended from a balance (± 0.01 mg). By lifting a container with destilled water with a speed of 0.2 mm s^{-1}, the soil covered plates were continually immersed up to a maximal immersion depth z_{max} of 10 mm, while the balance records the development of the effective sample weight, w_{eff}, as function of the immersion depth, z. The change of w_{eff} depends on the plate mass, m_P, the buoyancy $(F_b(z))$, the surface force (Fs) and the advancing contact angle, Θ_{adv}, and can be expressed as:

$$w_{eff} - w_p = F_s \cos\Theta_{adv} - F_b(z)$$

$$w_{eff} - m_p g = L_w \gamma_{lv} \cos\Theta_{adv} - \rho_w g A_p z$$

$$\frac{w_{eff} - m_p g}{L_w \gamma_{lv}}(z) = \cos\Theta_{adv} - \frac{\rho_w g A_p}{L_w \gamma_{lv}} z \qquad (3\text{-}1)$$

where w_p is the plate weight, L_W is the wetted length, γ^{lv} is the liquid-vapor interfacial tension, ρ_W is the density of water and g is the acceleration of gravity. Then $\cos\Theta_{adv}$ can be calculated from the axis intercept of Equation (3-1). For ideal smooth plates, L_W is equal to the geometric circumference of the plate, U_P. For coarse surfaces (e.g., soil samples), L_W has to be estimated. We assumed that the effective surface of the soil covered plate is formed by close-packed solid hemispheres and is in Wenzel's state (no entrapped air) from the first moment of immersion. Under these assumptions, L_W is the sum of the arc lengths of semicircles, U_i, (in the intersecting planes of the hemisphere particles), while U_P is the sum of diameters, d_i, of these semicircles. L_W and U_P can be expressed as a function of d_i and L_W estimated as following:

$$U_P = \sum_i d_i \qquad L_W = \sum_i U_i = \frac{\pi}{2}\sum_i d_i \qquad L_W = \frac{\pi}{2} U_P \tag{3-2}$$

If L_W is larger than assumed by the hemispheric particle shape, Θ_{adv} is overestimated in the range larger than 90° and underestimated in the range smaller than 90°. If part of the gaps between the soil particles remains air filled after immersion, what probably happens in the range > 90°, Θ_{adv} is overestimated as well. J. Bachmann (personal communication) obtained a factor of 0.7-0.8 to reduce the cos Θ_{adv} measured by Wilhelmy Plate Method and calculated the possible consequences for the wetted length and included air. The good accordance of Equation (3-2) with the estimation by J. Bachmann shows that our assumption is applicable, and therefore we corrected the geometric circumference U_P with the factor $\pi / 2$ according to Equation (3-2). From preliminary experiments, we obtained a statistic error of $\Delta\Theta = \pm 5°$.

Capillary Rise Method

Wettable samples ($\Theta_{adv} < 90°$), which did not stick to the adhesive tape, were measured according to the Modified Washburn Method or Capillary Rise Method (CRM). The Washburn equation for capillary flow in a porous medium (Washburn, 1921)

$$h^2 = \frac{\cos\Theta\ \gamma_{lv}}{2\eta}\ r\ t \tag{3-3}$$

modified by substitution of the height of the capillary rise for the mass of the risen liquid ($h = \frac{m}{\rho \pi C}$), and Equation (2-5) becomes:

$$\cos\Theta = \frac{m^2}{t}\left(\frac{2\eta}{\gamma_{lv} C \pi^2 \rho^2}\right), \tag{3-4}$$

where m is the mass, η is the viscosity and ρ the density of the risen liquid. The geometry factor, C, reflects, the porosity and tortuosity of the capillaries and depends on particle size and packing density of the measured medium.

The samples were filled in glass tubes (10 mm diameter) with a glass filter base. In order to obtain reproducible results, the tubes were slightly knocked for 12 times to compact the samples. The tubes with about 2 cm^3 compacted soil were suspended from the balance (± 0.01 mg). The glass frit base of the tubes samples were brought into contact to the surface of distilled water. The rate of water rise was measured by recording the increase in weight as a function of time. The geometry factor C has to be determined for each sample by additional measurements with n-hexane as an optimally wetting liquid, whose advancing angle is virtually 0°. The advancing contact angle was calculated based on Equation (2-7) in the range of linear increase of Δm^2 by the software SCAT (version 2.4.2.48 from dataphysics). All measurements were conducted in a temperature regulated sample chamber at 20°C (± 0.1 K) and repeated three times.

Time Dependent Sessile Drop (TISED)

In order to monitor wetting kinetics, we investigated the isothermal change in drop shape of sessile drops as a function of soil–water contact time. To distinguish between

spreading, evaporation and infiltration, three different experiments were conducted. In experiment I, the samples were filled into small vessels, smoothed with a spatula, and three drops of 100 µl were placed on the surface. In this configuration infiltration was possible. In experiment II, the samples were fixed as a thin layer by double sided adhesive tape on glass slides (Bachmann *et al.*, 2000). The drops placed on it could not infiltrate. The experiment II was conducted only with the samples B1 and B2 from Buch. In experiment III, in order to minimise the evaporation during the monitoring of drop shape, the sample covered glass slide (prepared like in experiment II) was enclosed in a humidity chamber (volume: 4 l) with a relative humidity *RH* of 99.9 %. All three experiments were conducted at 5°C, 20°C and 30°C in a temperature regulated incubator (volume: 200 L) to guarantee constancy of the respective temperature. In each experiment, the time depending change of drop shape was recorded by a digital camera (Canon A300), which took pictures in increasing time intervals from minimal 12 s up to 0.5 h.

The objective of the evaluation is to monitor changes in surface characteristics. The digital pictures were used as templates to fit ellipses to the drop shapes. The parameters of the ellipses and the soil–water contact line were used to calculate the contact angle, Θ_{app}, as described in Figure 2-4 and Equation (2-20). As a measure of surface characteristics, we calculated the apparent work of adhesion, W_{app}, from the time dependent Θ_{app} (Equation (2-15). In order to monitor the volume loss and to improve the experimental design, additionally, the drop volume V_{drop} was approximated by Equation (2-21).

The current state of knowledge does not allow formulating a mechanistic model for the wetting mechanism. Therefore, kinetic parameters were derived in a model independent way, fitting zero-order and first-order kinetics to the volume- and W_{adh}–data with the software Origin V. 7.5, and evaluating the respective rate constant parameters as function of temperature.

3.4 Results and Discussion

3.4.1 Drop Volume

Figure 3-1 a shows the volume, *V,* of sessile drops as a function of time, exemplarily for the initially wettable samples from Buch, B2, for the three experiment types at 5°C. In experiment I and II the drop volume decreases linearly with a rate *k.* and can be described as:

$$V(t) = V_0 - k\,t \qquad (3\text{-}5)$$

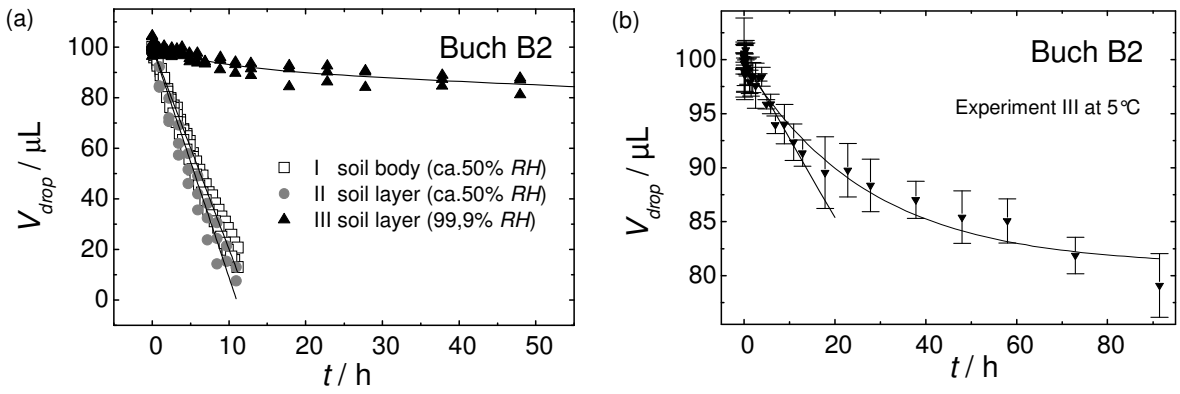

Figure 3-1 (a) Volume of sessile drops on the dried sample B2 at 5°C in different measurement conditions: I on soil body, at ca. 50% RH, II on a thin soil layer, at ca. 50% RH and III on a thin soil layer, at >99,9% RH, (b) Curve III: Figure 3-1 (a) in a smaller scale with deviation range and exponential and initial linear fitting curve

In experiment I, the drops on sample T2 infiltrated too fast to monitor the volume decrease at all temperatures. In contrast to the two first experiments the volume decrease is distinctly slower in experiment III and shows a different curve shape. In the first 10 – 120 min the drop volume decays fast and evolves to a slow decrease in the further course. Therefore, a different function is required for the mathematical description. However, the volume data reveal remarkable scattering, because small errors in drop height fitting have a cubed effect on the volume (Equation (3-5)). Testing even simple kinetic models (zero order and first order models) showed that the data quality did not allow choosing a definite function (see Figure 3-1 b).

As a model independent way to obtain kinetic data, we used linear approximations for the initial volume decrease (see Figure 3-1 b), and used the slope to calculate the activation energy of the intitial fast decrease.

Table 3-2 Means of linear rate of apparent volume decrease, *k*, during observation of sessile drops on all samples at all temperatures in different measurement conditions: I on soil body, at ca. 50% *RH*, II on a thin soil layer, at ca. 50% *RH* and III on a thin soil layer, at >99,9% *RH* (standard errors of fitting in brackets)

	Buch	initially water repellent B1			initially wettable B2		
Experiment	k / µL h^{-1}	5°C	20°C	30°C	5°C	20°C	30°C
I	Linear rate	8.0 (0.1)	20.7 (0.6)	48 (1)	8.5 (0.1)	20.3 (0.6)	49.2 (0.7)
II	Linear rate	9.1 (0.2)	17.2 (0.4)	53 (1)	8.8 (0.2)	17.7 (0.8)	43.3 (0.4)
III	Initial rate	0.37 (0.02)	0.6 (0.3)	26 (14)	0.64 (0.22)	6.9 (2.3)	30 (5)
	Tiergarten	initially water repellent T1			initially wettable T2		
Experiment	k / µL h^{-1}	5°C	20°C	30°C	5°C	20°C	30°C
I	Linear rate	8.2 (0.1)	10.8 (0.2)	39.6 (0.5)	6800 (1300)	1620 (150)	/ *
III	Initial rate	5.2 (3.3)	15.9 (0.3)	3.1 (2.2)	13 (8)	35 (14)	51 (4)

In Table 3-2 , the rate constants of volume decrease for all samples and temperatures are listed for the three experiment types. The linear rate *k* increases with increasing temperature and is comparable between experiment I and II. This is the first indication

suggesting comparable mechanisms responsible for drop volume reduction on a soil body and on the thin soil layer. On the samples from Tiergarten, the drop volume decreases slower on the initially repellent sample T1 than on the initially wettable sample T2, whereas the rate constants of volume decrease are comparable for the initial wettable and repellent samples from Buch.

Table 3-3 shows the activation energy E_A of the drop volume decrease calculated from the temperature dependence of k according to Equation (2-30). In experiment I and II, E_A of the linear volume decrease ranges for all investigated samples between 40 and 50 kJ mol^{-1}, whereas in experiment III, E_A of volume decrease is higher for the samples from Buch with 86-120 kJ mol^{-1} than for the samples from Tiergarten. with -14 - 44 kJ mol^{-1}. The negative E_A of the repellent sample from Tiergarten makes no physical sense and in view of the large error it has to be interpreted as close to zero.

Table 3-3 Activation energy, E_A, of the apparent decrease of drop volume during the spreading under 3 different conditions on the initially repellent samples B1 and T1 and the initially wettable samples B2 and T2 from Buch (B) and Tiergarten (T), (standard errors of fitting in brackets; n.d. - not determined; a - Infiltration was too fast to monitor.)

Experiment	E_A / kJ mol-1	B1	B2	T1	T2
I	linear decrease	48 (1)	49 (1)	41 (1)	/*
II	linear decrease	43 (1)	47 (1)	n.d.	n.d.
III	Initial rate	120 (36)	86 (12)	-14 (24)	44 (11)

The comparability of k in experiments I and II (Table 3-2) leads to the conclusion, that the infiltration of drop water into the soil body is improbable for the repellent samples, and evaporation of the drop water is probably the main process observed in experiments I and II. This assumption is further supported by the activation energy (Table 3-3), which is comparable to the latent heat of evaporation of water of 40.5 kJ mol-1 (Franks, 2000). As expected, in experiment III, evaporation was drastically reduced due to high relative humidity (99.9 %) and a different curve shape of the volume decrease as a function of time was observed (Figure 3-1). The observed influence of evaporation on sessile drops leads to a critical view on *WDPT* measurement. The comparison of high *WDPT* has to be regarded carefully. If the measurement conditions like air movement, *RH* and temperature as well as drop size are not standardised and evaporation cannot be prevented, penetration time might be comparable or higher and, thus, not distinguishable from evaporation time.

In order to minimize the effect of evaporation based volume decrease on shape and contact angle of a sessile drop, we conducted the further studies only under the condition of the experiment III at 99.9 % *RH*. In experiment III, the volume decrease starts with a faster decay (Figure 3-1 a) with an activation energy obtained by linear rate constants significantly higher than the latent heat of evaporation (Table 3-3) This leads to the conclusion that the observed fast initial volume decrease during the experiment III can not be caused by evaporation. Consequently, the volume decrease can only be explained by a transition of the water-solid contact area of the drops from the Cassie-Baxter state into the Wenzel's state driven by a continuous change in Θ_Y, as described in paragraph

2.3 and Figure 2-5. While the air filled gaps beneath the drop are step by step filled by the drop water, and the fitted water-soil contact line remains constant in the course of wetting, the volume necessary to fill the gaps, reduces the observed drop volume above the fitted contact line.

3.4.2 Apparent Work of adhesion

Figure 3-2 shows the development of the apparent work of adhesion, $W_{app}(\Theta_{app})$, between sessile drop and soil surface as a function of the contact time according to Equation°(2-15). After a fast initial increase, W_{app} grows slower and approaches asymptotically a final value, W_{app}^{∞}, between 120 and 150 mN m^{-1}. The W_{app}–time curves, obtained from the two sample sites, vary remarkably in their shapes. The curves obtained from the samples from Tiergarten (T1, T2) are more strongly curved and approach their final value earlier than those from Buch (B1, B2). While for the samples from Buch, the effect of temperature on the curve shape was more strongly, in the samples from Tiergarten, the effect of the initial water repellency on curve shape exceed the temperature effect.

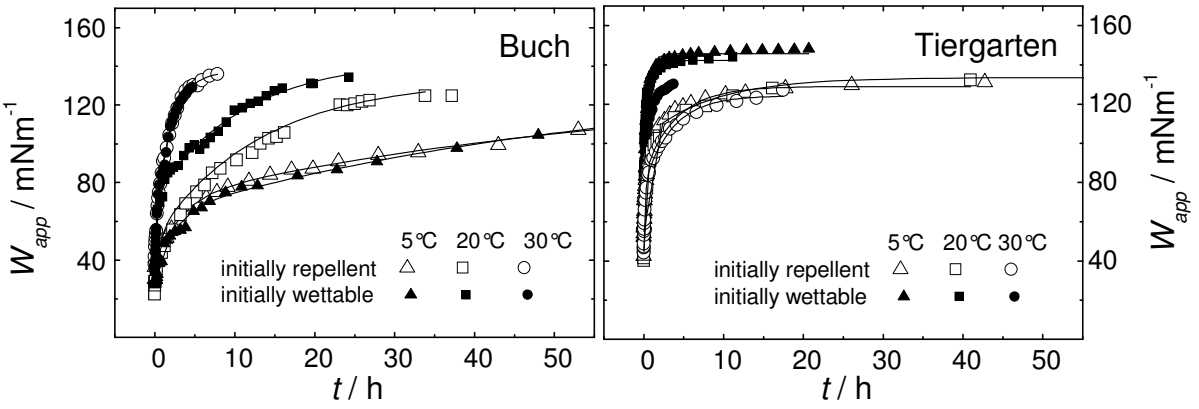

Figure 3-2 Apparent work of adhesion, W_{app}, according to Eq 3 as a function of contact time of one representative sessile drop on all investigated samples at 5°C, 20°C and 30°C and the respective double exponential fitting curves (standard deviation ± 5 mN m^{-1})

In order to describe the time dependence of W_{app}, fittings of first- and second-order kinetics as well as varying combinations of exponential and linear functions were tested. Simple first- or second order kinetics does not adequately describe the change in W_{adh}. The best description was achieved by a sum of two exponential decays with the following equation:

$$W_{app} = W_{app}^{0} + B_1(1-e^{-k_1 t}) + B_2(1-e^{-k_2 t}), \qquad (3\text{-}6)$$

where W_{app}^{0} is the initial work of adhesion for $t = 0$, B1 and B2 are the weightings of the subprocesses at the whole process, and k_1 and k_2 are the rate constants of the respective subprocesses. This would imply the occurrence of two independent processes. As, however, our current state of knowledge does not allow the development of a mechanistic model of wetting, we additionally applied the model independent evaluation by linear approximation as described for the volume data analysis.

Table 3-4 Parameters of double exponential fitting according to Eq 19 and of linear fitting of the initial increase for W_{app} as a function of time in course of wetting of sessile drops on all investigated samples at all temperatures, (standard errors of fitting in brackets)

		double exponential					linear	
Buch		W_{app}^{0}	B_1	k_1	B_2	k_2	W_{app}^{0}	k
		(mN m^{-1})		(h^{-1})		(h^{-1})	(mN m^{-1})	(mN m^{-1} h^{-1})
initially	5°C	41 (1)	25 (3)	0.32 (0.09)	64 (3)	0.02 (0.003)	42 (5)	7.7 (1.0)
repellent	20°C	32 (1)	20 (3)	2.2 (1.2)	78 (3)	0.08 (0.01)	34 (6)	19 (4)
sample B1	30°C	37 (1)	28 (4)	3.4 (0.7)	72 (3)	0.47 (0.05)	38 (3)	84 (22)
initially	5°C	31 (0.4)	38 (2)	0.36 (0.03)	68 (4)	0.02 (0.003)	33 (2)	8.9 (0,7)
wettable	20°C	36 (2)	34 (3)	2.9 (0.7)	70 (3)	0.12 (0.01)	42 (2)	33 (1)
sample B2	30°C	38 (1)	19 (5)	4.9 (1.8)	83 (3)	0.50 (0.1)	40 (6)	86 (17)
		double exponential					linear	
Tiergarten		W_{app}^{0}	B_1	k_1	B_2	k_2	W_{app}^{0}	k
		(mN m^{-1})		(h^{-1})		(h^{-1})	(mN m^{-1})	(mN m^{-1} h^{-1})
initially	5°C	49 (1)	48 (2)	1.9 (0.2)	31 (2)	0.08 (0.02)	53 (6)	45 (4)
repellent	20°C	41 (1)	32 (2)	5.4 (0.7)	48 (2)	0.24 (0.03)	46 (5)	58 (13)
sample T1	30°C	46 (1)	33 (2)	8.6 (1.4)	46 (2)	0.43 (0.05)	52 (4)	92 (3)
initially	5°C	59 (2)	47 (3)	12 (2)	39 (3)	1.1 (0.1)	70 (1)	166 (14)
wettable	20°C	58 (2)	50 (2)	13 (1)	33 (2)	1.1 (0.1)	71 (9)	213 (42)
sample T2	30°C	57 (1)	34 (2)	23 (3)	40 (2)	1.4 (0.1)	62 (5)	319 (25)

Table 3-4 shows the results of the double exponential and the initial linear fitting for all samples and temperatures. Although different ways of evaluation, the respective parameter show comparable relations between the samples, which are: W_{app}^{0} for the samples from Buch (30 -40 mN m^{-1}) is lower than for the samples from Tiergarten (40 - 70 mN m^{-1}). While W_{app}^{0} of all samples from Buch are within the same range, those from Tiergarten differ significantly between the initially repellent (41 - 53 mN m^{-1}) and the initially wettable samples (57 - 70 mN m^{-1}).

The rate constants of the change of the observed W_{app} on the samples from Buch are more strongly affected by the temperature than those of the samples from Tiergarten. On the other hand, the differences between the rate constants of the initially repellent and those of the related initially wettable samples are lower for the samples from Buch than for the samples from Tiergarten.

As shown in Figure 2-5, without exact information about the roughness and the gravity influence on the contact angle, the change of the observed W_{app} cannot unambiguously and directly be related with the change of the surface characteristics of the soil. But, under the assumption that the temperature influence on the roughness and gravity effect is either negligible or comparable at least within the sample pairs of each location, the temperature dependence of the rate constants derived from Θ_{app} is expected to be comparable to that derived from Θ_Y.

In Table 3-5 the activation energy, E_A, calculated by the temperature dependence of the exponential rate constants k_1 and k_2 (Equation (2-30)) is compared with E_A obtained by initial linear rates. The E_A of the double exponential approximation shows comparable values of both processes at both samples from Buch with 65 - 95 kJ mol^{-1} and distinctly smaller values at the samples from Tiergarten with 42 kJ mol^{-1} at the repellent sample T1 and 8 - 20 kJ mol^{-1} at the wettable sample T2. With the linear approximation, differences in *EA* between the sample sites could be confirmed with 63 - 64 kJ mol^{-1} at Buch and 18 - 19 kJ mol^{-1} at Tiergarten. But the linear approximation does not confirm the differences in E_A between the repellent and the wettable samples from Tiergarten.

Table 3-5 Activation energy, E_A, obtained by double exponential and initial linear fitting of wetting by sessile drops on all investigated samples, (standard errors of fitting in brackets)

E_A / kJ mol^{-1}	B1	B2	T1	T2
double exponential	65 (5)	85 (7)	42 (7)	20 (10)
	89 (8)	94 (6)	42 (10)	8 (6)
linear	64 (8)	63 (3)	19 (4)	18 (4)

The change of W_{app} in sessile drop consists of a fast initial and a slow final increase, which is associated with a respective fast initial and slow final apparent drop volume decrease. The E_A values (Table 3-3) show that the volume decrease can not be solely based on evaporation on the Buch samples. Muster and Prestidge (2002) recorded comparable time dependent sessile drop contact angle- and drop volume-curves on unsaturated compressed sulfathiazole powder in a time scale of up to 120 s. They suggested an influence of volume loss by imbibitions on the observable contact angle as a result of changing advancing into receding contact angle. These physical effects will probably occur in our measurements, but, in the case of the samples from Buch, the E_A shows, that they cannot be the rate limiting steps. We currently assume that the change in drop shape is controlled by a complex interplay between sinking and spreading. Detailed elucidation of the mechanism, however, requires additional targeted studies.

In the samples from Buch, the rate limiting step of apparent volume decrease as well as for W_{app} increase (Table 3-5) is in the range of chemical reactions indicating chemical changes of the solid surface characteristics. This is in good accordance to the results of Todoruk and co-workers(Todoruk *et al.*, 2003b). Because they found activation energy of > 80 kJ mol^{-1} for slow water distribution processes in repellent soils, Todoruk and co-workers (2003b) proposed hydrolysis of ester linkages formed between –COOH and -OH groups during drying as a possible reaction. They also suggested more generally, that by air drying, hydrophilic functional groups of the SOM may maximize non bounded van der Waals interactions, internal hydrogen bonds and charge transfer interactions, as water is lost. Re-wetting then would require a cooperative re-organisation to restore the hydrophilic groups to water binding (Todoruk *et al.*, 2003b). As hydrolysis of the biopolyester Poly-R-3-hydroxybutyrate, synthesised and accumulated in many bacteria as carbon storage, requires an activation energy of 82 kJ mol^{-1}(Chen & Yu, 2005), we found further evidences for the suggestion of Todoruk and co-workers that hydrolysis of ester

linkages may explain the high activation energy of the wetting process of the Buch samples.

On the other hand, the E_A values of apparent drop volume decrease and W_{app} increase of the samples from Tiergarten (Table 3-3 and Table 3-5) are distinctly lower than those from Buch and indicate physical or physico-chemical processes as rate limiting steps like diffusion and water film formation or conformational changes in molecules.

The processes occurring on the repellent sample from Tiergarten differ strongly from those proceeding on the samples from Buch. We therefore conclude that the repellency of the sample from Tiergarten has other origins than those from Buch. The samples from Buch have higher organic content, their wettability seems to depend mainly on water content (the wettable sample became repellent by drying), and wetting is controlled by chemical reactions. In contrast, the samples from Tiergarten with lower organic content kept their difference in wettability after air-drying, and even the repellent samples require a distinctly lower activation energy for re-wetting than the samples from Buch. Further, the repellent samples from Tiergarten did not reach the W_{app} values of the corresponding wettable sample within the observation time of our experiment. In another study, we found *pH*-dependence of the *WDPT* for Tiergarten, but not for Buch (Hurraß & Schaumann, 2006; Bayer & Schaumann, 2007). The maximum of repellency around neutral *pH* found in the study of Bayer and Schaumann (2007) may be indicative for acid/base catalysed ester hydrolysis reducing repellency at *pH* below 4 and above 8, but only for Tiergarten samples. This may indicate that the chemical energy barrier to overcome repellency at the sample from Tiergarten was not reached under the gentle conditions of our experiment, but needs to be catalysed. In the absence of chemical modification of organic soil surface, the rate limiting step of wetting is then only diffusion and water film formation. In contrast, the organic matter of the samples from Buch may undergo quasi-reversible hydrolysis-condensation reactions according to the loss or supply of water. The hypothesis of ester hydrolysis is currently being validated by spectroscopic methods (^{1}H-NMR and FT-IR).

Figure 3-3 shows the conceptual model we suggest to explain the different drying and re-wetting behaviour of the investigated samples. According to the suggestion of Bayer and Schaumann (2007), wettability is controlled by two independent parameters, which are the surface characteristics and the water coverage. Both parameters may change in the course of drying and re-wetting. While water coverage changes in Buch and in Tiergarten, we suggest that surface characteristics change predominantly in the Buch samples. Here, the water loss due to drying is compensated by an increase of H-bonds and probably ester linkages of the hydrophilic functional groups towards the interior, which results in a lower number of hydrophilic molecule domains orientated outwards. Re-wetting requires high activation energy for the disruption of these linkages followed by an outward re-orientation, which enhances wettability.

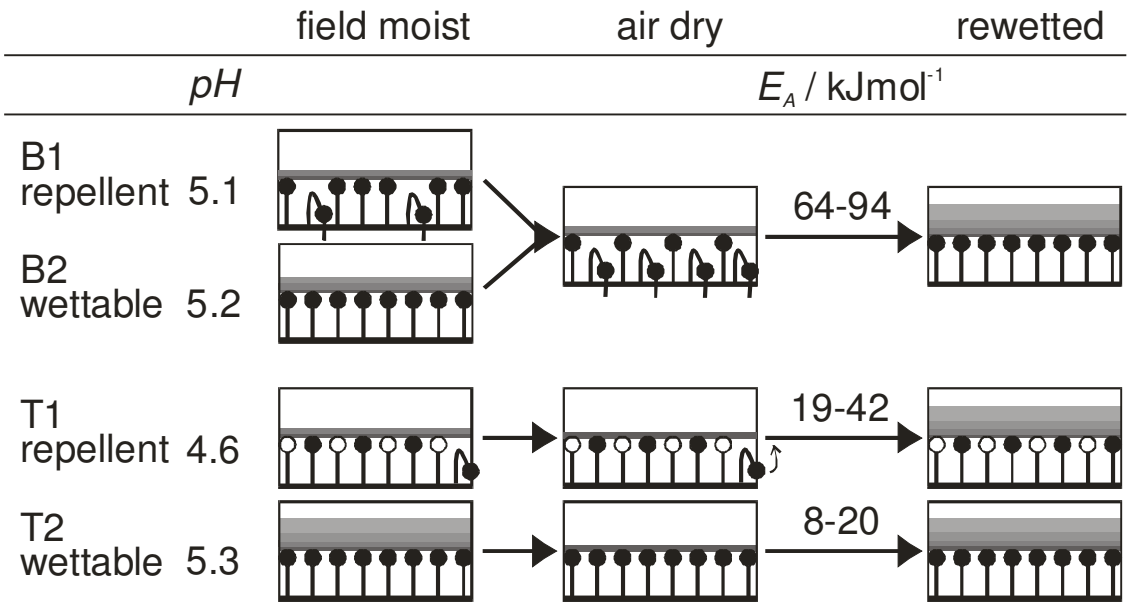

Figure 3-3 A model visualising different re-wetting behaviour of the investigated samples. *Buch*: Hydrophilic functional groups (black circles) are linked chemically towards the interior of SOM in the air-dried sample. Re-wetting requires high activation energy, E_A, to disrupt linkages. Tiergarten: Surface characteristics do change only slightly during drying and re-wetting. Probably, *pH*-differences result in differing percentage of charged functional groups (uncharged groups as white circles) and persist drying and re-wetting. Re-wetting requires medium E_A at repellent samples for conformational re-orientation of some hydrophilic functional groups (physico-chemical process) and low E_A at wettable samples for changes in water coverage (physical process).

In contrast, the surface characteristics of the Tiergarten samples do not change during drying and re-wetting. They differ between repellent and wettable samples, probably due to differences in *pH*, which may result in differing percentage of charged functional groups as suggested by Hurrass and Schaumann (2006) and Bayer and Schaumann (2007) and/or of ester linkages. These differences persist throughout our experiments, and changes of wettability are mainly caused by changes in water coverage, which are of physical nature and therefore require lower activation energy. The differences in activation energy between the repellent and the wettable Tiergarten sample (only found with a double exponential fitting), may be due to an additional conformational re-orientation of a part of the hydrophilic functional groups.

3.5 Conclusions

The comparison of change of sessile drop volume in three different experimental designs tested in this study, lead to the conclusion, that measurement conditions like air movement, *RH* and temperature as well as drop size, strongly affect the value of *WDPT*. At high *WDPT,* it has to be considered, that evaporation may overbalance penetration.

Under the assumption that the temperature dependence of gravity and roughness influence on the sessile drop shape does not affect the temperature dependence of the rate constants of wetting, the activation energy can be related to the change of the respective surface characteristics.

We found principal differences in the nature of water repellency between the two investigated locations Buch and Tiergarten: The samples from Buch, which differed significantly in wettability in the field moist state, lost their differences in wettability upon air drying and storage in 31 - 35 % *RH*. The wetting of these samples required activation energy of 63 - 94 kJ mol^{-1}, which indicates that chemical reactions are the rate limiting step. In contrast to the samples from Buch, the samples from the inner city park Tiergarten kept their initial differences in wettability after drying and storage and re-wetting required activation energy between 19 and 42 kJ mol^{-1} for the repellent samples and 8-20 kJ mol^{-1} for the wettable samples. This indicates that physico-chemical reactions like conformational changes in molecule structures or physical processes like diffusion and water film formation represent the rate limiting step for the samples from Tiergarten.

Our study showed for the first time that the process of wetting on soil samples can be monitored by sessile drop assessment, and that the temperature dependence of the wetting kinetics allows distinguishing between different natures of wetting and soil water repellency. Combination of such approaches with spectroscopic investigations will help to deepen our understanding on possible causes of water repellency. They further help to understand the great variety of suggested causes of repellency and indicate locational and soil-material specific effects rather than one general cause for water repellency.

4 Influence of drying conditions on wettability and DRIFT spectroscopic C-H band of soil samples

4.1 Summary

This study assesses the effect of various drying procedures on water repellency measured by water drop penetration time (*WDPT*) and spectroscopic parameters gauged by Diffuse Reflectance Infrared Fourier Transform spectroscopy (DRIFT) of two anthropogenically-influenced soils at sites in Berlin. Wettable and water repellent samples were dried at various temperatures and at prescribed relative humidity. *WDPT* and DRIFT spectroscopic characteristics were obtained from both dried and field-moist subsamples.

Normalization of DRIFT spectral C-H band intensity ('surface hydrophobicity') against the integral absorption intensity over the wave number range 4000 – 400 cm^{-1} resulted in an apparent resolution between the effects of water content and changes in C-H absorption at the surface. To our current knowledge, the latter could be best explained with changes in the three-dimensional re-arrangement of organic molecules or moieties on inner and outer soil organic matter (SOM) surfaces, whereas the former could be a direct consequence of the fraction of inner and outer soil surfaces covered with water and of the mean thickness of the respective water films. Further evidences for this model are required from other investigations focusing on the surfaces in soil, before drawing final conclusions. The results show that the method of drying affects *WDPT* to a greater extent than soil water content after drying. DRIFT spectra suggest that exposure to high temperature results in some reorganisation of SOM in the outer layer. It is further suggested that short exposure may result in a heterogeneous distribution of water leading to localized variation and inconsistency in *WDPT*s. Drying for four weeks under controlled relative humidity at 20°C is suggested as a reference preparation method combining the benefits of an almost unchanged SOM surface compared with field moist samples with homogeneous moisture distribution.

4.2 Introduction

Soil water repellency is a world-wide phenomenon with a large impact on plant growth, transport of nutrients and contaminants through the soil and thereby on soil function(Doerr *et al.*, 2000). Occurrence of soil water repellency is often linked with increasing dryness of soil(Doerr & Thomas, 2000). Dekker & Ritsema (1994) defined actual and potential soil water repellency determined in field-moist and dried samples, respectively, and concluded that below a critical water content, soil tends to become repellent. Ziogas et al (2003) showed that oven-drying might render samples fully wettable. Other studies investigating soil water repellency as a function of water content upon drying found one, sometimes even two repellency maxima, especially at intermediate to small water contents between air-dried states and wilting points (King,

1981; Bayer & Schaumann, 2007). Equilibration of soils at high relative humidity resulted in an increase of repellency (Hurraß & Schaumann, 2006; Wallach & Graber, 2007). As changes in repellency are not fully reversible after rewetting (Doerr & Thomas, 2000; Bayer & Schaumann, 2007) water content seems to be an inadequate characteristic to predict soil water repellency. Soil texture (de Jonge *et al.*, 1999) and soil organic matter (*SOM*) as well as additional factors such as drying duration and temperature (Bayer & Schaumann, 2007) together with equilibration time (Hurraß & Schaumann, 2006; Wallach & Graber, 2007) influence changes in soil water repellency.

Organic coatings on mineral particles or particulate organic material are considered to be responsible for water repellency (van't Woudt, 1959; DeBano, 1969; Fink, 1970). Numerous investigations indicate that soil water repellency is not caused by single substances (McGhie & Posner, 1980; Ma'shum & Farmer, 1985), whereas the amount of polar and non-polar functional groups in amphiphilic organic substances appear to be of great importance (Horne & McIntosh, 2000; Doerr *et al.*, 2006).

Infrared spectroscopy (IR) is commonly used to measure the abundance of functional groups in organic molecules. Infrared measurements of acid washed sand coated with soil lipids showed a good correlation between lipid concentration, aliphatic C-H absorption intensity and water repellency (Ma'shum *et al.*, 1988). Capriel et al. (1995) defined the aliphatic *CH / SOC* (soil organic carbon content) ratio as an index of hydrophobicity of soil organic matter. In contrast, other studies of natural soil samples found no correlation between spectroscopic values and their water repellency (Doerr *et al.*, 2005b; Hurraß & Schaumann, 2006). Correlations were obtained when spectroscopic data was combined with clay and/or SOC content (McKissock *et al.*, 2003; Ellerbrock *et al.*, 2005). This led to the conclusion that the extent of surface coverage and thickness of the organic layer on soil mineral particles control the effective water repellency of functional groups in SOM (Ellerbrock *et al.*, 2005). These observations are in accordance with the concept of three-dimensional re-arrangement of molecules, in whole or in part, in the outer layer of the organic coatings as suggested by several authors as a mechanism leading to different wetting characteristics (Tschapek, 1984; Horne & McIntosh, 2000; Hurraß & Schaumann, 2006). According to this concept, hydrophilic functional groups exposed to the outside increase wettability, whereas outward directed hydrophobic aliphatic chains increase water repellency.

In contrast to the transmission Fourrier Transformed IR technique, DRIFT spectroscopy provides information about the outer 6 – 8 µm layer of a sample, penetrated by the incident light (Gottwald & Wachter, 1997) and suggests that it has potential for the investigation of soil water repellency. It has to be kept in mind that soil water repellency gives information mainly about the outer surfaces of soil particles whereas DRIFT, within the penetration depth, senses both the outer and inner surfaces of SOM as well as water. Therefore, a suitable method for normalization of DRIFT spectroscopic data is required. Normalization against *SOC* (Capriel, 1997) refers to bulk SOM and so dilutes the signal from the SOM on the surface. The absorption band at 1081 cm^{-1} used by Ellerbrock *et al.* (1999) in transmission IR is not detectable in our DRIFT spectra, the C-O stretching absorption at 1720 cm^{-1} and 1620-1600 cm^{-1}, also used by Ellerbrock in

transmission IR (Ellerbrock *et al.*, 2005), cannot be distinguished from mineral absorption in DRIFT spectra of undiluted soil material. Therefore, normalization by various other references was tested in the present study in order to resolve the non-specific effect of water content.

The objective of our study was to verify the extent to which changes in water repellency are (i) related to changes in the relative abundance of hydrophobic molecular parts in the outer layer of soil organic matter and (ii) caused solely by changes in water content. In this paper we present the relationship between the relative abundance of hydrophobic moieties in the surface layers of soil, assessed using DRIFT, the *WDPT* water repellency and reduction in water content resulting from various drying regimes for both, wettable and water repellent soil.

4.3 Materials and methods

4.3.1 Sample Sites

Soil samples were obtained from two strongly anthropogenically-influenced sites, a former sewage disposal field north east of Berlin (Buch) and a city park in Berlin (Tiergarten). The sample area is homogeneously covered with couch grass (mainly *Elytrigia repens*) at Buch and with a grass cover consisting of *Festuca rubra rubra*, *Lonium Perenne* and *Poa pratensis* at the Tiergarten. At both sites, the topsoil consists of medium sized sand with low clay content and is characterized by large *SOM* contents (Schlenther, 1996; Hoffmann, 2002; Täumer *et al.*, 2005; Diehl & Schaumann, 2007).

Sampling took place in spring after a rainy day following a long dry period. The grass cover was removed in an area of approximately 1 m^2. Samples were taken at a depth of 10 - 20 cm, directly beneath the dense root network, from clearly separate dry and wet patches of soil as reported and shown by Hurraß & Schaumann (2006). At both sites, the dry patches were much smaller than the wet patches, so at each site only two repellent samples were taken from two separate dry patches. Eight samples were taken from the wet patches at Buch and four wet patch samples were taken at the Tiergarten. The wet and dry patch samples differ widely in their degree of repellency, but soil characteristics such as texture and organic content were comparable (Table 4-1). Consequently, these 16 individual samples are classified in the following four groups as follows: the wettable samples from Buch and from the Tiergarten are referred to as BW (n = 8) and TW (n = 4), respectively, and the repellent samples from Buch and Tiergarten as BR (n = 2) and TR (n = 2), respectively.

Earlier studies on soils from the specific locations used in the present study showed (i) “a strong relation between the actual water repellency (which triggers the preferential flow process on the site) and the water content” (Täumer *et al.*, 2005; Taumer *et al.*, 2006) and (ii) significant differences in repellency between moist and dry samples chosen in the same way as in our study (Hurraß & Schaumann, 2006). This clearly showed that the actual repellency controlled the water content after rainfall. Differences in the water

supply caused by differences in plant canopy are minimal because of the uniform plant coverage in the sampling area.

Table 4-1 Number (*n*) of individual samples, water content (*WC*), soil organic matter content (*SOM*), *pH* and water drop penetration time (*WDPT*) of field moist wettable samples (BW) and repellent samples (BR) from Buch and from the Tiergarten (TW, TR, respectively). Estimates of errors, *WC* ± 15% and of *SOM*, *pH* and *WDPT* (from triplicate measurements) are shown in parentheses.

	n	*WC* / %	*SOM* / %	*pH*	*WDPT* / min
BW	8	15 (3)	10 (2)	4.5 (0.3)	0.01 (0.02)
BR	2	10 (1)	11 (1)	4.6 (0.1)	300 (200)
TW	4	14 (2)	7 (2)	3.9 (0.1)	0.05 (0.04)
TR	2	9 (1)	9 (1)	3.9 (0.1)	700 (400)

4.3.2 Sample preparation and characterization

Prior to homogenizing field moist samples, large stones and root material were removed and large aggregates disrupted. Sample *pH* was measured using 12 g portions in 25 ml 0.01 M $CaCl_2$-solution (DIN ISO 10390). The water content (*WC*), was determined gravimetrically by drying samples for 24 hours at 105°C (DIN ISO 11465) and is expressed on a dry basis. The dried material is defined as having a *WC* of zero. The *SOM* was assessed by ashing the < 2 mm fraction of dried material for five hours at 550°C (DIN 18128).

Each of the 16 samples was separated into five subsamples that were subjected to one of the following treatments: (i) airtight storage at 5°C (“moist”), (ii) drying for seven days at 35°C (“35°C), (iii) drying for three days at 65°C (“65°C”), (iv) air-drying (open to atmosphere at approximately 20°C / ~50% *RH*) for two days and subsequent storage for > 28 days at 20°C / 31% *RH* over saturated $CaCl_2$-solution (“31% *RH*”) and (v) oven-drying for 24 hours at 105°C, (”105°C”).

For the subsequent *WC* measurement of the treated subsamples, we took a maximum relative error of 15% (based on numerous preceding *WC* measurements from these two specific locations) into consideration, which is more realistic than the standard error between replicates of the small and random subsample groups. The 80 subsamples were then sieved to < 1 mm in order to reduce soil heterogeneity and stored in airtight glass flasks.

4.3.3 Measurement of soil water repellency

The resistance to wetting of the 80 subsamples of soil was determined using the water drop penetration time (*WDPT*) (Letey, 1969). Soil was placed in small containers and the surface was gently smoothed. They were then placed in an incubator at 20°C. Digital micrographs of the water droplets were taken automatically at increasing intervals from 12 s to 10 minutes. *WDPT*s were determined to within ± 5% by inspection of the

micrographs (Diehl & Schaumann, 2007). A minimum *WDPT* of 0.1 s was used to provide a finite value for log(*WDPT*) for readily-wettable soil.

4.3.4 DRIFT spectra

DRIFT spectra were obtained with a BioRad® FTS 135 (Bio-Rad Corp., Hercules, CA) over a wave number range of 4000 to 400 cm-1 with 16 scans for each replicate at a resolution of 1 cm^{-1}. Soil material (< 1 mm) was used without any further preparation in order to maintain the integrity of both *SOM* and *WC*. The consequent heterogeneous particle size distribution and large sample concentration have an adverse effect on DRIFT spectra. This does not allow absolute quantitative analysis or direct comparison with pressed KBr disc spectra (Nguyen *et al.*, 1991; Tremblay & Gagne, 2002), but still permits relative comparison between subsamples with comparable composition and characteristics drawn from the same location.

Dried, finely ground KBr was used to obtain a background reference spectrum. Spectra were of five drying treatments with reference spectra obtained within each batch of three replicates. Because of technical problems, for four of the eight BW samples and one of the four TW samples, DRIFT spectra could not be obtained with the 35°C and at 65°C treatments. In order to subtract the background including absorption by water vapour and CO_2 in the sample environment, the 210 single spectral data were automatically corrected for background and transformed into Kubelka-Munk (K.-M.) units after measurement using Bio-Rad® Win IR Foundation® software (Digilab, Randolph, MA). Smoothing, baseline correction, identification of peaks and evaluation of peak heights and peak areas were performed using Origin 7.5 SR6 (v7.5885-B885) software (OriginLab Corp., Northampton, MA). Linear baselines were created from minima of the spectra in the regions of 3800 and 480 cm^{-1}.

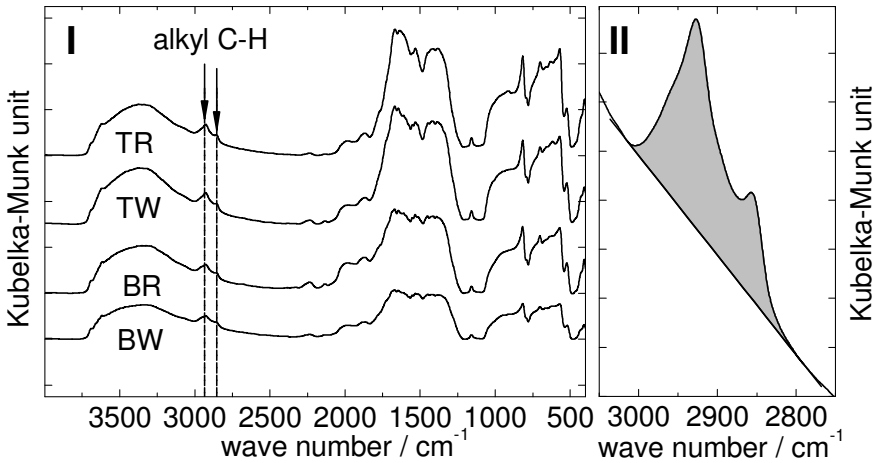

Figure 4-1 (I) DRIFT spectra of initially wettable Buch samples (BW) and repellent Buch samples (BR) and initially wettable Tiergarten samples (TW) and repellent Tiergarten samples (TR) dried at 105°C and (II) expanded spectral region showing peaks, associated with selected C-H bands and a typical baseline for evaluation of peak area.

The combined integral area under the peaks at 2930 and 2850 cm^{-1}, which were superimposed on a broad O-H band at 3800 – 2500 cm^{-1}, were calculated relative to a linear baseline under that band (See Figure 4-1– II) and denoted as *CH*. These peaks

represent the asymmetric and symmetric C-H-stretching vibrations of aliphatic CH_3 and CH_2 groups (Capriel *et al.*, 1995; Celi *et al.*, 1997; Ellerbrock & Kaiser, 2005). Furthermore, the integral area under the broad O-H band between 3800 and 2500 cm^{-1} and under the spectra between 4000 and 400 cm^{-1} were calculated and denoted as *OH* and *Ref*, respectively. As explained in detail in the Result section, a normalization of *CH* and *OH* areas was necessary and performed by dividing the respective areas by the *Ref* area, denoting the normalized values as CH_N and OH_N, respectively.

4.4 Results & discussion

4.4.1 Normalization of DRIFT spectra

DRIFT spectra typical of BW, BR, TW and TR samples dried at 105°C, show *CH* absorption bands at 2930 cm^{-1} and at 2850 cm^{-1} superimposed on the broad *OH* absorption band between 3800 and 2500 cm-1 (Figure 4-1 – I). The spectra possess two additional absorption bands located between 2000 cm^{-1} and 1200 cm^{-1}.

The *Ref* area showed no correlation with corresponding sample *SOM* (Table 4-2) but did show a weak correlation with the sample *WC* whereas the *OH* area did not correlate with *WC*; however the *CH* area did have a weak negative correlation with *WC* (Table 4-2). It is assumed that the expected, but not found, *SOM* effect on the *Ref* area and the specific *WC* effect on the *OH* area are outweighed by a broad non-specific interference and contribution to absorption over the entire reference band arising from the presence of water.

A significant correlation was found between OH_N and *WC*, indicating a specific effect of *WC* on the O-H band, whereas CH_N had no significant correlation with *WC* (Table 4-2). These correlations show that the use of normalized spectra provides information that reflects better the links between soil properties and the vibrational modes of the chemical constituents that they represent.

Table 4-2 Correlation coefficient (*R*), number (*n*), and probability of error (*P*) for the integral area under the DRIFT spectra from 4000 to 400 cm^{-1} (*Ref*) against soil organic matter (*SOM*) and water content (*WC*) and the areas under the *OH* and *CH* peaks against *WC* and, similarly, for the normalized peak areas OH_N and CH_N.

	Ref - SOM				*OH - WC*				*CH - WC*		
	R	*n*	*P*		*R*	*n*	*P*		*R*	*n*	*P*
BT	0.06	70	0.6115	BT	0.04	72	0.7575	BT	-0.40	72	0.0013
B	-0.05	42	0.7473	B	0.01	42	0.9294	B	-0.50	42	0.0020
T	0.22	28	0.2602	T	0.02	30	0.9069	T	-0.40	30	0.0405
	Ref - WC				OH_N *- WC*				CH_N *- WC*		
	R	*n*	*P*		*R*	*n*	*P*		*R*	*n*	*P*
BT	-0.50	70	<0.0001	BT	0.68	72	<0.0001	BT	0.09	72	0.4757
B	-0.49	42	0.0011	B	0.84	42	<0.0001	B	0.02	42	0.9236
T	-0.53	28	0.0039	T	0.62	30	0.0003	T	0.24	30	0.2067

4.4.2 Effect of drying

In Figure 4-2, *WC*, *WDPT* and CH_N are depicted as functions of the applied drying treatments where the connecting lines trace the data of each original sample and can help to indicate the variety of effects of drying procedure on *WC*, *WDPT* and CH_N in individual samples which were dried in parallel.

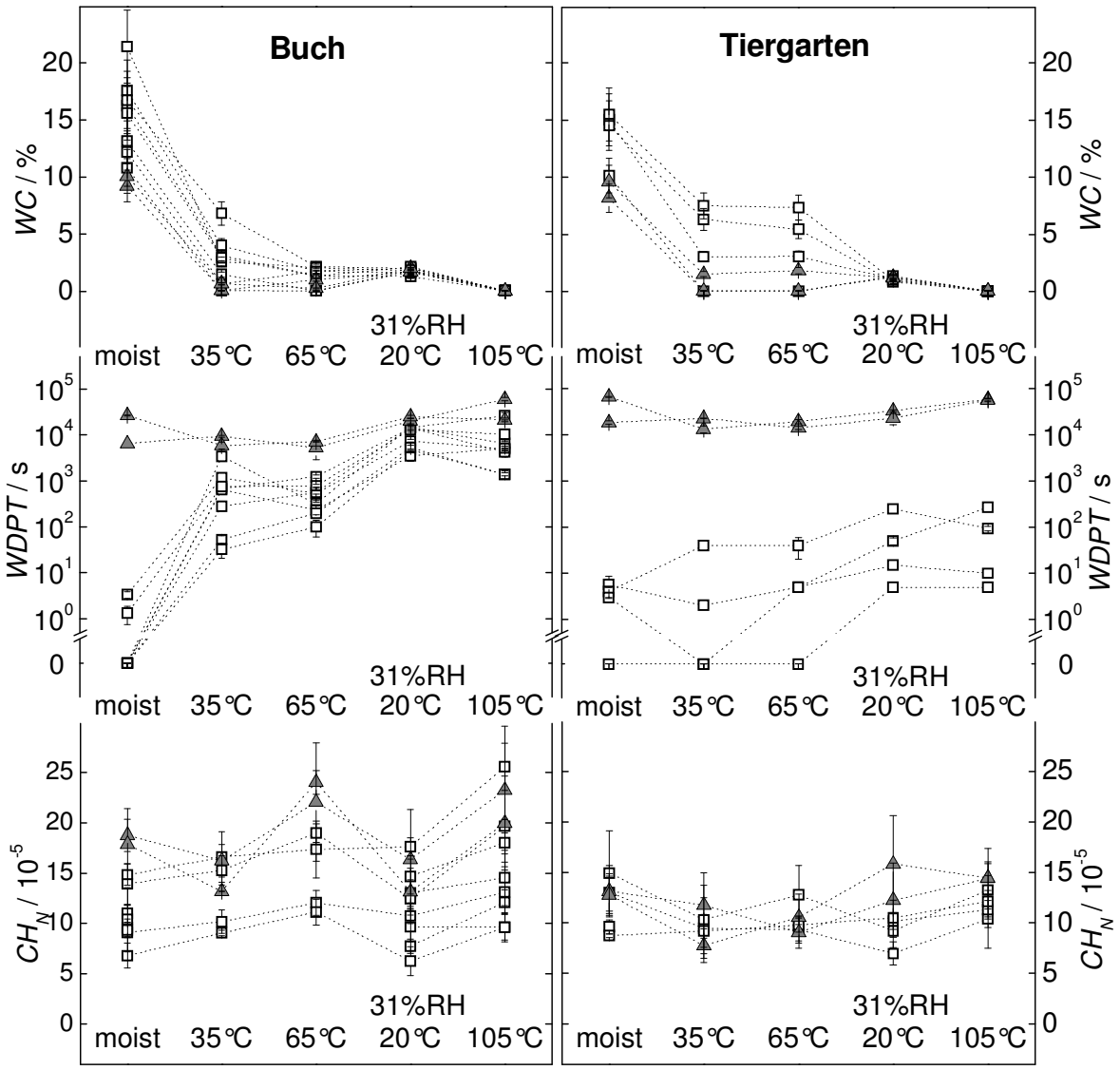

Figure 4-2 Effect of drying conditions on water drop penetration time (*WDPT*), water content (*WC*) and normalized C-H band intensity (CH_N) of initially wettable and repellent samples from Buch (BW □ and BR ▲) and the Tiergarten (TW □ and TR ▲, respectively) for field moist and dried samples. Lines connect the data points of subsamples drawn from the same soil sample. Error bars are *WC* ± 15% and estimates of the standard deviation from triplicate measurements of *WDPT* and DRIFT peak areas.

Buch field samples had a wider range of *WC* than those from Tiergarten (Figure 4-2, top). Drying at 35°C reduced *WC* in all samples with generally greater reductions in BR and TR than BW and TW. Drying at 65°C seemed to have the same effect as drying at 35°C on T samples, whereas the *WC*s of B samples were almost indistinguishable from each other. Drying at 20°C (31% *RH*) and at 105°C reduced the *WC* of all sample to similar values with the latter producing the smallest values.

*WDPT*s of BR samples were consistently long for field moist and virtually all the dried treatments (Figure 4-2, centre). Those values of BW samples, initially with short times in the field-moist treatment, increased significantly with drying, with the longest times associated with the 20°C (31 % *RH*) and 105°C procedures, although the former resulted in more tightly clustered values than the latter. *WDPT*s of TR samples were consistently in the range $104 < WDPT < 105$ s from the field-moist state and after all drying procedures. *WDPT*s of TW samples had a range of values from $0.1 < WDPT < 10^3$ s with the tightest clusters relative to the field- moist samples following drying at 20°C (31% *RH*) and 105°C and the widest ranges after drying at 35 and 65°C (Figure 4-2, centre). The drying treatments tended to lengthen the *WDPT*s of BW samples into the range of those of BR samples, but had only limited effect on those of TW which remained at least 100 times shorter then those of TR.

Table 4-3 Probabilities (P) in support of the alternative hypothesis (H_A) and rejection of the null hypothesis for normalized C-H peak areas (CH_N) obtained for sample pairs dried using two different procedures obtained from sample paired t-tests.

Alternative Hypothesis H_A	Buch (n = 18)	Tiergarten (n = 15)
CH_N (31% *RH* / 20°C) < CH_N (65°C)	0.001	0.550
CH_N (31% *RH* / 20°C) < CH_N (105°C)	<0.001	0.011
CH_N (35°C) < CH_N (65°C)	0.001	0.617
CH_N (35°C) < CH_N (105°C)	<0.001	0.005
CH_N (65°C) < CH_N (105°C)	0.583	0.001
CH_N (31% *RH* / 20°C) < CH_N (35°C)	0.575	0.384

The normalized peak areas for aliphatic carbon, CH_N, obtained from DRIFT spectra was in the range $4{\cdot}10^{-3} < CH_N < 12{\cdot}10^{-3}$ and $4{\cdot}10^{-3} < CH_N < 8{\cdot}10^{-3}$ for field moist B and T samples, respectively (Figure 4-2, bottom). Drying at 35°C caused a reduction in the range for B samples. The other treatments either maintained that range (20°C, 31% *RH*), moved it to $7{\cdot}10^{-3} < CH_N < 15{\cdot}10^{-3}$ (65°C) or moved and expanded it to $6{\cdot}10^{-3} < CH_N < 16{\cdot}10^{-3}$ (105°C). The values for BR samples were generally, but not consistently, greater than those of BW. Drying had a less marked effect on the range of CH_N values of the T samples, but values for TR samples were generally, but not consistently, greater than those of TW (Figure 4-2, bottom). In Buch samples, drying at 65°C and 105°C resulted in larger CH_N than drying at lower temperatures (paired sample t-test, Table 4-3).

Correlations between *WC* and *SOM* for sets of sub-samples involved in drying procedures (n = 16) were only significantly positive ($R = 0.81$; $P = 0.0002$) after long exposure to 20°C at 31% *RH*. The only other sets with a reasonable range of *WC*s (dried at 65 and 35°C) showed either a small negative or no correlation ($R = -0.54$; $P = 0.03$ and $R = -0.30$; $P = 0.25$, respectively).

4.4.3 Evaluation of the effects of drying

The smaller CH_N in Buch samples after drying at 31% *RH* at 20°C and at 35°C suggests a smaller surface concentration of hydrophobic structural elements than after drying at greater temperatures. This does not explain the larger *WDPT* after drying at 31% *RH* for more than four weeks, irrespectively of whether *WC*s were the same, smaller or larger than after drying at 35°C and 65°C for seven and three days, respectively.

The greater scatter of *WC* data of the latter drying treatments indicates that drying for seven and three days were not sufficient to overwhelm the differences in moisture content between individual samples. In contrast, the protracted drying at 31% *RH* at 20°C resulted in *WC*s which were in a narrow range for all samples from each site and which significantly correlate with *SOM*. It is likely that this drying procedure allows the samples to equilibrate better with the imposed conditions because of the longer period and the constant *RH*. The question remains as to whether this could be the cause for the increased extent of repellency.

Similar phenomena were observed in previous studies which observed changes in repellence during a protracted exposure to a particular drying regime (Bayer & Schaumann, 2007) or re-moistening regime (King, 1981; Wallach & Graber, 2007). The changes in repellence continued unexpectedly even after the *WC*s reached constant values. This suggests that a redistribution of soil moisture within the porous *SOM* structure may alter its surface characteristics and leads to changes in repellency. The equilibration at a constant *RH* and thereby the moisture redistribution without changes in *WC* may lead to (i) a more homogeneous moisture distribution with an increase in the area covered with water and a decrease in the mean thickness of the water cover or (ii) a more heterogeneous moisture distribution with a decrease in the area covered with water and an increase in the mean thickness of water cover. In this case local moist micro-spots or even micro-droplets would be concentrated on hydrophilic regions whereas hydrophobic regions would be water-depleted. The latter case does not explain the effect of drying at 31% *RH* at 20°C in Buch samples since because larger *WDPT*s after this treatment are coincident with smaller CH_N than after treatments at 65°C. It is therefore more likely that drying at 31% *RH* at 20°C leads to a more homogeneous moisture distribution with a smaller amount of water-depleted hydrophobic regions explaining the lower CH_N and a thinner water film.

The Frumkin-Derjaguin theory (Derjaguin & Churaev, 1986) explains the reduced wettability of a thin film with a bulk liquid of the same liquid. Below a certain thickness of water layers, interphase transition zones overlap, and the layer is exposed to an equilibrium pressure, the so-called ‘disjoining pressure’, exerted by long–range surface forces of the two confining phases. Theoretical calculations of the isotherm for disjoining pressure of water films on quartz surfaces indicate negative disjoining pressures for film thickness ranging between 60 and 7 nm resulting in increased Θ which was demonstrated experimentally (Derjaguin & Churaev, 1986).

Assuming a uniform water film on an inner and outer soil surface of 3.7 $m^2\ g^{-1}$, as measured by BET for the Tiergarten site (Jaeger *et al.*, under revision), a water molecule size of 0.27 nm and a water content of 1%, the respective water film would have a

thickness of approximately 2 nm and consist of seven layers of water molecules. Because material as porous and as heterogeneous as soil will not have a uniform water film, some part of the surfaces, probably the more hydrophilic, would be covered by a film thicker than 2 nm whereas other more hydrophobic parts of surfaces would have thinner water films or even remain dry.

A recent study (Goebel *et al.*, 2004) found a tendency for the contact angle maximum to be at soil water potentials of approximately 30 and 154 MPa, corresponding to an exposure to a constant *RH* of 80% and 32%, respectively: Goebel (2004) assumed that this effect is caused only by the impact of water films on the surface free energy as described by Derjaguin & Churaev (1986).

Although our results do not provide information about the distribution of moisture and water film thickness, it is evident that (at least) in the range $0\% < WC < 5\%$ there may be regions where water film thickness reduces wettability as previously described. Thin water films appear to be one of the few reasonable explanations presently available to explain the larger *WDPT* after drying at 31% *RH* at 20°C than after treatments at 65°C in Buch samples.

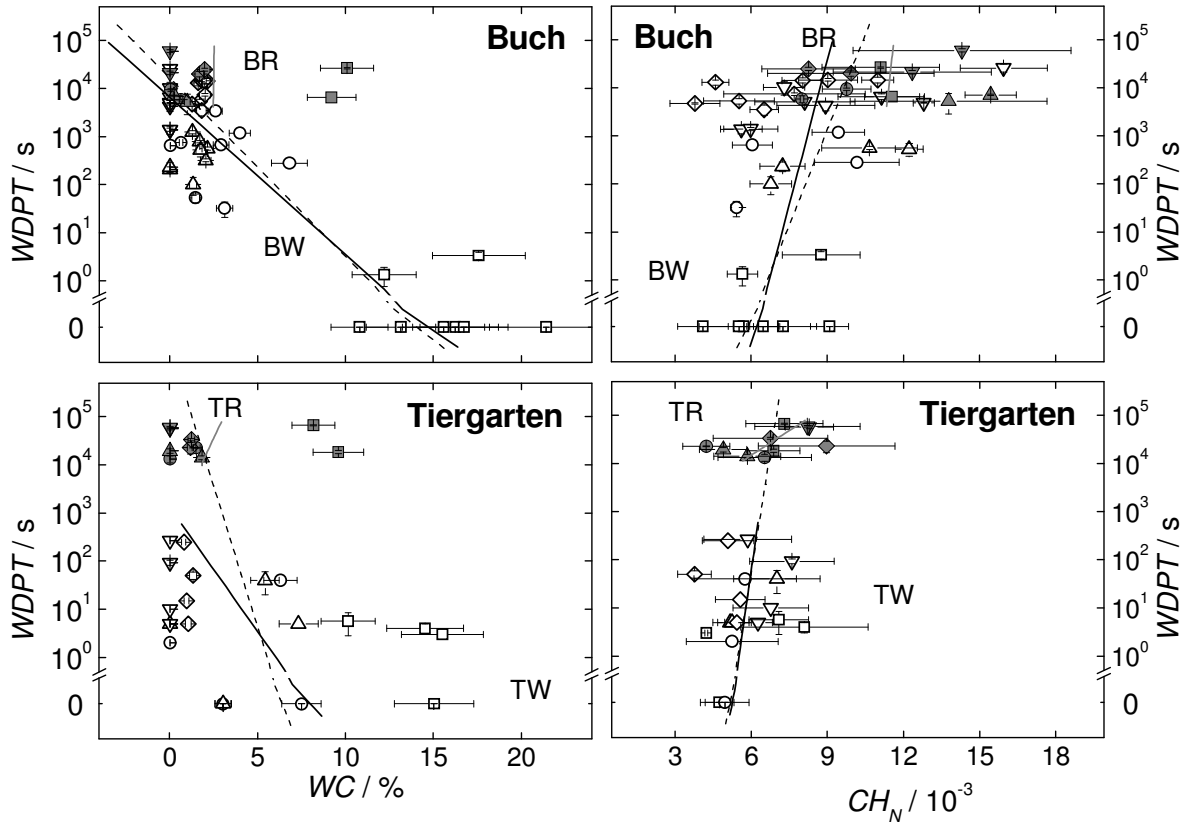

Figure 4-3 Water drop penetration time (*WDPT*) as a function of water content (*WC*), and as a function of normalized C-H band intensity (CH_N) of initially wettable (BW, $n = 32$, open symbols) and repellent Buch samples (BR, $n = 10$, solid symbols) and wettable and repellent Tiergarten samples (TW, $n = 18$; and TR, $n = 10$, respectively) in field moist state (□■) and after drying at 35°C (○●), 65°C (△▲), 105°C (▽ ▼) and at 31% *RH* (◇◆). Error bars are *WC* ± 15% and estimates of the standard deviation from triplicate measurements of *WDPT* and DRIFT peak areas.

4.4.4 WDPT as a function of water content and CH_N

Scatter diagrams of *WDPT* as a function of *WC* and CH_N (Figure 4-3) show that BW samples (*WDPT* < 10 s) had *WC* larger than 10% whereas those of TW fall in the range of 0% to 15%. *WDPT* of BW samples increased with decreasing *WC* and reached values in the range of those of BR samples, whereas *WDPT* of TW samples also increase with decreasing *WC* but remained distinctly smaller than those of TR samples. *WDPT* of TR and BR samples did not significantly change with *WC* (Figure 4-3) and a significant log*WDPT* correlation with *WC* was not found (Table 4-1).

Table 4-4 Correlation coefficients (*R*) for linear regression of log*WDPT* against water content (*WC*) and normalized C-H peak area (CH_N), and of *WC* against CH_N for all samples of both soils (BT) and the various sample subsets (see text)

BT	(*n* = 70)	*WC*	CH_N
	log*WDPT*	-0.61***	0.44**
	WC	1.00	-0.18

B	(*n* = 42)	*WC*	CH_N
	log*WDPT*	-0.81***	0.45*
	WC	1.00	-0.26

T	(*n* = 28)	*WC*	CH_N
	log*WDPT*	-0.34	0.42*
	WC	1.00	-0.07

BW	(*n* = 32)	*WC*	CH_N
	log*WDPT*	-0.88***	0.35
	WC	1.00	-0.23

TW	(*n* = 18)	*WC*	CH_N
	log*WDPT*	-0.39	0.22
	WC	1.00	0.00

BR	(*n* = 10)	*WC*	CH_N
	log*WDPT*	0.00	0.03
	WC	1.00	-0.12

TR	(*n* = 10)	*WC*	CH_N
	log*WDPT*	0.10	0.51
	WC	1.00	0.04

* Probability of error $P < 0.05$; ** $P < 0.01$; *** $P < 0.001$

A significant negative correlation was found between log*WDPT* and *WC* for all Buch samples (Table 4-4), mainly dominated by the strong negative correlation between log*WDPT* and *WC* of the BW samples. A weak negative correlation between log*WDPT* and *WC* was found for TW but not for TR.

The correlation between *WDPT* and CH_N (Figure 4-3) is weaker than that between *WDPT* and *WC* and is only significant for Buch samples (B), which dominates the correlation for the full BT dataset (Table 4-4). A significant correlation between CH_N and *WC* is not found either for Buch or Tiergarten samples.

4.4.5 Water content and CH_N as descriptors for the degree of repellency

As both *WC* and CH_N, had significant correlations with log*WDPT* for the BT dataset, whereas no significant correlation was found between CH_N and *WC*, it was assumed that CH_N and *WC* are independent from each other. Under this assumption, they were used as independent variables in a simple multiple regression analysis against log*WDPT*:

$$\log (WDPT) = \alpha + \beta\, WC + \gamma\, CH_N \qquad (4\text{-}1)$$

Table 4-5 Multiple regression parameters α, β and γ, their standard errors and correlation coefficients (R) of log$WDPT$ against water content (WC) and normalized C-H peak area (CH_N) for all samples (BT) and those from Buch (B) and those from Tiergarten (T).

	$\log WDPT = \alpha + \beta\ WC + \gamma\ CH_N$			
	α (±)	β (±) / %$^{-1}$	γ (±) / (K.-M. unit)$^{-1}$	R
BT	1.7 (0.5)**	-0.20 (0.03)***	220 (60)**	0.74***
B	2.5 (0.5)***	-0.23 (0.02)***	150 (50)*	0.87***
T	-1 (1)	-0.14 (0.06)*	500 (200)*	0.56*

* Probability of error P < 0.05; ** P < 0.01; *** P < 0.001

We used log$WDPT$ because Buczko (2006) found a linear relationship between sessile drop contact angle and log$WDPT$ indicating a correlation between surface free energy and the persistence of repellency. Parameters α, β, γ (Equation (4-1)) and the R values of this analysis for all samples (BT) and those of Buch (B) and Tiergarten (T) separately indicate a significant correlation (P < 5 %) between log$WDPT$ and the two descriptors (Table 4-5). This multiple regression is of much greater significance than the single regression analysis (Table 4-4).

In all cases, the parameters β and γ are significantly different from zero (Table 4-5), with greater significance for Buch samples than for those of the Tiergarten. The parameter β is negative and indicates a decrease in $WDPT$ with increasing WC. The differences in γ between the regressions of the three data sets (BT, B, T) fall within their standard error. The positive parameter γ decreased in the order of the respective data sets: $\gamma^T < \gamma^{BT} < \gamma^B$.

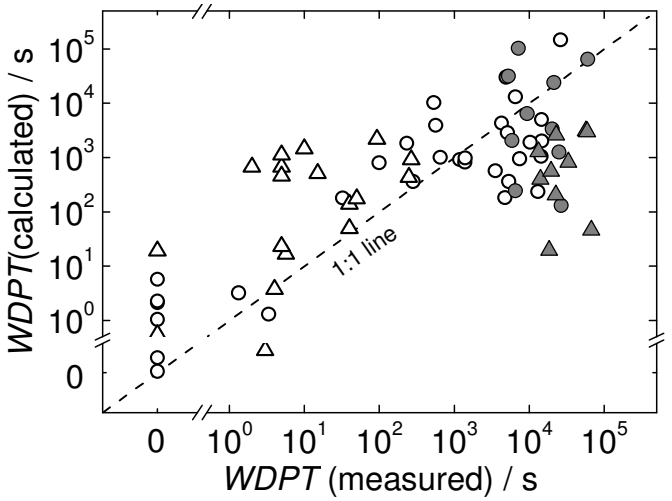

Figure 4-4 Water drop penetration time ($WDPT$) calculated using Equation (1) and the values of α, β and γ shown for BT in Table 4-4 as a function of the experimentally determined $WDPT$s of wettable (○, n = 32) and repellent (●, n = 10) Buch samples and wettable (△, n = 18) and repellent (▲, n = 10) Tiergarten samples, respectively.

The relation between measured log$WDPT$ and that calculated with Equation (4-1) and α, β and γ derived from BT dataset (Table 4-4) cluster around the 1:1 line (Figure 4-4). The T dataset appears to differ in a systematic way from the 1:1 line, which illustrates a difference between the datasets of the two locations.

4.4.6 Surface model of repellency changes in Buch and Tiergarten samples

The dependency of *WDPT* on *WC* and CH_N depicted as a plane in the three-dimensional space as predicted by Equation 1 shows drying patterns for wettable and repellent samples from Buch and the Tiergarten which are symbolized as arrows on this plane (Figure 4-5). The increase in repellency upon drying of the wettable Tiergarten samples, as expressed by longer *WDPT*, seems to arise from the reduction in *WC*, which is a physically controlled process. In addition to the reductions in *WC*, changes in surface hydrophobicity of wettable Buch samples suggested by changes in CH_N result in a more pronounced increase in repellency than for the Tiergarten samples.

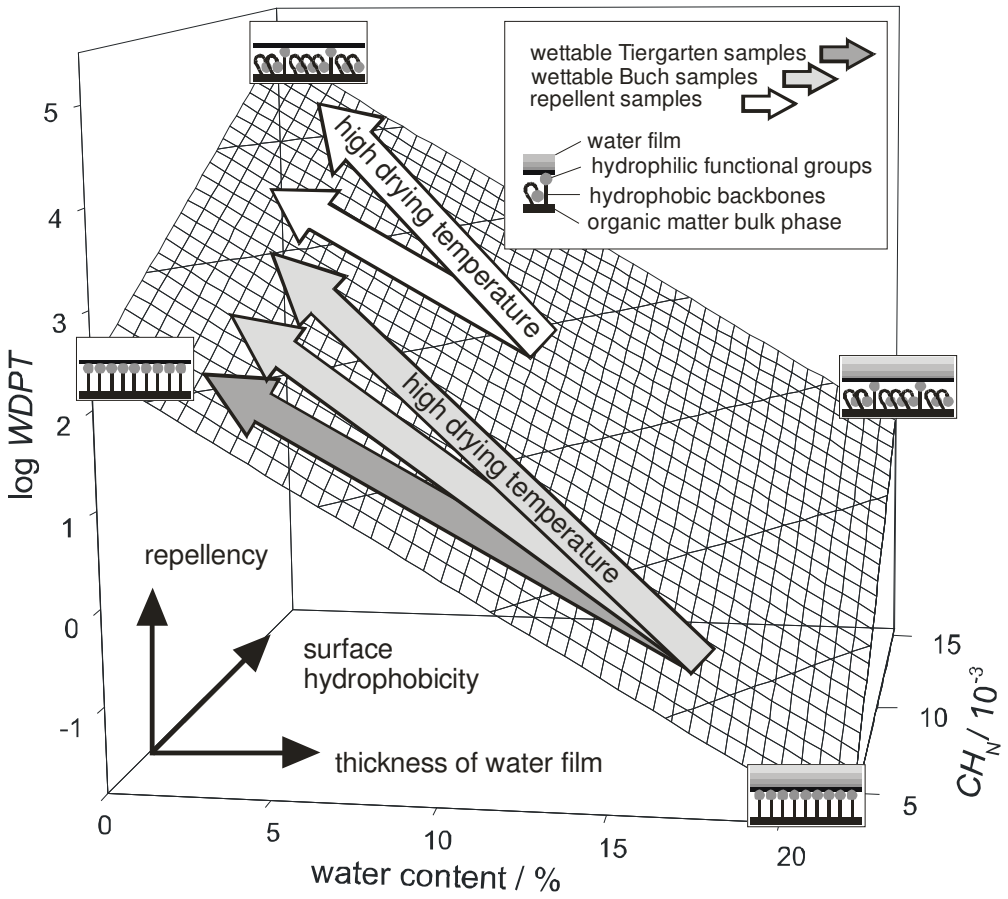

Figure 4-5 Plane of wettability (water drop penetration time, *WDPT*) as a function of water content (*WC*) and surface hydrophobicity (normalized peak height of C-H band intensity, CH_N) of Buch (B) and the Tiergarten (T) soils as calculated by Equation 1 in combination with the schematic model of three dimensional arrangement of outer organic molecules and the average thickness of a water film for homogeneous moisture distribution suggested by Bayer & Schaumann (2007).

As greater drying temperatures cause a stronger increase in CH_N in Buch samples than lower drying temperatures, the changes in surface hydrophobicity seem to be controlled rather by chemical processes. This is confirmed by greater activation energy of wetting in Buch samples than in the Tiergarten samples as observed with time-dependent sessile drop analysis (Diehl & Schaumann, 2007) where temperature and time dependent change of contact angles of spreading sessile drops was used to calculate the activation energy of wetting. The quantitative analysis of this study may be visualized with the aid of the qualitative model suggested by Bayer & Schaumann (2007) depicting the

interactions between molecular arrangements and mean thickness of the water film (Figure 4-5).

The effect of increasing water content on the degree of repellency may be interpreted as the formation of an increasing film thickness where the water film properties continuously tend towards those of bulk water (Goebel *et al.*, 2004; Bayer & Schaumann, 2007) or by an increasing degree of surface covered by a water layer. In contrast, an increase in the parameter CH_N would be indicative of an increase in the proportion of outward-oriented hydrophobic moieties, because of changes in orientation of amphiphilic compounds in the outer SOM layers with increasing dryness (Kleber *et al.*, 2007). Although the description of *WDPT* via a *WC*-dependent term and a surface-specific term (CH_N) has significantly improved the correlation, the deviation between measured and calculated *WDPT* is still up to three orders of magnitude. This indicates that additional factors affecting soil water repellency, such as a heterogeneous moisture distribution as suspected in the samples dried at 35°C and 65°C need to be considered.

4.4.7 Evaluation of the DRIFT method to detect drying-dependent surface changes

The results show that changes in the surface of SOM relevant to water repellency are detectable. However, the penetration depth of IR radiation exceeds the surface-active molecular layer and so the signal is diluted by the additional contribution from bulk SOM over that depth. The scatter of DRIFT spectral data may further arise from spectral distortions because of the use of untreated samples and interference from soil moisture and minerals. This scatter could be reduced by an IR technique with a lower penetration depth of IR radiation (e.g. ATR-IR technique) or by greater sample homogeneity in finer-sieved or ground samples. The latter would, however, require a detailed evaluation of the effect of grinding and sieving on SOM surface, the creation of new surfaces and therefore on soil water repellency dynamics.

Interference from minerals may be compensated by subtracting some proportion of a suitable reference spectrum of the sample's minerals obtained after the removal of organic material by oxidation or acid treatment. Reduction of interference by dilution of the sample with an inert solid seems impractical as the commonly used KBr and KCl are likely to affect the moisture content and distribution and most other materials absorb in the IR region. The small changes in IR absorption, following various drying procedures, reported here correspond with subtle modifications to soil surface chemistry. The differences between the IR absorption of samples from the different locations are much larger. This renders precise quantification of the small changes difficult with standard DRIFT technology.

4.5 Conclusions

DRIFT spectroscopy has been found to be qualitatively useful, but not precise in quantifying hydrophobicity in untreated, un-fractionated soil samples. The scattering of the data indicates that the technique needs to be improved. The variations in CH_N suggest that there are changes in SOM surface structure, which correlate with water repellency.

As DRIFT probes a relatively thick outer layer of the sample, its sensitivity to the outer most layers is too low to confirm that changes in the conformation of SOM at the surface have actually occurred. However, this appears to be one of the few reasonable explanations presently available to account for changes in soil water repellency.

The drying procedure has more influence on the *WDPT* than the water content of the soil samples. Care and control is required when assessments of some reference soil water repellency follow drying. High temperatures may increase hydrophobicity, but short drying events may be not sufficient to overwhelm initial differences in moisture content. Reproducible repellency under laboratory conditions requires a drying procedure which allows equilibrating the *WC* of all samples with the same imposed conditions. Drying at 20°C at a constant *RH* of 31% for periods in excess of four weeks seems to best to preserve some characteristics of the field moist samples with relevance to soil hydrophobicity. This procedure is therefore recommended as a means to maintain a reference estimate of water repellency which is insensitive to minor changes in the soil moisture content. In contrast to this reference repellency, the currently used potential repellency is measured on samples dried at greater temperatures, where more energy is available to promote conformational rearrangements of SOM components.

An improved correlation between *WDPT*, as an indicator of water of repellency, and *WC* together with CH_N, estimated using DRIFT spectroscopy, provides some resolution of the contributions made by these properties to soil water repellency. Accordingly, changes in soil water repellency result from an interplay between (i) water content driven changes, probably induced by changes in micro-scale moisture distribution and thickness of the water film, and (ii) changes in SOM surface chemistry, promoted by re-orientation of amphiphilic moieties.

5 Reaction of soil water repellency on artificially induced changes in soil *pH*

5.1 Abstract

Few studies have systematically investigated the relationship between soil water repellency (SWR) and soil *pH*. The hypothesis that the *pH* may control repellency via changes in the variable surface charge of soil material has not yet been tested. Previously it has been shown that it is necessary to eliminate the direct influence of changes in soil moisture content so that the unique relationship between *pH* and SWR can be isolated.

A method has been developed which allows adjustment of the *pH* of soils with low moisture content via the gas phase with minimal change in moisture content. The method was applied to 14 soil samples from Germany, Netherlands, the UK and Australia, using the water drop penetration time (*WDPT*) as the indicator of SWR. Sessile drop and Wilhelmy plate contact angles (Θ_{sess} and Θ_{WPM} resp.) were measured on the four samples from Germany and the data correlated with those of *WDPT*. The titratable surface charge of these four soils was measured at selected *pH* values using a particle charge detector (PCD).

The comparison of repellency determination by *WDPT*, Θ_{sess} and Θ_{WPM} highlights the advantages and constrains of each individual method.

Changes in SWR with soil *pH* were found to be influenced by the density and type of sites able to interact with protons at the available surfaces of organic and mineral materials in soil. The maximum SWR occurred for soil at natural *pH* and where the charge density was minimal. As *pH* increased, negative surface charge increased due to deprotonation of sites and *WDPT* decreased. Two types of behaviour were observed: Those in which (i) *WDPT* shortened with decreasing *pH* and ii) *WDPT* was sensibly constant with decreasing *pH*. The data suggest that the availability and relative abundance of proton active sites at mineral surfaces, and those at organic functional groups influence the behaviour.

5.2 Introduction

Soil water repellency (SWR) is a world wide phenomenon leading to uneven water distribution in soils, preferential flow and enhanced surface runoff, which in turn may result in a lack of water to support plant growth, accelerated leaching and transport of surface nutrients and contaminants toward groundwater, top soil degradation and erosion. The causes and mechanisms affecting SWR are many fold and not fully understood. Soil wettability was observed to improve following addition of lime, kaolinite clay, ammonia and sodium hydroxide solution (van't Woudt, 1959; Karnok *et al.*, 1993; Roper, 2005) This led to the general acceptance that, among others, soil *pH* influences SWR (Wallis & Horne, 1992). Roberts & Carbon (1971) found that water repellent sandy soils from

south-western Australia were more likely to have a lower *pH* than wettable soils. Similar trends were reported for 3000 garden and agricultural samples from New York State by Steenhuis et al. (2001) for 66 samples from calcareous forest soils with a generally very narrow range of *pH* (Mataix-Solera et al., 2007) and for soils from ants' nests (Cammeraat et al., 2002). Hurrass & Schaumann (2006) observed that, from a batch of 46 soil samples from an inner city park "Tiergarten" in Berlin, repellency was only detected in those with *pH* below 4.5. However, they did not find any correlation between *pH* and water repellency of samples drawn from a former sewage disposal field in Berlin.

Several mechanisms for the pH – SWR relationship have been proposed:

I) Changes in the surface charge of organic material: The hydrophobicity of humic acids (HA) was observed to increase with decreasing *pH* in the ranges $8 < pH < 11$, caused by protonation of phenolic groups (MacCarthy *et al.*, 1979; Duval *et al.*, 2005) and $4 < pH < 7$ by protonation of carboxylic groups (Terashima *et al.*, 2004). In these ranges this results in a reduction of negative surface charge which in turn leads to a less polar and, therefore, less wettable surface. Holmes-Farley et al. (1985) observed the same *pH* effect on sessile drop contact angle (Θ_{sess}) at a polymer surface (PE) with covalently attached carboxylic acid groups. The same mechanisms could be responsible for a decrease of soil water repellency as observed in field studies after increasing the *pH* via lime addition (van't Woudt, 1959; Roper, 2005) or the application of 0.1 M NaOH to repellent soils (Karnok et al., 1993). A further decrease in *pH* may lead to positive charge, e.g. by protonation of amine groups. On heptylamine plasma polymer surfaces this leads to an increasing wettability of the material (Chatelier et al., 1997).

II) Conformational changes in the organic matter: HA are not completely hydrophobic, but have amphiphilic character, and can render a soil water repellent when orienting the non-polar groups towards the pore space (Tschapek, 1984). Changes in *pH* may result in the rearrangement of moieties, fragments or entire molecules of SOM, which may influence their hydrophobicity (Ohashi & Nakazawa, 1996; Terashima *et al.*, 2004; Duval *et al.*, 2005). Deo *et al* (2005) observed, that at low *pH,* carboxylic groups on organic macromolecules with hydrophobic side chains, were orientated toward the bulk water, protecting the hydrophobic groups by encasing them in the inner part of coiled macromolecules. As *pH* increased and carboxylic groups were deprotonated, electrostatic repulsion was considered responsible for the observed swelling, loosening and/or chain expansion of hydrophobic nano-domains leading to an increased outward orientation of hydrophobic groups. Similar mechanisms were also suggested for water repellent soils (Ma'shum & Farmer, 1985; Valat *et al.*, 1991). A decrease in *pH* from 7 to 5 was found to facilitate a membrane-like aggregation of HA on mineral surfaces by hemimicelle or admicelle-like formations with increasing hydrophobicity of HA (Terashima et al., 2004). This was caused by protonation of carboxylic and phenolic groups leading to a reduction in repulsion forces between these moieties (Ohashi & Nakazawa, 1996) and to the formation of H-bridges and a more compact structure of HA with a maximum compaction around the pK_a of carboxylic sites.

III) Leaching of fulvic acid (FA)s: The relatively high solubility of FA at low *pH*, in comparison with those of HA, provide opportunities for preferential dissolution and

transport that do not arise at higher *pH* (>7). These high solubilities reflect a wettable character to FA so the quantities of FA and HA, and their relative abundances, may influence SWR (Chen & Schnitzer, 1978; Tschapek, 1984; Babejova, 2001); high FA/HA may confer wettability and low FA/HA may lead to SWR. Generally, the addition of HA to soil samples has been shown to increase their water repellency, and stable humic acid complexes were identified as an important contribution to water repellency in some sandy soils (Roberts & Carbon, 1972). The contact angle of FA and HA extracts was found to be the inversely related to their *pH*, indicating that *pH* might be an indicator for the hydrophobic potential of these materials (Lin et al., 2006).

IV) Changes in bacterial and fungal communities: Fungal exudates could be an agent for local *pH* reduction. This could lead to polymerization and/or precipitation of FA and HA and, therefore, be responsible for the resulting SWR observed in areas of high fungal activity (Lin et al., 2006). Liming may increase soil wettability not only by increasing its *pH* directly, but also by promoting microbial activity of wax degrading bacteria (Roper, 2005). However, some studies (Hurraß & Schaumann, 2006; Bayer & Schaumann, 2007) did not find increased fungal growth within water repellent areas of soil.

Few studies have systematically investigated the influence of *pH* changes on soil sample wettability. Instead of changing the soil *pH* directly, Graber *et al.* (2009) used Na^+ and Ca^{2+} solutions at various *pHs* to measure drop penetration times (a modified form of the *WDPT* test). The maximum time occurred using drops in the range $7 < pH < 9$ near to the original soil *pH* (~7.3 - 7.7) which was not adjusted. Only in the presence of Ca^{2+} did the water repellency of their samples increase with increasing *pH*. This was explained as the complexation of free undissociated fatty acids with the mineral surface via Ca^{2+} bridges leading to a higher density of fatty acid groups on the mineral surface and hydrocarbon tails left to express water repellency above them.

Bayer & Schaumann (2007) investigated the change of *pH* and its influence on soil wettability following the addition of aqueous HCl and NaOH solutions to soils. These actions only affected the wettability of samples from “Tiergarten” with a distinct maximum in SWR occurring in the range $4.5 < pH < 6.5$ and a similar wettability when brought to similar *pH* by addition of liquid NaOH. However, they found no such effect on samples from “Buch”. As soil moisture content is altered by the addition of aqueous reagents, this approach provides opportunities for partial solvation and re-arrangement of large organic molecules or flexible side-chains, which would not arise in the field where SWR has developed through natural drying. It is, therefore, difficult to resolve the effects of the imposed *pH* change from the impact of the method on soil moisture content on SWR (Bayer & Schaumann, 2007). Differences in repellency following drying have been observed between Buch and Tiergarten soils. Some mechanisms for the influence of water content on repellency in them (such as conformational changes in SOM at the surface, together with water coverage) were suggested by Diehl *et al. (2009)*. Diehl & Schaumann (2007) discussed this in the context of several chemical reactions with activation energies of 65 – 94 kJ mol^{-1}, 42 kJ mol^{-1} and 8 - 20 kJ mol^{-1} for the wetting process of dried Buch, repellent and wettable Tiergarten samples respectively.

This study presents an alternative approach to the investigation of the relationships between soil *pH* and SWR where the soil moisture content is essentially unaffected so that the mobility of organic material is not enhanced by solvation effects. The method involves exposing samples to various concentrations of gaseous hydrogen chloride or ammonia (drawn from the headspace gas above their respective concentrated solutions) for 24 h. The outcomes of the method are compared with those of previous studies (Täumer *et al.*, 2005; Hurraß & Schaumann, 2006; Diehl & Schaumann, 2007) concerning SWR of soils from "Buch" and "Tiergarten" sites, in Berlin, Germany, and the differences between them. The method was also applied to soil samples from the Netherlands, the UK and Australia and correlated with *WDPT* data. The *pH* data, from processed German soils, are compared with those from water drop penetration times (*WDPT*), water contact angles, estimates of both surface charge density and potential cation exchange capacity (CEC_{pot}) and an assessment of the influence of interactions between surface sites and protons in relation to *pH* and SWR is presented.

5.3 Material and Methods

5.3.1 Soil samples

German soil samples originate from two strongly anthropogenically influenced sites, a former sewage field in the north east of Berlin "Buch" and an inner city park in Berlin "Tiergarten". The locations are in a transition zone between temperate oceanic and continental climates with moderate precipitation (< 500 mm a^{-1}) and highest yield in the summer months.

At both sites the topsoil consists of medium sized sand with clay content below 5 % and is characterized by high soil organic matter content (*SOM)* between 5 and 20 % (Schlenther, 1996; Hoffmann, 2002; Täumer *et al.*, 2005; Diehl & Schaumann, 2007).

Samples were collected at the sites in spring 2007. The grass cover was removed (~ 1 m^2) and four individual samples taken in a depth of 10-20 cm from visibly distinguishable dry or wet patches known to reflect different SWRs (Hurraß & Schaumann, 2006). The wet and dry soil samples differ strongly in actual wettability (Table 5-1 and Table 5-2). Samples are identified by their source locations and SWRs as initially determined in their field moist states: Buch-wettable (BW), Buch- repellent (BR), Tiergarten-wettable (TW) and Tiergarten-repellent (TR).

Samples from the Netherlands were obtained from an individual profile (4). Samples of topsoils were collected from the UK (3) and Australia (3) between October 1999 and May 2001. Each set consisted of 2 or 3 water repellent samples (NLR, UKR and AUR) and one wettable sample (NLW, UKW and AUW, respectively). Wettable samples were collected as close as possible to the sites of water repellent soils to eliminate, insofar as possible, variations in soil type and land use. Sample information (Table 5-1) was obtained from Llewellyn (2004) and Mainwaring (2004) and further details of precise locations are available (Doerr *et al.*, 2002; Doerr *et al.*, 2005a; Doerr *et al.*, 2005b; Morley *et al.*, 2005; Douglas *et al.*, 2007).

Table 5-1: Sample characteristics

Code	Country	Region	Site	Vegetation	Depth (cm)	Soil particle size mean diameter / distribution width (mm)	*TOC* (g kg^{-1})	*pH*	*WDPT* air dried (s)
TR	Germany	Berlin	Tiergarten	turf grass	0-10	0.23 / 0.08	26.2 (±0.7)*	4.0	3,500 (±1,100)
TW				turf grass	0-10	0.23 / 0.08	48 (±1)*	4.4	5 (±1)
BR			Buch	couch grass	0-10	0.24 / 0.08	47 (±1)*	4.6	9,900 (±1,000)
BW				couch grass	0-10	0.24 / 0.08	50 (±1)*	4.6	1,200 (±100)
NLR1	Nether-lands	Zuid Holland	Ouddorp	grass, moss	0-10	0.27 / 0.22	36 (±3)	4.7	6,700 (± 700)
NLR2				grass, moss	10-20	0.23 / 0.10	5.9 (±0.3)	3.9	6,900 (± 700)
NLR3				grass, moss	20-30	0.22 / 0.08	0.8 (±0.2)	3.9	1,600 (± 400)
NLW				grass, moss	30-40	0.22 / 0.07	n. d.	4.1	0.1 (± 0.1)
UKR1	UK	Gower	Nicholaston Dunes	dune herbs, grasses	0- 5	0.33 / 0.08	11 (±3)	4.1	6,000 (± 1,000)
UKR2			Pennard Golf Course	turf grass	0- 5	0.30 / 0.08	8 (±1.0)	4.5	90 (± 10)
UKW			Nicholaston Dunes	unvegetated	0- 5	0.39 / 0.12	3.1 (±0.6)	7.0	0.1 (± 0.1)
AUR1	Australia	Nara-coorte	Pine Views	paddock	0-10	0.25 / 0.16	11.7 (±1.0)	4.8	450 (± 40)
AUR2				paddock	0-10	0.29 / 0.23	14.4 (±0.5)	4.3	1000 (± 200)
AUW			Myome	paddock	0-10	0.24 / 0.14	2.2 (±0.4)	5.1	0.1 (± 0.1)

* *TOC* values are estimated from *SOM* content (loss of ignition)

All samples are sandy soils representing various locations, covering vegetation, and climates (Table 5-1).

The Australian samples (AU) are from a Mediterranean-type climate with long dry periods during the summer, whereas those from the Netherlands (NL) and the United Kingdom (UK) are exposed to oceanic humid-temperate climates with rainfall throughout the year.

Table 5-2: Water content (*WC*) and wettability as water drop penetration time (*WDPT*), as contact angle measured by Wilhelmy Plate method (Θ_{WPM}), and by sessile drop method (Θ_{sess}) in field moist state and dried at 19°C at a constant relative humidity of 31%*RH*, and soil organic matter content (*SOM)* and potential cation exchange capacity (CEC_{pot}) of the 4 German samples.

	WC (%) moist	*WDPT* (s) moist	Θ_{WPM} (°) moist	Θ_{sess} (°) moist	*SOM* (%)
TW	32 (±2)	0	80 (±4)	< 10	8.2 (±0.3)
TR	5.4 (±0.3)	17,000 (±2,000)	129 (±4)	111 (±5)	4.5 (±0.1)
BW	23 (±1)	0	80 (±3)	< 10	8.6 (±0.1)
BR	9.6 (±0.5)	>30,000	123 (±1)	103 (±5)	8.0 (±0.2)
	WC (%) dried	*WDPT* (s) dried	Θ_{WPM} (°) dried	Θ_{sess} (°) dried	CEC_{pot} ($cmol_c\ kg^{-1}$)
TW	2 (±0.3)	5 (±1)	98 (±6)	43 (±6)	25 (±1)
TR	1.5 (±0.2)	3,500 (±1100)	123 (±3)	94 (±3)	17 (±1)
BW	1.8 (±0.3)	12,000 (±100)	126 (±4)	86 (±3)	27 (±2)
BR	1.6 (±0.2)	9,900 (±1000)	134 (±6)	103 (±4)	25 (±2)

5.3.2 Sample preparation and characterization

Sample storage

The German samples were air dried and then stored (> 8 weeks at 19°C) over saturated $CaCl_2$-solution at ~ 31% relative humidity (*RH*). The NL, UK and AU samples were dried at 20ºC in an oven and then stored in closed bottles at ambient conditions without temperature control. Prior to assessments of SWR these samples were equilibrated at 20ºC and *RH* ~ 50% for 24 h.

SOM content

The *SOM* content of the German samples was assessed by loss of ignition (samples sieved < 2 mm, heating at 550°C for 5 h, DIN 18128) and total organic carbon content (*TOC)* estimated by dividing *SOM* by the factor 1.72 (AG Boden, 2005). *TOC* of NL, UK and AU samples was determined using a Solid Sample TC Analyser (Primacs^{SC}, Skalar, Netherlands) controlled by a PC. Oxygen was used as the oxidant. Samples were ground, by hand, to improve the rate of combustion and heated to 1050ºC for seven minutes. As

samples were free of inorganic carbon, total carbon (*TC*) content was considered equivalent to *TOC*. The quantity of CO_2 released on combustion was determined, at a wavelength of 4.2 µm, using an IR detector. The instrument was calibrated using oxalic acid as a standard.

Water content, soil pH and electrical conductivity

Soil *pH* and electrical conductivity were determined using field moist un-sieved soil (~ 12 g) in $CaCl_2$-solution (25 ml, 0.01 M) (DIN ISO 10390) using a pH-meter (Qph 70, VWR International). Similar *pH* determinations were also made using less material (German samples ~ 2g soil and 4 ml $CaCl_2$-solution or AU, NL and UK samples ~ 5 g and 11 ml $CaCl_2$-solution). Soil water content of un-sieved material (*WC*) was determined gravimetrically by oven drying for 24 h at 105°C (DIN ISO 11465). The values are reported on a dry weight basis.

Potential cation exchange capacity (CECpot)

CEC_{pot} was determined by complete displacement of all cations by Ba^{2+} ions at *pH* 8.1 and a subsequent replacement of Ba^{2+} by Mg^{2+} ions. 8 – 9 g of air dried soil sample (m_0) were placed in a centrifuge tube (m_1) and shaken in an overhead shaker for one hour with 30 mL of a 1:1 mixture of 1 mol L^{-1} $BaCl_2$-solution and a triethanolamine solution (9 vol%, adjusted at *pH* 8.1 with HCl). The samples were then centrifuged for 10 min at 3000 g. Afterwards, the supernatant was decanted. This procedure was repeated twice. After manual shaking with water and subsequent centrifugation and decantation, the centrifuge tube was weighted again (m_2). Finally, 30 mL of a 0.02 mol L^{-1} $MgSO_4$ solution was added and shaken overnight. The concentration (c) of Mg ions in the solution was determined by FAAS (Perkin Elmer) and CEC_{pot} calculated as:

$$CEC_{pot} = \frac{3000\left(c_{bl} - c\,\frac{(30 + m_2 - m_1)}{30}\right)}{m_0} \qquad (5\text{-}1)$$

Water drop penetration time

The resistance of soil samples to wetting was determined using water drop penetration time, *WDPT* (Letey, 1969). Samples were placed in small containers, the surface gently smoothed and the containers placed in a incubator at 20°C. Three drops (100 µL) of distilled water were placed on each sample and the period required for complete penetration was determined. When *WDPT* exceeded 1 min, the period was determined from magnified digital photographs (Canon A300) taken automatically at increasing intervals from 12 s up to 10 min, such that the relative error of *WDPT* did not exceed 5 % (Diehl & Schaumann, 2007). *WDPT* of UK, NL and AU samples were determined using drop volumes of 35 µL.

Contact Angle: Wilhelmy Plate Method

Advancing contact angles (Θ_{WPM}) were determined by the Wilhelmy Plate Method using a Dynamic Contact Angle Meter and Tensiometer (DCAT 21, Data Physics, Filderstadt, Germany). Half a glass microscope slide (76 x 26 x 1 mm) was covered completely with double sided adhesive tape and a thin layer of soil attached to it. The Θ_{WPM} of the slide was measured as an advancing contact angle (Diehl & Schaumann, 2007).

Contact Angle: Sessile Drop Method

A thin layer of the soil sample was attached to one side of a glass microscope slide using double sided adhesive tape (Bachmann *et al.*, 2000a). Three drops of water (100 µl) were placed on the surface. After one minute a digital image was taken (Canon A300) and the sessile drop contact angle (Θ_{sess}) was calculated from the tangent to the three-phase contact point associated with the ellipse that best fitted the drop shape (Diehl & Schaumann, 2007).

Modification of soil pH

Soil samples were exposed to various concentrations of gaseous HCl and NH_3 in air to change their *pH*.

pH increase: Ammonia solutions 32% and 35% were obtained from Carl Roth and Fisher Scientific Ltd (Germany and UK, respectively). A known sample volume of ammonia gas (5 - 100 mL) was drawn from the headspace of an ammonia solution using a glass syringe via a silicone septum fitted in the screw cap of a containing bottle. The sample was then injected through a similar septum in the cap of a small bottle containing soil (~10 or 40g) (Figure 5-1 A). AU, NL, UK soil samples were treated with ammonia from the 35% solution and those from Germany with that from the 32% solution). After 24 h, the bottle containing the soil was opened and the wettability and then *pH* and of the soil were determined.

pH reduction: Hydrochloric acid solutions, 37%, and 36%, were obtained from Carl Roth, Germany and 36 % Fisher Scientific Ltd., UK resp. A known sample volume between (25 - 500 mL) of air was introduced into a dispersion tube and passed through a gas wash bottle (250 mL) filled with HCl. The air enriched in HCl was passed through flexible silicone tubes and glass stopcocks into a second wash bottle (250 mL) containing soil (~10 g) (Figure 5-1 B). AU, NL and UK soil samples were treated with fumes from the 36% solution and those from Germany with fumes from the 37% solution. After 24 h, the bottle containing the soil was opened and the wettability and the *pH* of the soil were determined.

pH range: Both procedures were applied to known masses of soil and various volumes of HCl and NH_3 fumes to determine the range of adjustment possible to soil *pH*.

Surface charge

Particle surface charge of selected soil samples (sieve fraction < 0.063 mm), at native and adjusted *pH* (as described above), were determined by titration following dispersion of

the samples in laboratory water (prepared by deionisation and reverse osmosis; 5.4 < pH < 6.6; specific conductivity < 2 µS) using a particle charge detector (PCD 02, Mütek company, Germany). Stepwise additions of cationic polyelectrolyte (polydiallyl-dimethylammonium chloride, 0.01, 0.1 or 1 mmol L^{-1}) were made in for negatively charged particles, and anionic polyelectrolyte (sodium polyethylene-sulfonate, 0.1 mmol L^{-1}), for positively charged particles, using an automatic titrator (Mettler Toledo DL 25) to effect neutralization of electrokinetic charge. The amount of polyelectrolyte of charge (c) in volume (V) required to reach the isoelectric point (*IEP*) of a sample mass (w), was detected by the PCD as an electrokinetic potential of zero. The titratable charge (Q) of the sample was calculated as:

$$Q = \frac{V \cdot q}{w} \qquad (5\text{-}2)$$

Provided that the PCD signal is only used in combination with polyelectrolyte titration to detect the sign of particle charge and to indicate the isoelectric point (*IEP*), PCD technique is reported to produce reasonable results for titratable surface charge (Böckenhoff & Fischer, 2001).

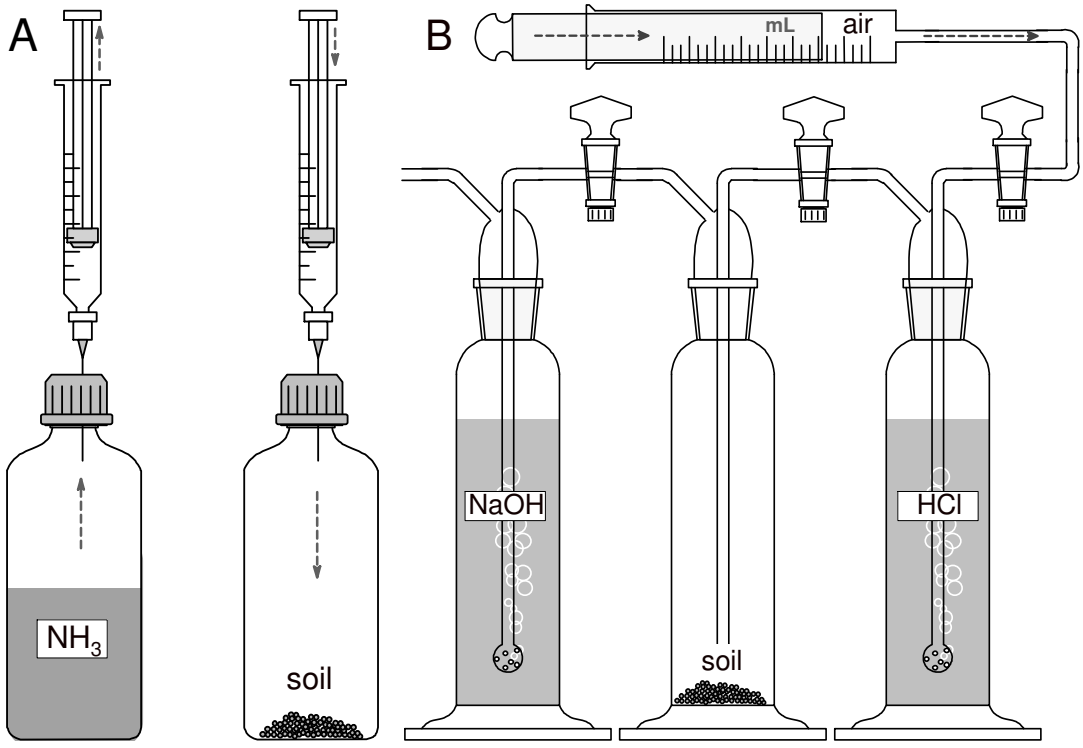

Figure 5-1: Experimental design of modification of soil-*pH*. **A** Exposition of soil to gaseous ammonia enriched atmosphere. **B** Exposition of soil to HCl enriched atmosphere.

Long-term investigation of Buch and Tiergarten site

Between spring 2002 and spring 2004, the sample sites Tiergarten and Buch (Germany) were subjected to a long-term study of seasonal sampling and characterisation of wettable and repellent samples, amongst others, *pH,* electrical conductivity (*EC*), *C/N* ratio and "Mehlich" extractable iron (Mehlich, 1984). Some *EC* and *pH* data were presented by

Hurraß & Schaumann (2006). *C/N* ratio was determined by combustion and quantification of CO_2 and N_2 using gas chromatography and thermal conductivity detector (C/N NA 1500 N Carlo Erba).

5.4 Results

5.4.1 General sample characteristics

The long-term investigations showed that repellent samples in Tiergarten were restricted to a range $3.5 < pH < 4.5$ whereas wettable Tiergarten samples and all Buch samples were found in a range of $3.5 < pH < 5.5$ (Figure 5-2 A). Wettable samples from both sites had *EC* values < 350 µS cm^{-1}, whereas repellent samples had maximum *EC* values of < 1300 µS cm^{-1} and < 550 µS cm^{-1} for Tiergarten and Buch sites, respectively (Figure 5-2 B). Although Tiergarten samples have higher *C/N* ratios than Buch samples (Figure 5-2 C), absolute *N* content is comparable in both sites (data not shown). Tiergarten samples possessed significantly higher contents of "Mehlich" extractable iron than Buch samples, in absolute values (Figure 5-2 D) as well as related to SOM content (data not shown).

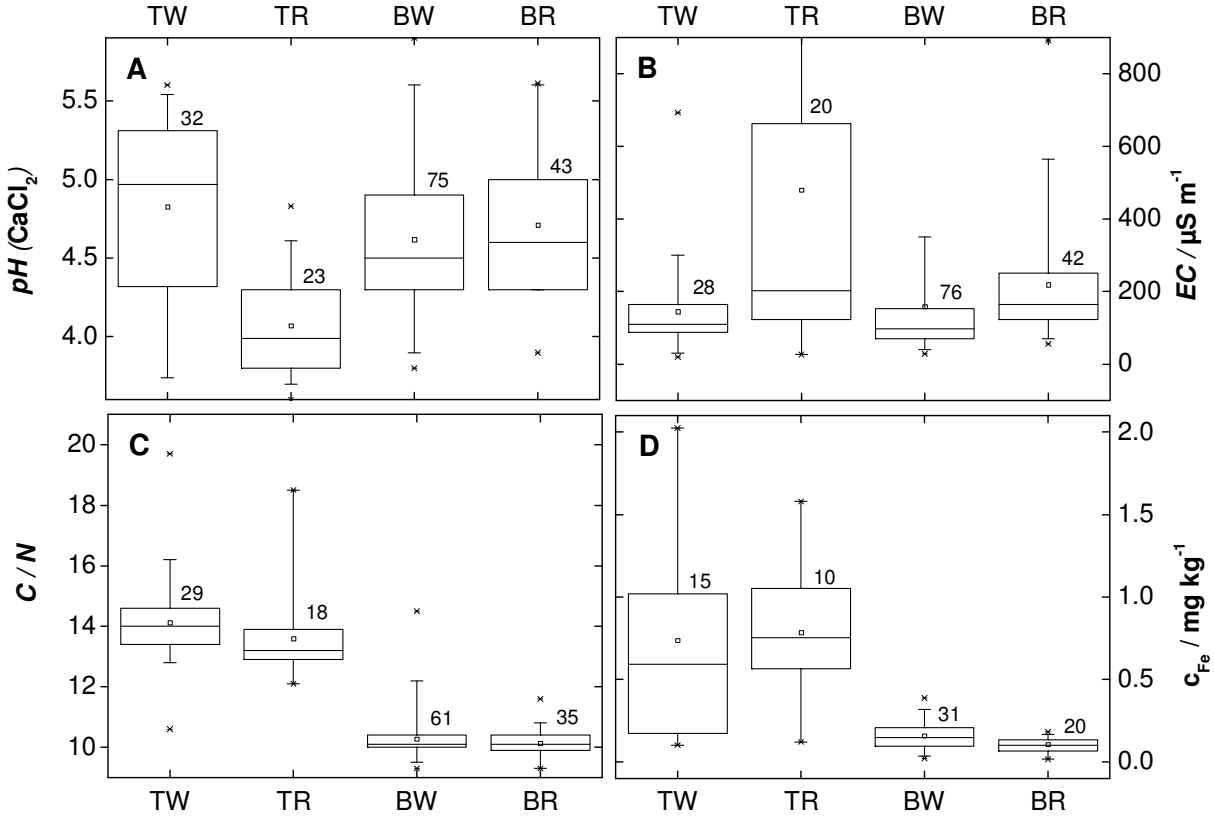

Figure 5-2: **A** *pH*, **B** electrical conductivity (*EC*), **C** Soil C/N ratio, and **D** "Mehlich"-extractable iron measured in wettable and repellent soil samples from Tiergarten (TW, TR) and from Buch (BW, BR, respectively) from a study of seasonally sampling between spring 2002 and spring 2004.

Water repellency (WDPT) of the originally wettable samples from Germany (TW, BW) changed significantly after drying at 19°C at constant relative humidity of 31%*RH*. Values for BW samples increased from 0 s in field moist state up to 1200 s following drying (Table 5-2). In contrast, values for TW samples increased from 0 s in field moist state to 5 s following drying and so the soil remained wettable. The effect of drying on *WDPT* of the repellent samples (TR, BR) was the inverse: After drying *WDPTs* were shorter than those for field moist samples (Table 5-2).

CEC_{pot} was significantly lower (17 $cmol_c\ kg^{-1}$) in the TR sample than in the other 3 German samples (25-37 $cmol_c\ kg^{-1}$) which may reflect the low *SOM* content in the TR samples, 26 g kg^{-1} in comparison with ~ 50 g kg^{-1} TOC of the others (Table 5-2). The TR sample also has a noticeably lower pH (4.0) in comparison with the others (4.4 - 4.6) (Table 5-1).

TOC in the NL samples decreased with increasing depth from 36 g kg^{-1} in the topsoil (0-10 cm) down to 0 (the detection limit) at a depth of 30-40 cm. The *TOC* of UK and AU samples varied between 2 and 14 g kg^{-1}. Original *pH* values of the samples from vegetated sites ranged between 3.9 in NLR2 and NLR3 (in a depth of 10-30 cm of the NL soil profile) and 5.1 in sample AUR2. Only the *pH* of the UKW sample, from a vegetation-free site, was distinctly higher (7.0) than those of the others (Table 5-1).

5.4.2 Effects of exposure to gaseous NH_3 and HCl

As the volumes of gaseous ammonia or hydrogen chloride, added to soil samples B and T increased, the resulting *pH* changes increased and decreased respectively away from the initial value and form sigmoidal curve (Figure 5-3 D). The slope of *pH* increase / decrease is steepest around *pH* 4 – 5 (untreated samples) and flattens with increased gas volume. The *pH* approaches a value of 8.8 – 9.3 after addition of 10 mL/g of NH_3-enriched air and to a value of 1.8 – 2.4 after addition of 50 mL/g of HCl-enriched air.

The *pH* of the TR sample was slightly more sensitive to increases in concentration of NH_3 in comparison with its wettable counterpart (TW). In order to increase *pH* of TW sample from 5.2 to 8.1, ~ 4 mL/g of NH_3 enriched air is needed, whereas TR sample requires only ~ 3 mL/g to increase *pH* from 5.3 to 8.3. The difference between *pH* of this pair vanished after the addition of 1 mL/g NH_3 (*pH* 5.3) and reappears clearly inverted after the addition of 4 mL/g NH_3.

The initial *pH* of untreated BW and BR were identical, but addition of NH_3 (up to 4 mL/g) resulted in slightly higher *pH* change for BR than for BW. With further additions of NH_3, the *pH* of the TR-TW pair converged at 9.3 and at 8.8 – 9.0 (Figure 5-3 D).

The *pH* of the repellent sample TR decreased with a steeper slope, than that of TW after addition of HCl (up to 15 mL/g). Within this range, the *pH* of the TW sample is higher than that of TR, whereas the *pH* of BW is slightly lower than that of BR. Only after addition of volumes (20 and 50 mL/g) of HCl enriched air, did the *pH* of all samples converge to specific values of 1.8 for T and 2.4 for B pairs (Figure 5-3 D). In order to decrease the *pH* of TW from its original value (4.4) to that of TR (4.0), it was necessary

to add ~ 3 mL/g of HCl enriched air. A further reduction to *pH* 3.0 required additions of ~ 12 mL/g and 7.5 mL/g to TW and TR respectively.

Samples from Buch have comparable *TOC* content for the wettable and the repellent sample (50 and 47 g kg^{-1}) respectively). In contrast, *TOC* of the wettable TW sample (48 g kg^{-1}) was almost twice as high as that of its repellent counterpart TR (26 g kg^{-1}) (Table 5-1).

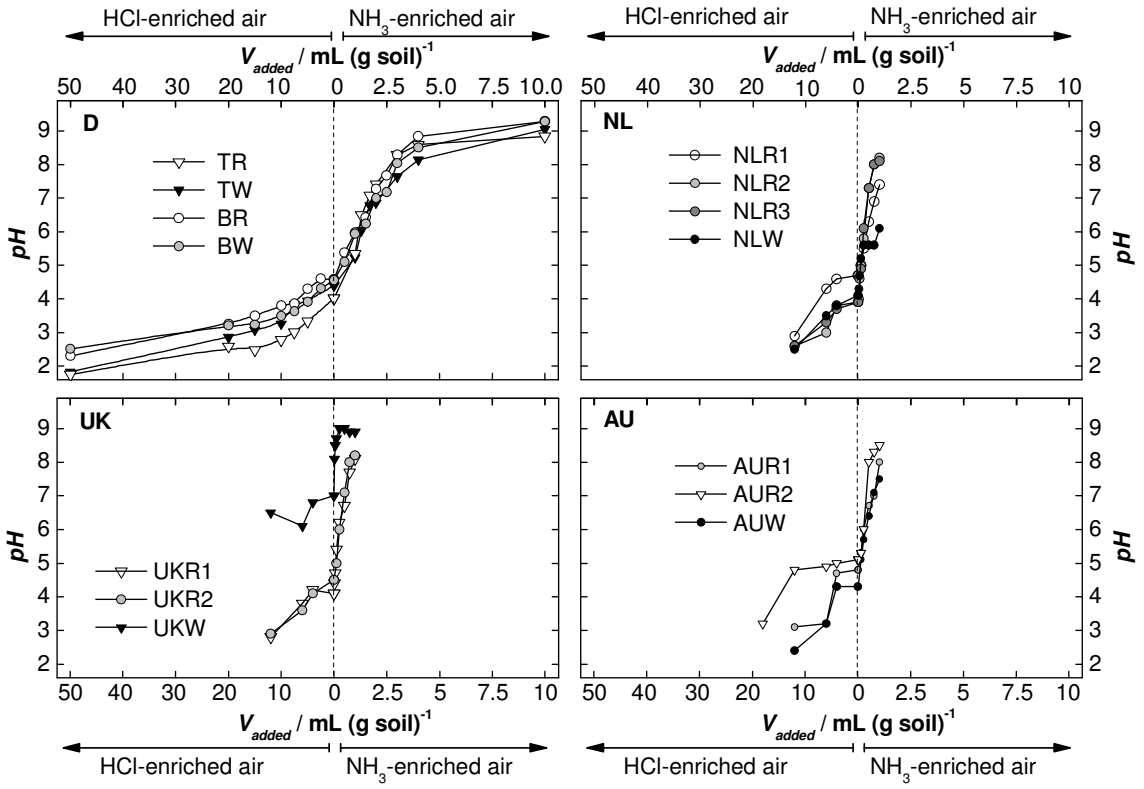

Figure 5-3: Artificially induced soil-*pH* as a function of the added volume of HCl- and NH_3-enriched air for **D** samples from Germany, **NL** samples from Netherlands, **UK** samples from the UK, and **AU** samples from Australia.

Most curves of *pH* as a function of the applied gas volume obtained from NL, UK and AU samples were sigmoidal in shape, similar to those obtained from the German samples. However, the limits of the induced *pH* change were narrower than those of the German samples. Most curves have more than one inflexion point so that in some cases the convergence to a maximum (e.g. NLC, AU1) and minimum *pH* values (e.g. NL1, AU2) was not readily observed within the range investigated (Figure 5-3 NL, UK, AU).

In most NL, UK and AU samples, a second inflexion point in the curve shape forming a plateau like shape is indicated in the range just below the original *pH* of the samples, suggesting a buffering system in this *pH* range. This buffering zone is most strongly pronounced in the sample AU-R2 (Figure 5-3).

In good accordance to the TW and TR samples, the slope of *pH* as a function of added NH_3 volume seems to be steeper for samples with a lower *TOC* than for samples with a higher *TOC*: As ammonia was added, the *pH* of NLR2 and NLR3 (with *TOC*s of 6 and 1 g kg^{-1} resp.) increased with a steeper slope than that of NLR1 (with a *TOC* of

36 g kg^{-1}), similarly the *pH* of UKW (with a *TOC* of 3 g kg^{-1}) increased with a steeper slope than those of UKR1 and UKR2 (with *TOC*s of 11 and 8 g kg^{-1} resp.) and the *pH* of AUR2 (with a *TOC* of with 2 g kg^{-1}) increased with a steeper slope than those of AUR1 and AUW (with *TOC*s of 12 and 14 g kg^{-1} resp.) (Figure 5-3 NL, UK and AU).

The sparse array of data (3-4 points) available for acidified samples is not sufficient to provide a detailed description of the behaviour of NL, UK and AU samples. Whilst this method of soil acidification appears useful, the experimental design does not provide a relationship between the added HCl-enriched air volume and the specific HCl concentration in the wash bottle containing the soil sample.

5.4.3 Reaction of repellency on changes in soil pH

*WDPT*s of the German samples whose *pH* was adjusted were found to fall in the range 0 < WDPT < 14400 s with increasing maxima (TR 1 h, BW 2 h and BR 3 h) and minima (at 2, 12 and 90 s respectively). Data for TW fell in the range 0 < *WDPT* < 5 s indicating a minimal influence of *pH* in the range 2 < pH < 9. *WDPT* decreased with increasing *pH* for all samples ((Figure 5-4 D). Slopes of the best fit linear regression lines of log *WDPT* vs *pH* in the alkaline direction were -0.36 ± 0.02 and -0.42 ± 0.03 ($p < 0.0001$, both) comparable for BW and BR, respectively, but significantly steeper (-0.66 ± 0.04, $p < 0.0001$) for the TR. This sample became wettable (*WDPT* < 10 s) above *pH* 8.3, whereas both Buch samples remain repellent (*WDPT* > 10 s) up to the limit of *pH* 9.3 ((Figure 5-4 D).

As *pH* was reduced, *WDPT* behaved in an inconsistent manner: The *WDPT* of TR decreased with a maximum at the original *pH*. Variations in the relatively short *WDPTs* of TW are probably of little practical significance (with little net change in relation to the value at the original *pH*). Contact angles measured either from sessile drops or using the Wilhelmy Plate method decrease with decreasing *pH* for all Tiergarten samples (Figure 5-4 B, C). In contrast, *WDPTs* of both Buch samples did not decrease upon *pH* reduction, but remained within a range of 2 < WDPT < 4 h for BR and increased from 0.3 h to 1 h for BW.

Changes in *WDPT* arising from adjustment of soil *pH* of the repellent NL, UK, and AU samples follow the trends shown by the repellent German samples (BR and TR): In all cases, *WDPT* decreased with increasing *pH* (Figure 5-4).

Two types of behaviour were observed as *pH* decreased: I) samples with a maximum *WDPT* in the region of the original *pH* and *WDPT* decreasing with decreasing *pH* (TR, NLR1, UKR2, AUR1 and AUR2) and II) samples with constant or increasing *WDPT* (BW, BR and UK-R1) after reduction of *pH*. Samples NLR2 and NLR3 possessed local maxima in *WDPT* at the original *pH*, and *WDPT* decreased with *pH*, except for the lowest induced *pH*, where *WDPT* reached a second maximum with a value comparable with or higher than, that at the original *pH* (Figure 5-4 NL).

In contrast to TW, all wettable NL, UK, and AU sets exhibited instant penetration (WDPT ~ 1 s) over the *pH* range examined. Sample BW became repellent after drying and, suffered a reclassification as repellent.

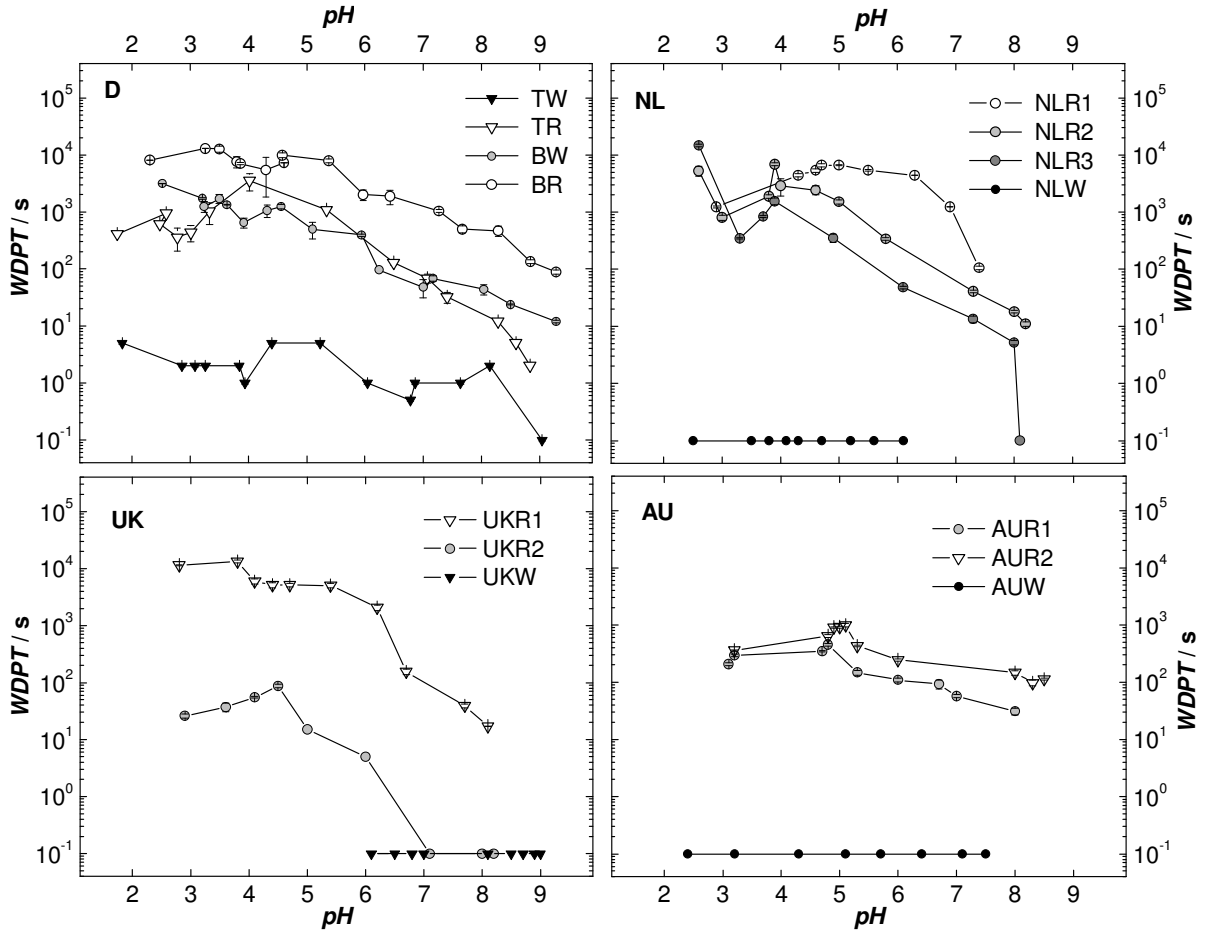

Figure 5-4: Water drop penetration time (*WDPT*) as a function of artificially induced *pH* of repellent samples and wettable control samples: **D** from two sites in Germany, **NL** from a profile in the Netherlands, **UK** from two sites in UK, and **AU** from two sites in Australia.

5.4.4 Comparison of contact angle and WDPT data

Contact angle measurements (Θ_{sess}) made on the German samples show qualitatively comparable trends with *WDPT*. In principle, all three curves (Figure 5-5 A, B, C) indicate a decrease in repellency upon increase from the original *pH* for all samples, and a decrease in repellency upon decrease from the original *pH* for TW and TR samples and only small or negligible changes in repellency upon decrease from the original *pH* for BW and BR samples. Correlation of *WDPT* and Θ_{WPM} with Θ_{sess} (Figure 5-5 D) shows clustering about a linear regression line of log(*WDPT*) data of the form:-

$$\log(WDPT) = 0.038\,\Theta_{sess} - 0.29 \qquad (5\text{-}3)$$

with a range of ~ 40° over the range 0 < WDPT < 10 s.

Contact angles Θ_{WPM} cluster in a similar manner to Θ_{sess} only at low values with a significant departure at high values indicating a relative insensitivity of Θ_{WPM}. These effects can be seen in the scatter Θ_{WPM} as a function of Θ_{sess}, where Θ_{WPM} data cluster around the line:

$$\Theta_{WPM} = 0.73\,\Theta_{sess} + 80° \qquad (5\text{-}4)$$

in the range $0° < \Theta_{WPM} < 120°$, whereas in the range $120° < \Theta_{WPM} < 130°$, where $\Theta_{sess} > 60°$ scatter is random about the horizontal. The regions of low sensitivity of the *WDPT* method and Wilhelmy plate method, in relation to sessile drop method, are shown shaded in Figure 5-5 A and C, respectively.

The WPM method did not resolve the differences between BW and BR detected in the *WDPT* and Θ_{sess} data. There is little clustering of data in the vertical direction to suggest regions where Θ_{sess} is insensitive to *WDPT* or Θ_{WPM}. The boundary between wettable and repellent samples defined as *WDPT* ~ 5 s (Dekker et al., 1998) correspond with Θ_{sess} of ~ 26° and Θ_{WPM} of ~ 100° using Equation (5-4) and (5-3), respectively.

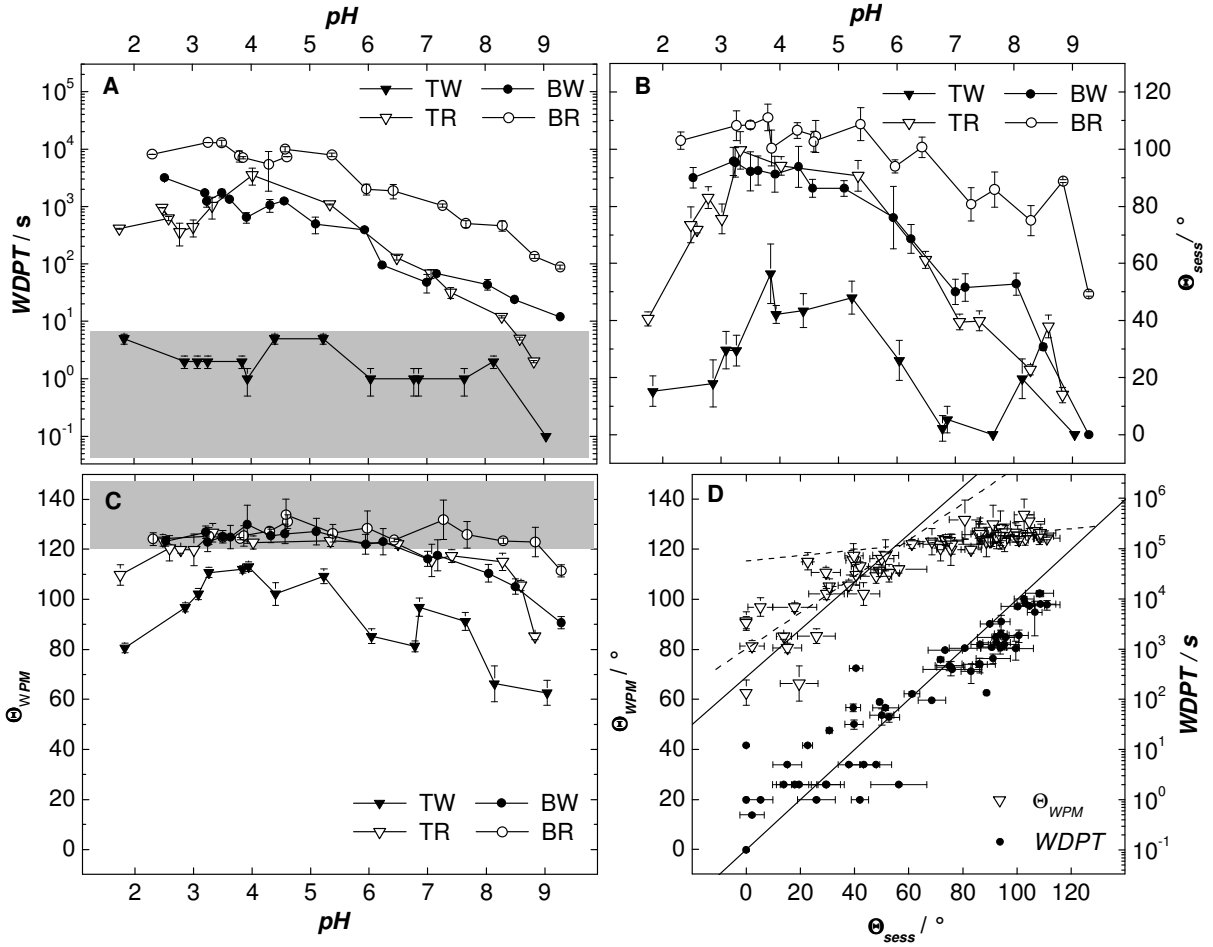

Figure 5-5: Wettability of the German Tiergarten (TW, TR) and Buch (BW, BR) samples as a function of artificial induced soil *pH*: **A** as contact angle measured by Wilhelmy Plate Method (Θ_{WPM}), **B** as contact angle measured by sessile drop method (Θ_{sess}), and **C** measured as water drop penetration time (*WDPT*). **D** *WDPT* and Θ_{WPM} as a function of the respective Θ_{sess}.

5.4.5 Surface charge changes of German samples

Negative surface charge (*Q*) strongly increased with increasing *pH* in all samples (Figure 5-6). and data from repellent and wettable samples from Buch (BW, BR) did not differ significantly from each other in surface charge over the range of *pH* investigated. At the lowest investigated *pH* (1.7 for BW and 2.3 for BR), both revealed minima in *Q* of -0.9 (±0.9) $cmol_c\ kg^{-1}$ and -0.5 (±0.6) $cmolc\ kg^{-1}$, respectively. Both samples had

maximum Q of -20 $cmol_c\ kg^{-1}$ at the highest *pH* (9.3) (Figure 5-6). Both Tiergarten samples had positive Q (1.1 (±0.2) $cmol_c\ kg^{-1}$ for TW and 3.5 (±0.4) $cmol_c\ kg^{-1}$ for TR) at their lowest *pH* (1.7 and 1.8, respectively). At their highest *pH* of 9 and 8.8 (TW and TR, respectively) both had more negative charge than the Buch samples at similar *pH* (TW: -39 (±4) $cmol_c\ kg^{-1}$, TR: -30 (±3) $cmol_c\ kg^{-1}$, Figure 5-6). The slope of Q as a function of *pH* showed a minimum between *pH* ~ 3 and pH ~ 6 for all samples (Figure 5-6), suggesting the elements of a sigmoidal shaped curve, with at least one inflexion point, whose detail is not made clear by the sparse data points. As Q data were available for four only *pH* values, estimates of Q values at intermediate *pH* were made by linear interpolation between these (Figure 5-6).

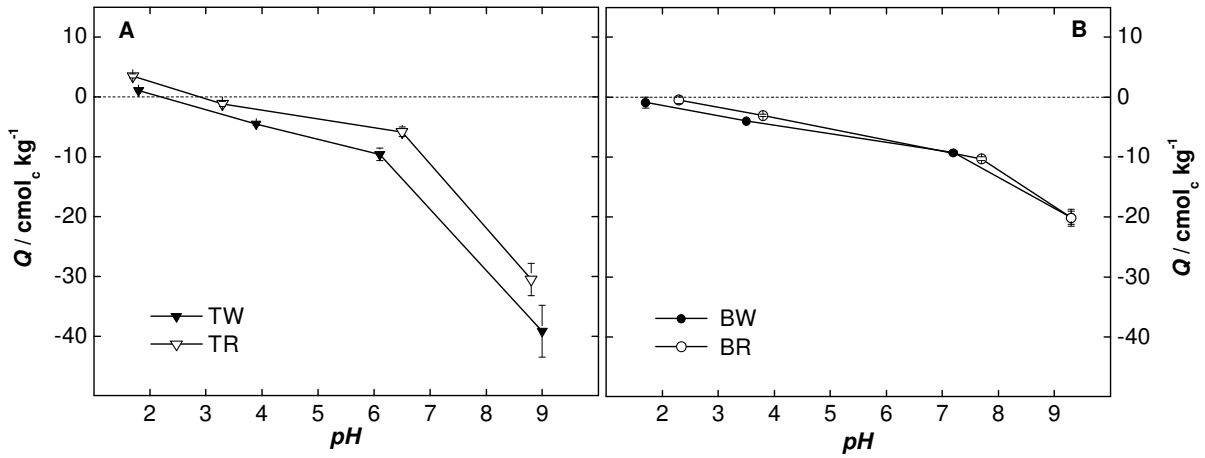

Figure 5-6: Particle surface charge (Q) of soil fraction < 63 µm of selected *pH*-treated sub-samples with highest, lowest and medium artificially induced *pH* from the wettable and repellent Buch samples (BW, BR) and Tiergarten samples (TW, TR, respectively).

The *pH* of isoelectric point (pH_{iep}), at which negative and positive surface charge are equal, resulting in a net zero surface charge, was found to be higher for TW and TR (~ 2 < *pH* < ~ 3) than for BW and BR (~ 1 < *pH* < ~ 2), respectively and below the *pH* region of maximum repellency ($pH_{(max.\ Repell)}$) for TW and TR (Table 5-3)

Table 5-3: Point of zero charge, pH_{pzc} (PCD) suggested by PCD measurement, *pH* of maximum repellency ($pH_{(max\ Repell)}$) and particle charge of maximum repellency ($Q_{(max\ Repell)}$).

	TW	TR	BW	BR
pH_{pzc} (PCD)	2.0	2.6	< 1.7	< 2.3
$pH_{(max\ Repell)}$	3.5 … 5.5	3 …4.5	< 5	< 5
$Q_{(max\ Repell)}$ / $cmol_c\ kg^{-1}$	-3 … -7	-1 … -4	> -5	> -5

The relationships between Θ_{sess} (which was the measure of repellency that exhibited the highest sensitivity to *pH*) and (measured and estimated values of) Q show maxima ($Q_{(max\ Repell)}$) (Figure 5-7) at ~ -2 and ~ -5 $cmol_c\ kg^{-1}$ for TR and TW, respectively (Table 5-3). Above $Q_{(max\ Repell)}$ Θ_{sess} decreases with increasing Q. Compared with TW, Q values of TR were found to be shifted to higher Θ_{sess} and less negative Q values. Θ_{sess} of BW and BR samples decreased with decreasing Q, but remained constant above

Q ~ -5 $cmol_c\ kg^{-1}$. Compared with BR, Q values of BW were shifted to lower Θ_{sess}, but Q values were found to be within a similar range. The differences between Θ_{sess} data of BW and BR are more pronounced at low Q and tend to converge as electroneutral conditions are approached.

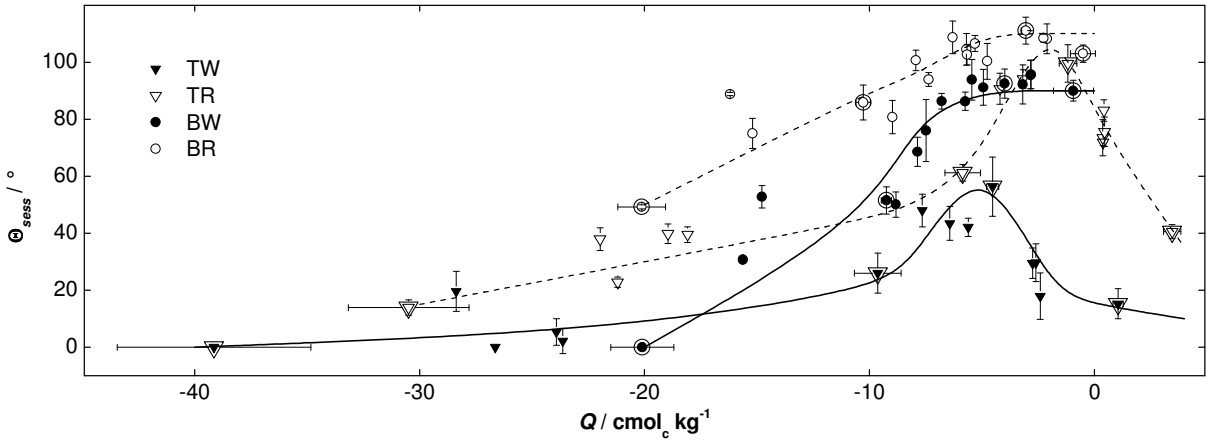

Figure 5-7: Wettability of the German Tiergarten (TW, TR) and Buch (BW, BR) samples as contact angle measured by sessile drop method depicted as a function of particle surface charge (Q) of soil fraction < 63 µm. Particle surface charge data are measured at four data points for each sample (indicated by double symbol frame) and linearly interpolated between these four points by their *pH* dependency (Figure 5-6).

5.5 Discussion

5.5.1 Comparison of contact angle and WDPT data

The differences in sensitivity between the various methods for assessment of water repellency probably arise as a consequence of various factors involved in the measurements and associated properties of soil. *WDPT* measurements involve the process of infiltration and any time dependent changes of soil surfaces arising from chemical interaction with water. Penetration depends on surface characteristics, particle and pore size distributions and the accessibility and continuity of pores. Soil texture and compaction will, therefore, influence the resistance to flow. At short *WDPT* (< 10s) the effects of minor changes in the resistance to flow will contribute a large relative error in *WDPT* reducing the sensitivity to detection of purely surface effects. The contact angle methods should avoid significant depth penetration of liquid and so avoid this error (see, for example, data for sample TW, in Figure 5-5 A-C). At *WDPT* < 5s the drop penetration in response to the hydrostatic pressure may form a significant component of the time measurement effected by the texture and compactness of the soil, and a subjective judgement as to when drop penetration is complete.

In the range $\Theta_{WPM} > 90°$, small differences in the surface characteristics of soil particle layers may enhance hydrophobicity through entrapment of air between particles. At $\Theta_{WPM} < 90°$ this entrapment is known to be less significant.

However, measurements are influenced, for example, by surface roughness, temperature and drop volume and useful comparisons arise when these are known and/or controlled.

5.5.2 Conformational arrangement of SOM molecules

All samples exhibited maximum repellency at *pH* 3 - 5, in good agreement with the *pKa* of carboxylic acids in HA from peat (Duval et al., 2005), at which a reduction in repulsion forces between these moieties may cause micelle-like aggregation or a more compact structure of HA with outward orientated hydrophobic moieties (Ohashi & Nakazawa, 1996; Terashima *et al.*, 2004; Duval *et al.*, 2005). However, such conformational changes may arise from changes in surface charge density likely to occur as soil moisture is gained or lost from soil electrolyte solution. Direct evidence of changes in conformational arrangement of SOM is not available from macroscopic methods; molecular scale investigations are required.

5.5.3 pH dependent changes in surface charge

Buffer systems in the German samples

The similarity of titration curves for BR, BW and TW (all with similar *TOC* contents) and the greater sensitivity of TR to HCl addition may reflect the significantly lower *TOC* and an associated lower buffering capacity of this sample.

Increase in pH

The decrease of soil water repellency with increasing *pH* may arise from an increased population of dissociated acidic functional groups associated with conjugate acid (ammonium) ions. NH_3 readily hydrolyses on contact with soil moisture, forming hydroxyl and ammonia ions. The ionic strength will increase, favouring further dissociation of carboxylic groups at $4 < pH < 7$ (Terashima *et al.*, 2004) and of phenolic groups at $8 < \mathrm{pH} < 11$ (MacCarthy *et al.*, 1979; Duval *et al.*, 2005). Our results suggest that sufficient deprotonated sites became available at the surface, to enhance its affinity for water, as *pH* was increased.

Decrease in pH

The decrease in repellency observed with reduction of soil *pH,* for TW, TR, NLR, UKR2, AUR1 and AUR2 samples, may arise from a surplus of a small quantity of acid, albeit in a concentrated form, able to maintain local acidic organic functional groups in protonated forms on contact with water. Basic functional groups such as amine groups, with $pK_a \sim 5$ are protonated with decreasing *pH* and rendered positively charged. If *C/N* data (Figure 5-2 C) is used as a surrogate measure of the mass concentration of amine groups, responsible for positive surface charge at low *pH*, then, the decrease in wettability with decreasing *pH* observed for TR and TW but not with BR and BW suggest that amines were of little influence.

Amphoteric mineral sesqui(hydr)oxides, (like iron, aluminium, manganese or silicon (hydr)oxides) may contribute to both positive and negative surface charge at high and low *pH* respectively. Samples from Tiergarten generally have a higher concentration of "Mehlich"-extractable iron than those from Buch (Figure 5-2 D). These iron species are neutral at about *pH* 4 and become positively charged with decreasing *pH*. Only in Tiergarten samples may the availability of surface active mineral proton acceptors (e.g. sesqui(hydr)oxides) be sufficient to achieve a net positive surface charge density with decreasing *pH* and, therefore, contribute to the increased wettability of Tiergarten samples at low *pH*.

The development of net positive titratable surface charge in TR and TW (Figure 5-6) at $2.5 < pH < 3$, below the *pH* where measurements of water repellency reach maxima, suggests that mineral oxides may be responsible. As samples from Buch, did not develop net positive charge and exhibited no significant reductions in measurements of water repellency at low *pH,* perhaps there was insufficient Fe-oxide available.

Net surface charge and wettability

The close proximity of the maximum *WDPT*s with the natural *pH* of the samples suggests that this coincides with the lowest density of ionisable sites. The presence of pH_{iep} consistently below $pH_{(max\ Repell)}$ for all B and T samples suggests that both, negatively and positively charged sites are present and some negative sites may be permanent. The net surface charge is then determined by the sum of (i) permanent charge ($Q_{perm.}$), (ii) variable charge caused by protonation/deprotonation reactions of organic functional groups (Q_{SOM}) and (iii) mineral compounds ($Q_{mineral}$) and can be expressed in a simplified form on the basis of averaged pK_i as follows:

$$\sum Q_i\,(pH) = Q_{perm.} + Q_{SOM} + Q_{\min eral}$$
$$= Q_{perm.} + \frac{Q_{\max,\,SOM}}{10^{(pK_{SOM}-pH)}+1} - \frac{Q_{\max,\,\min eral}}{10^{(pK_{1,\ \min eral}-pH)}+1} + \frac{Q_{\max,\,\min eral}}{10^{(pH-pK_{2,\ \min eral})}+1} \quad (5\text{-}5),$$

where $Q_{max,SOM}$ is the maximum negative charge from deprotonation of the organic functional groups, $Q_{max,mineral}$ is the maximum negative or positive charge from deprotonation or protonation of mineral compounds, pK_{SOM} is the deprotonation constant of *SOM* surfaces and $pK_{1,mineral}$ and $pK_{2,mineral}$ are the deprotonation and the protonation constants of mineral surfaces, respectively. At pH_{iep}, positive and negative charges have the same value and the net surface charge becomes zero. However, maximum repellency is probably not related to the zero net surface charge but rather with a minimum of the absolute equivalent number of charged sites ($\Sigma\sqrt{Q_i^2}$), which is expressed as follows:

$$\sum\sqrt{Q_i^2}\,(pH) = \sqrt{Q_{perm}^2} + \sqrt{[Q_{SOM}\,(pH)]^2} + \sqrt{[Q_{\min eral}\,(pH)]^2} \qquad (5\text{-}6)$$

Equations (5-5) and (5-6), and the measured ΣQ_i as a function of *pH*, allow a search of *pH* dependent contributions of Q_{SOM}, $Q_{mineral}$ and Q_{perm} to the net surface charge fulfilling the condition that a minimum $\Sigma\sqrt{Q_i^2}$ coincides with $pH_{(max\ repell)}$ (Figure 5-8, Table 5-4).

Figure 5-8 shows a combination of the measured net surface charge values (ΣQ) and a suggestion, how Q_{SOM} and $Q_{mineral}$ may change with *pH* resulting in a sum of absolute equivalent charge values ($\Sigma\sqrt{Q_i^2}$) which could explain the measured *pH* dependent wettability. At $pH_{(max\ Repell)}$ the lowest total number of charged sites is reached and at this *pH*, negatively charged sites dominate in all samples. In Tiergarten samples, below $pH_{(max\ Repell)}$, with the total number of charged sites, wettability increased with increasing Q and decreasing *pH* (Figure 8 TW, TR). This led to the assumption that in these samples mineral surfaces are probably available, where the positive surface charge increases with decreasing *pH*, exceeding the negative permanent charge. In contrast, in Buch samples, the lack of changes in wettability in the range of $pH_{(max\ Repell)}$ with < 5 indicates a nearly constant total number of charged sites (Figure 8 BW, BR). The number of protonable mineral surface sites is probably not high enough to increase wettability with decreasing *pH*.

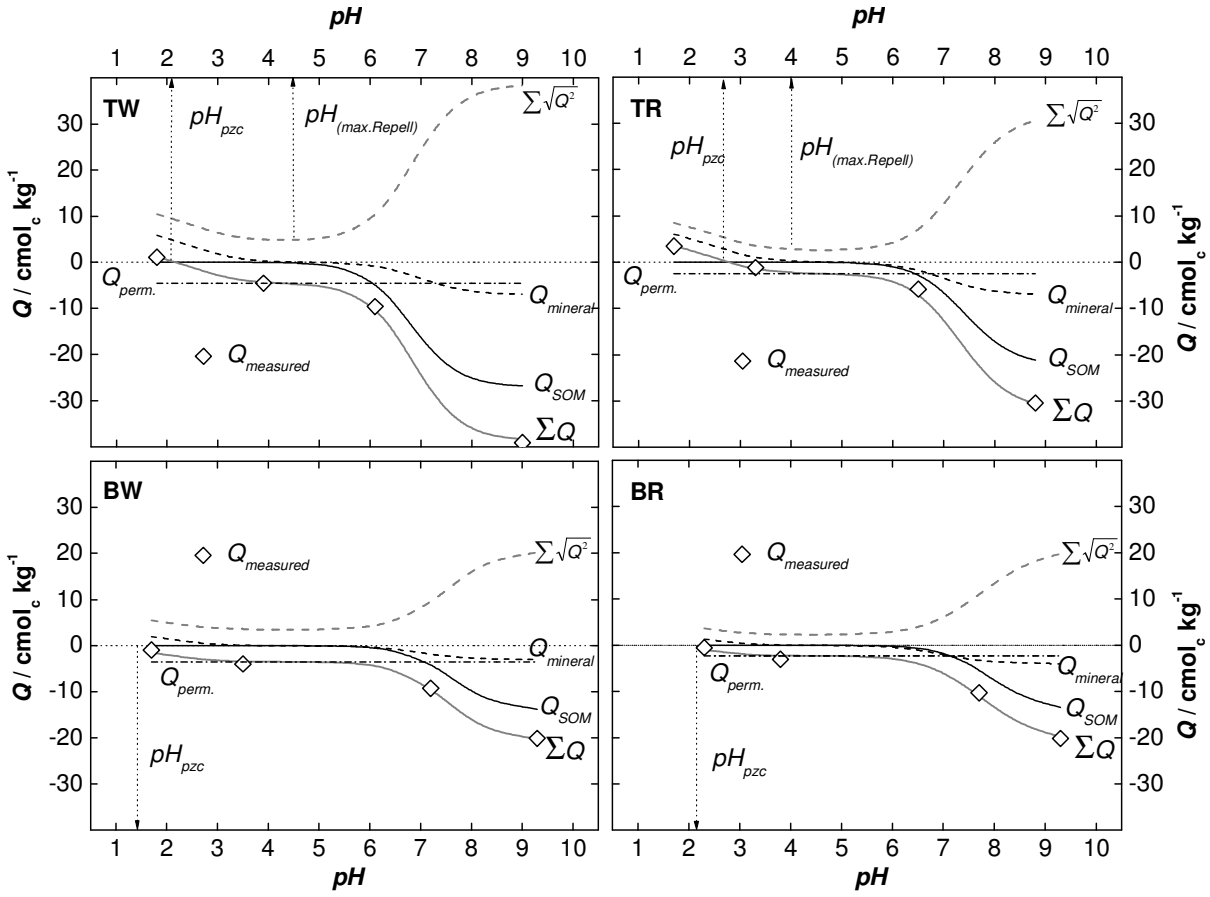

Figure 5-8: Simplified schematic *pH* dependent interplay of negative and positive surface charge provided by SOM surfaces (Q_{SOM}), by mineral surfaces ($Q_{mineral}$), and by permanent surface charge ($Q_{perm.}$) using equation 4 and 5 with parameters (Table 5-4) chosen to create a scenario with minimum $\Sigma\sqrt{Q_i^2}$ at $pH_{(max\ Repell)}$ and a ΣQ-curve crossing the data points of measured net surface charge of the respective German samples.

The parameters of equation 4 and 5 were adapted to create a scenario with minimum $\Sigma\sqrt{Q_i^2}$ at $pH_{(max\ Repell)}$. A ΣQ-curve was laid through the data points of the measured net surface charge of the respective German samples (Figure 5-8, Table 5-4).

This offers the following hypotheses which are not adequately tested with present data: (i) The wettable samples have higher Q_{perm} than the repellent samples and (ii) Tiergarten samples have higher $Q_{max,\ SOMl}$ and higher $Q_{max,\ mineral}$ than Buch samples (Table 4). (iii) The values of pK_{SOM} are with ~7 lower for Tiergarten samples than for Buch samples with ~8. Compared to generally postulated *pKa* values of 3 – 4 for strong acidic carboxylic surface groups, 5 – 6.5 for weak acidic groups and 7 – 8 for phenolic groups (Scheffer and Schachtschabel, 2002), the pK_{SOM} used in the scenario (Table 4) are rather high, which imples high amounts of weaker acidic functional groups and considerable amounts of phenolic groups. The chosen values for $pK_{mineral}$ and the resulting pH_{iep} of $Q_{mineral}$-curves at *pH* 4.5 – 5 suggest a higher influence of manganese-(hydr)oxide surface species which reveal a pH_{iep} of 3 – 5, than of silicium-, aluminium- or iron-(hydr)oxide surface species with pH_{iep} of 2 – 3.5, 5 – 9 and 7 – 10, respectively (Scheffer and Schachtschabel, 2002). However, it has to be kept in mind that the parameters in Table 4 are based on only 4 data points of measured surface net charge. Further investigations need to focus on distinguishing between different surface species, e.g. weak and strong acidic carboxylic sites, phenolic sites and the different relevant minerals compounds as clay minerals and sesqui(hydr)oxides and their contribution to the surface charge.

Table 5-4: Parameters chosen in order to create a scenario with minimum $\Sigma\sqrt{Q_i^2}$ at $pH_{(max\ Repell)}$ and a ΣQ-curve crossing the data points of measured net surface charge of the respective German samples (Figure 5-6) using equation 4 and 5: permanent charge ($Q_{perm.}$), maximum negative surface charge obtainable by deprotonation of SOM ($Q_{max,\ SOM}$) and the respective deprotonation constant (pK_{SOM}), maximum negative and positive surface charge obtainable by deprotonation / protonation of mineral surfaces ($Q_{max,\ mineral}$) and the respective deprotonation and protonation constants ($pK_{1,\ mineral}$ / $pK_{2,\ mineral}$).

	TW	TR	BW	BR
$Q_{perm.}$	-4.6	-2.5	-3.5	-2.3
$Q_{max,\ SOM}$	-27	-22	-14	-14
pK_{SOM}	6.8	7.4	7.6	7.9
$Q_{max,\ mineral}$	7	7	3	4
$pK_{1,\ mineral}$	7	7	7	7
$pK_{2,\ mineral}$	2.5	2.5	2	2

More detailed information about the contributions of the various surface species (e.g. weak and strong acidic carboxylic sites, phenolic sites and the fine mineral component clay minerals and sesqui(hydr)oxides) is required.

The occurrence of the peak in the Θ_{sess}-Q curve of TR at higher (more positive) Q than that of TW (Figure 5-7) may arise from the relatively low CEC_{pot}, of the former, which indicates a generally low negative charge density and, therefore, a generally lower wettability in TR than in TW. The occurrence of positive charge in the low *pH* range in T samples coincides with a decrease in repellency with decreasing *pH* which indicates a close relation between surface charge and repellency.

5.5.4 Chemical reactions

An alternative explanation for *pH* dependent changes in repellency is a change of SOM surface properties caused by chemical reactions. Acidic hydrolysis and condensation reactions as suggested in earlier studies as mechanisms controlling SWR in Buch samples (Diehl & Schaumann, 2007) are equilibrium reactions highly related to changes in water content and their influence maybe therefore minimized in the dried samples of the present study. Irreversible base catalyzed hydrolysis reactions, however, are less influenced by water content and may therefore be an additional explanation for decreasing repellency with increasing *pH*.

5.5.5 Comparison with former studies

In agreement with the results of Graber *et al.* (2009), the maximum of *WDPT* was found in the range of the original *pH* of the soil samples.

Previous studies involving adjustment of soil *pH* by addition of aqueous reagents to samples from the Buch site (Bayer & Schaumann, 2007) found that, following drying, samples were completely wettable over the range $3 < pH < 11$, whereas pronounced repellency occurred in these soils when the *pH* was adjusted using gases, with minimal effect on soil moisture content. The observed decrease in repellency with increasing *pH* of soils from the Netherlands, UK and Australia indicate that it is a soil characteristic spanning various locations. However, Tiergarten samples, exhibited a maximum repellency irrespective of how the *pH* was adjusted, but the repellency of Buch samples seem to be influenced by changes in water content resulting from the use of liquid reagents. The maximum repellency of Tiergarten samples reported by Bayer & Schaumann (2007) was at a higher *pH* than found in this study, despite a similar original soil *pH*. The addition of liquid NaOH may lead to additional SOM alteration which causes a shift in surface charge (Bayer & Schaumann, 2007) whereas the use of acidic and basic gases as reagents to modify soil *pH* without significant impact on soil moisture content appears to provide a useful route to examine the *pH* dependency of SWR.

Bayer & Schaumann (2007) observed that wettable and water repellent Tiergarten samples exhibited similar wettability when brought to similar *pH* by addition of liquid NaOH. In contrast, when *pH* was altered via the gas phase Tiergarten samples kept their original repellency differences, even at the same *pH*. The addition of moisture to the soil which accompanies the addition of liquid NaOH probably caused an equalisation of repellency differences between wettable and repellent samples. This indicates that the *pH* alteration via the gas phase applied in this study provide a new method with reduced side effects and is, therefore, suitable for changes in soil *pH* and investigations of those changes on SWR.

5.6 Conclusions

The comparison of 3 different methods for repellency determination showed the advantages and disadvantages of each method: In the range below ~ 10 s, *WDPT* showed a reduced sensitivity compared to the other two methods. In contrast to that, the

Wilhelmy plate method seemed to be less sensitive in the range of very strong repellency ($\Theta_{WPM} > 120°$) compared to *WDPT* and sessile drop method. The sessile drop method seemed to have no repellency range with reduced sensitivity, but revealed higher standard deviation between measurement repetitions compared to the two other methods.

By using a newly developed method to change the *pH* in soil samples via the gas phase without changing the moisture status, the influence of changes in soil *pH* on wettability was related to the number and type of protonable and de-protonable surface sites of organic and mineral surfaces in soils. The highest level of repellency is reached at the original *pH* when the number of charged sites is minimal. With increasing *pH* repellency decreased and negative surface charge increased caused by de-protonation. With respect to the repellency reaction on *pH* decrease, two types of soil can be distinguished: i) soils, in which repellency decreased with decreasing *pH* because of a sufficient number of protonable surface sites with a significant amount of positive surface charge and ii) soils, with no or not sufficient protonable surface sites to exhibit significant positive surface charge and, therefore, their repellency did not decrease with decreasing *pH*. Evidences suggested, that the protonable sites in case of the two Tiergarten samples, which are of the soil type I, were rather presented by mineral surfaces, than by organic functional groups.

5.7 Acknowledgments

The study was financed by the German Research Association DFG (research group Interurban, subproject HUMUS; SCHA 849/4-3). We thank Lydiya Shemotyuk for her help with the laboratory work and all members of the research group “U-Chemie” for lively discussions and constructive teamwork. We also want to thank Marta Casimiro for the help with lab work on the NL, UK and AU samples. The data of the long-term study of Buch and Tiergarten site are provided by the subproject SOIL from the Interurban research group and published here by the courtesy of Prof. Dr. Gerd Wessolek. We therefore want to thank him and the laboratory staff of Department of Soil Protection (Technical University Berlin).

6 Synthesis and general conclusions

6.1 Summary of observations

In order to link the individual results and conclusions of the present studies with each other and to find a more general explanation for the role of SOM for SWR, Table 6-1 gives an overview of the main observations made in this and in earlier investigations. Although repellency generally increased with gentle drying, the specific effects of drying on SWR vary between samples from different sites. In Buch samples, drying resulted in an approach of SWR of initially wettable and repellent samples. In contrast, the difference in SWR between initially wettable and repellent samples persists in Tiergarten. In Buch samples, higher drying temperatures lead to an increased degree of surface hydrophobicity. Since wetting, the reverse process, requires high activation energy, the surface hydrophobization is probably controlled by chemical processes. In Tiergarten samples, higher drying temperatures do not significantly increase surface hydrophobicity and activation energy of the wetting process is low. In these samples, water content dependent changes in SWR are thus likely controlled by physical processes e.g., water evaporation and condensation, or by physicochemical processes, e.g., changes in orientation of organic molecules without changes in chemical bonds.

Artificially induced *pH* changes in Buch and Tiergarten samples clearly show that *pH* has an effect on SWR At the original *pH*, the samples reveal the lowest number of charged surface sites and thus the highest SWR. The same pattern was observed in soil samples from sites of various geographical origins and with various vegetations. This indicates that under field conditions, the state with the lowest number of charged sites and with the highest degree of repellency is an equilibrium state for both initially wettable and repellent samples. A possible explanation is that at field *pH* a maximum of charged sites are occupied by counter ions. With changes in *pH*, additional charged sites develop which are not immediately occupied by the respective counter ions.

Only at the Tiergarten site do the aqueous extracts of repellent samples tend to have lower *pH* values and higher *EC* than aqueous extracts of wettable samples. In contrast, SWR in the Buch samples does not significantly decrease with decreasing *pH* below the original *pH*. This indicates that there is a significantly lower number of protonable and positively chargeable sites accessible for wetting in the Buch samples than in the Tiergarten samples.

The *pH* alteration via the liquid phase and subsequent drying of samples from the same sites (Bayer & Schaumann, 2007), however, results in complete wettability of both originally wettable and repellent Buch samples throughout almost the entire *pH* range. In contrast, Tiergarten samples show a maximum of SWR at *pH* 4.5-6.5, which are above their original *pH* levels. Furthermore, differences between wettable and repellent samples are completely compensated for after *pH* alteration in Tiergarten samples via the liquid

phase. This shows that in the liquid phase additional mechanisms gain in importance and superimpose the pure *pH* effect on repellency in the Tiergarten samples.

Table 6-1 Overview of the main observations of differences in soil characteristics and in responses on changes in environmental conditions between wettable and repellent samples from Buch and Tiergarten

	Buch	*Tiergarten*
Drying	*Increases repellency; differences between wettable and repellent samples decrease.*	*Increases repellency; differences between wettable and repellent samples remain.*
High drying temperature	*Increases surface hydrophobicity (DRIFT-CH_N).*	*Does not significantly affect surface hydrophobicity (DRIFT-CH_N).*
Activation energy of wetting	*65-94 kJ mol^{-1} Chemical reactions.*	*8-42 kJ mol^{-1} Physicochemical processes.*
pH alteration via gas phase	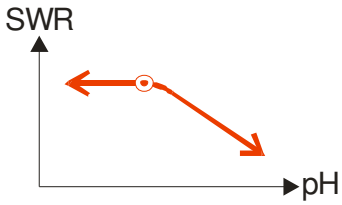 *Wettable = repellent samples.*	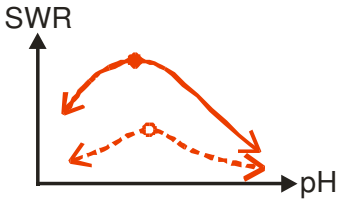 *Wettable < repellent samples.*
pH alteration via liquid phase	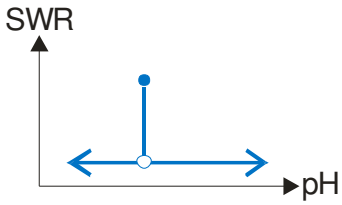 *Wettable = repellent samples.*	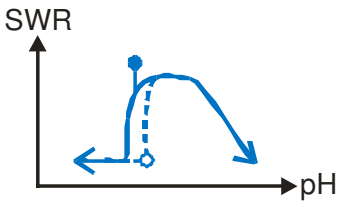 *Wettable = repellent samples.*
Field pH	*No significant relation with SWR.*	*Only samples with pH<4.6 exhibit repellency.*
Electrical conductivity	*No significant relation with SWR.*	*Higher conductivity for repellent samples.*
Surface tension of aqueous extracts	*Lower surface tension for repellent samples.*	*Lower surface tension for repellent samples.*

This overview not only shows a correlation of repellency with environmental conditions but also that responses of repellency to changes in environmental conditions are highly dependent on the specific location. The differences in the nature of repellency between the sites and between wettable and repellent samples within each site may help to draw some conclusions on the appearance of SWR and on the factors which determine the degree and nature of SWR. In order to explain these differences in nature and appearance of SWR, two theoretical models are developed.

6.2 Chemical nature of repellency in Buch samples

The activation energy of the wetting process for the Buch samples indicates that chemical reactions are involved in changes of SWR. Ester hydrolysis has already been suggested as a possible chemical reaction in the course of wetting of water repellent samples (Todoruk *et al.*, 2003b). Grasset & Amblès (1998) found that ester groups crosslink macromolecular chains of the matrix of humins. Bound by ester groups, aliphatic dicarboxylic acids may act as bridges between alkyl chains and fatty acids, alcohols and aromatic acids. These ester bonds may be disrupted by base catalysed hydrolysis (Grasset & Amblès, 1998) leading to an increasing number of carboxylate groups, i.e., an increasing number of charged sites at the SOM surface and thus an increased wettability. In the first reaction step of base catalysed hydrolysis, OH^- is reversibly added at the carboxyl carbon atom forming a tetrahedral activated intermediate. In alkaline solutions, this intermediate is irreversibly decomposed to the carboxylic acid anion and an alcohol in the second step (Schmeer *et al.*, 1990). For the second step, two competing reaction pathways were observed; one pathway involves a direct proton transfer, whereas a second pathway involves a water-assisted proton transfer through which the energy barrier for the decomposition of the tetrahedral intermediate is significantly lower than through the direct proton transfer (Zhan *et al.*, 2000). Thus, under dry conditions, these reactions are slow and accelerated only by increasing OH^- concentration, i.e. with increasing *pH*. This may explain why the dry Buch samples develop increasing wettability with increasing *pH* after treatment with gaseous NH_3 (Figure 6-1, red curve). The presence of water accelerates alkaline hydrolysis reactions (Zhan *et al.*, 2000). This explains why Buch samples are completely wettable after addition of liquid NaOH and subsequent incubation for 1 week at 20°C in closed containers (Bayer & Schaumann, 2007); (Figure 6-1, blue curve). Since alkaline hydrolysis is a non-reversible reaction, no recombination of esters is possible under alkaline conditions (Beyer & Walter, 1998):

$$R_1 - C(=O) - O - R_2 + OH^- \longrightarrow R_1 - C(=O) - O^- + R_2 - OH \qquad (6\text{-}1)$$

In contrast, long-term drying and drying at elevated temperatures under the original acidic *pH* conditions led to enhanced esterification and to an establishment of cross-linking between carboxylic and hydroxyl functional groups. This has been observed in solid state reactions between carboxylic acids and hydroxyl-groups of cellulosic material (Pantze *et al.*, 2008) and could explain why samples from Buch which reveal significant

differences in wettability in field moist state reached a comparable degree of repellency after long-term drying or after drying at elevated temperatures.

A reduction in *pH* favours acidic catalysed hydrolysis which is a reversible process:

$$R_1 - C(=O) - O - R_2 + H_2O \underset{}{\overset{[H^+]}{\rightleftharpoons}} R_1 - C(=O) - OH + R_2 - OH \qquad (6\text{-}2)$$

Acidic hydrolysis is driven by excess of water and the reverse reaction, e.g., the esterification is driven by deficiency of water. The ester concentration at the equilibrium point is independent from the *pH* but highly depends on the amount of available water. The *pH* solely determines the rate at which the equilibrium is reached. Therefore, at equilibrium under acidic conditions, the number of hydroxyl and carboxyl groups in dry samples is significantly lower than in wetted samples.

This can explain why the repellency of dry Buch samples remains constant with decreasing *pH* (Figure 6-1, red curve). Only the addition of liquid acid solution (Bayer & Schaumann, 2007) provides the excess of water necessary for shifting the equilibrium towards a significantly higher number of hydroxyl and carboxyl groups and leading to a decrease in repellency (Figure 6-1, blue curve). In that experiment, the subsequent air drying at 20°C at 50% *RH* for two days before measurement of repellency may not have reduced water content to a range in which the hydrolysis–esterification equilibrium is driven towards a re-esterification, or the equilibrium state was still not reached.

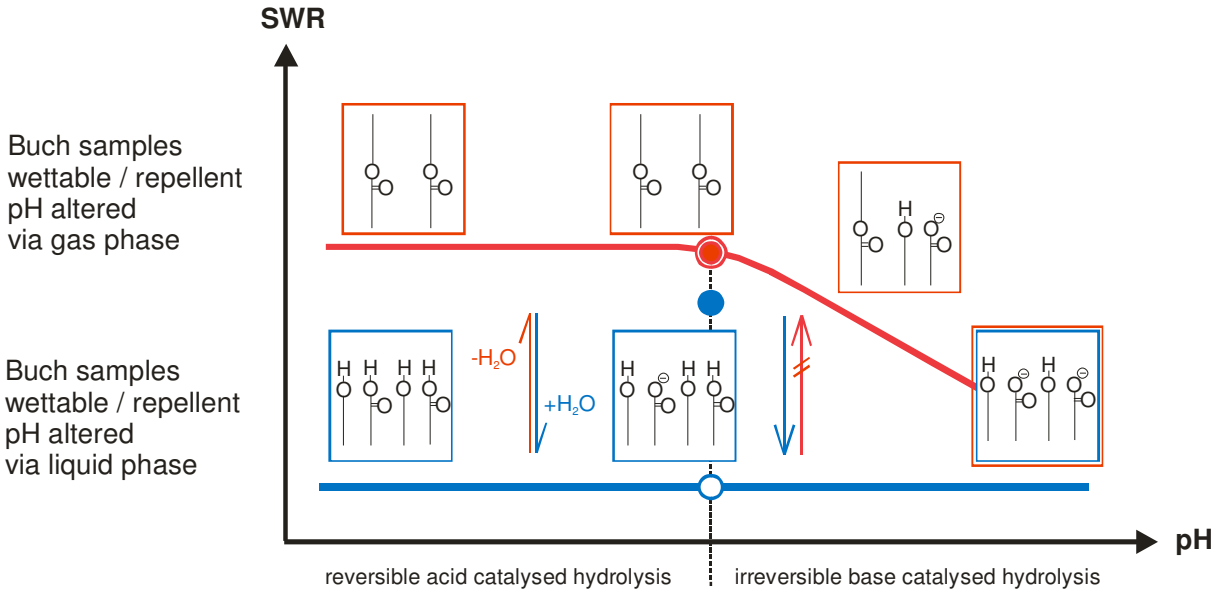

Figure 6-1 Schematic model of suggested mechanisms of changes in soil water repellency (SWR) upon altering pH via liquid phase and via gas phase in dried samples from Buch.

The suggested mechanism is not restricted to esterification but generally includes hydrolysis-condensation reactions which in SOM can occur between a variety of substances, e.g., carbohydrates, proteins, lipids etc.

In Buch samples, higher drying temperatures result in significantly higher relative abundance of aliphatic groups (CH_N) detectable by DRIFT than drying at lower

temperatures, and the correlation between *WDPT* and CH_N is of higher significance for Buch samples than for Tiergarten samples. Hydrolysis-esterification reactions are expected to occur not only in the outermost layer but also in deeper layers of SOM bulk phase, which are subjected to changes in water content. Since the penetration depth of IR radiation of DRIFT measurement exceeds the surface-active molecular layer, potential changes in the relative abundance of aliphatic groups caused by hydrolysis-condensation reactions are better detectable by DRIFT than changes of molecule arrangements in the very outermost layer as suggested for Tiergarten samples.

6.3 Physicochemical nature of repellency in Tiergarten

During gaseous *pH* alteration in dried Tiergarten samples, changes in wettability can be attributed to pure *pH* dependent charge effects as discussed in Chapter 5. The decrease in repellency with decreasing *pH* in Tiergarten but not in Buch samples coincides with the development of positive surface charge. The positive charge could arise from protonation of mineral surface sites e.g., Si-, Al-, Mn- or Fe-(hydr)-oxides. If this is the case, then such sites are expected to be less abundant in Buch than in Tiergarten samples which have a ~4% higher clay content than Buch samples (< 1 %).

The decrease in repellency with increasing *pH* can be explained by an increasing deprotonation of carboxylic and phenolic functional groups of humic substances. Base catalysed hydrolysis of ester bonds which requires activation energy, e.g., between 60 and 110 kJ mol^{-1} for sucrose laurates at *pH* 11 (Baker *et al.*, 2000), is not rate limiting in Tiergarten samples since the activation energy of the wetting process is below the range of the chemical reactions. Furthermore, increases in *pH* via the addition of liquid NaOH as investigated by Bayer & Schaumann (2007) resulted in a repellency-*pH* curve completely different from that of Buch samples (compare blue curves in Figure 6-1 and Figure 6-3, top). This leads to the conclusion that repellency in Tiergarten samples is controlled by additional mechanisms.

In Tiergarten samples, repellency differences between initially wettable and repellent samples remain following drying under various conditions as well as following artificially induced *pH* changes via gas phase. These differences disappear only after addition of liquid NaOH (Bayer & Schaumann, 2007). The addition of water and subsequent incubation and air drying result in a slight decrease of repellency of the repellent sample and an unchanged complete wettability of the wettable sample at their original *pH* (Bayer & Schaumann, 2007). In contrast to this, the addition of 0.05 M NaOH slightly increased the *pH* and resulted in a severe repellency for both the wettable and the repellent sample. This repellency maximum extends over a *pH* range between 4.5 up to 6.5. At *pH* ~10, both samples become completely wettable (Bayer & Schaumann, 2007). The broadening of *pH* range with maximum repellency and the shift toward a higher value compared to the *pH* alteration via the gas phase indicate that additional processes which favour the appearance of repellency in Tiergarten samples are induced by the addition of NaOH.

Since under field conditions repellent Tiergarten samples generally have *pH* values below 4.6, it is improbable that the increase in *pH* is responsible for the increase in repellency of the wettable samples observed in a *pH* range between 4.5 up to 6.5. A more plausible explanation arises from the differences in *EC* indicating a larger quantity of ions and suggesting a higher ionic strength in the aqueous extracts of repellent samples than of wettable samples. Addition of NaOH increases not only *pH* but also ionic strength. It is therefore also probable that the increase in ionic strength caused by NaOH addition induces a change in conformational arrangement of amphiphilic molecules at the SOM surface. At high ionic strength, repulsion forces between charged functional groups are effectively shielded by the counter ions (Fleer *et al.*, 1993). This allows charged groups to stay closer to each other and leads to more compact micelle-like structures. Upon drying, water evaporates slowly from the outside to the inside of the hydrated SOM surface layer. Hydrophilic groups orientate towards the inwards receding water front whereas hydrophobic chains orientate towards the air (Swift, 1999; Horne & McIntosh, 2000). Smaller, water-soluble amphiphilic molecules may form a hydrophobic layer by micelle-like intermolecular aggregations at the surface (Terashima *et al.*, 2004).

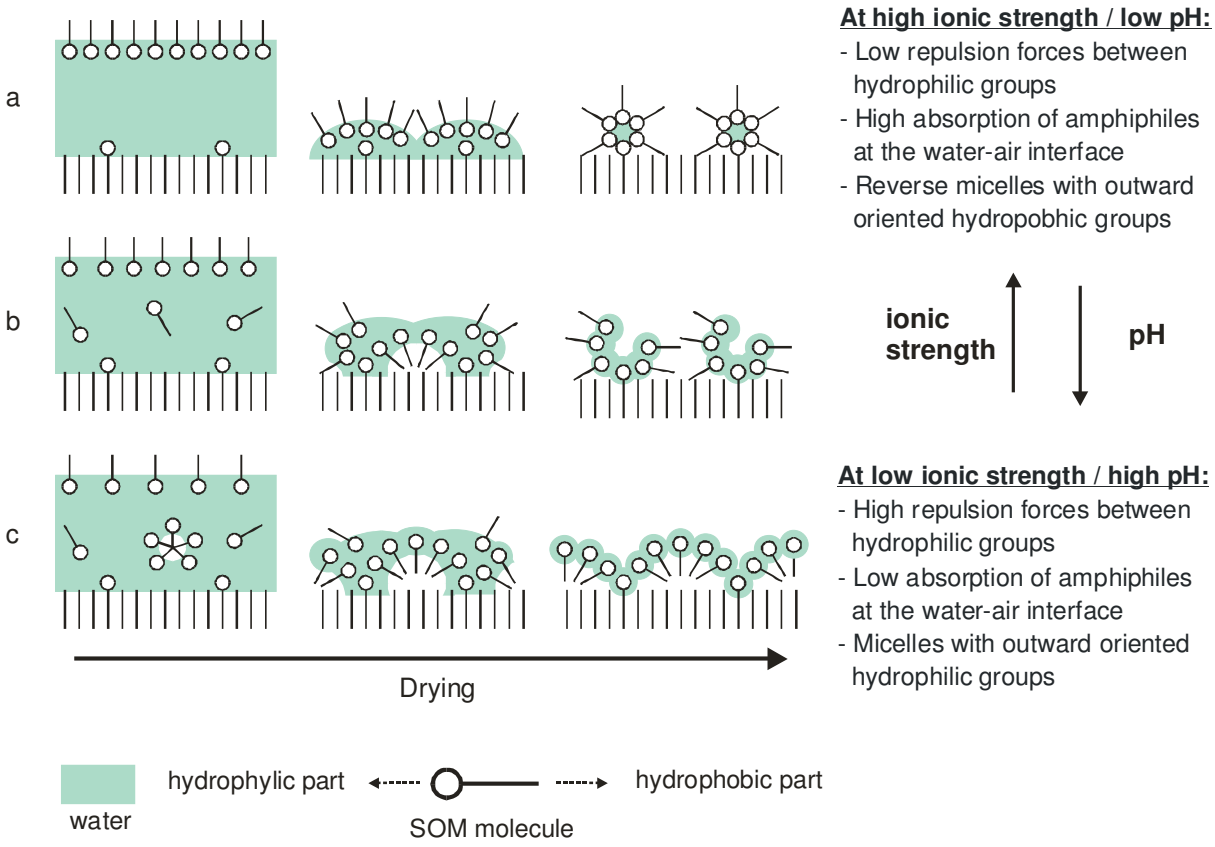

Figure 6-2 Suggested model of orientation of amphiphilic organic molecules at the SOM surface during drying in dependence of pH and ionic strength of the soil solution

Due to their polyelectrolytic character (Swift, 1989; Stevenson, 1994), larger HS may also undergo intramolecular micellization in principal as described by Engebretson & van Wandruszka (1994). At low *pH* and high ionic strength, these polyelectrolytes

preferentially form aliphatic loops and tails (Baßmann, 2001), which, together with aliphatic side chains, are directed outward and mask the inward-directed hydrophilic groups.

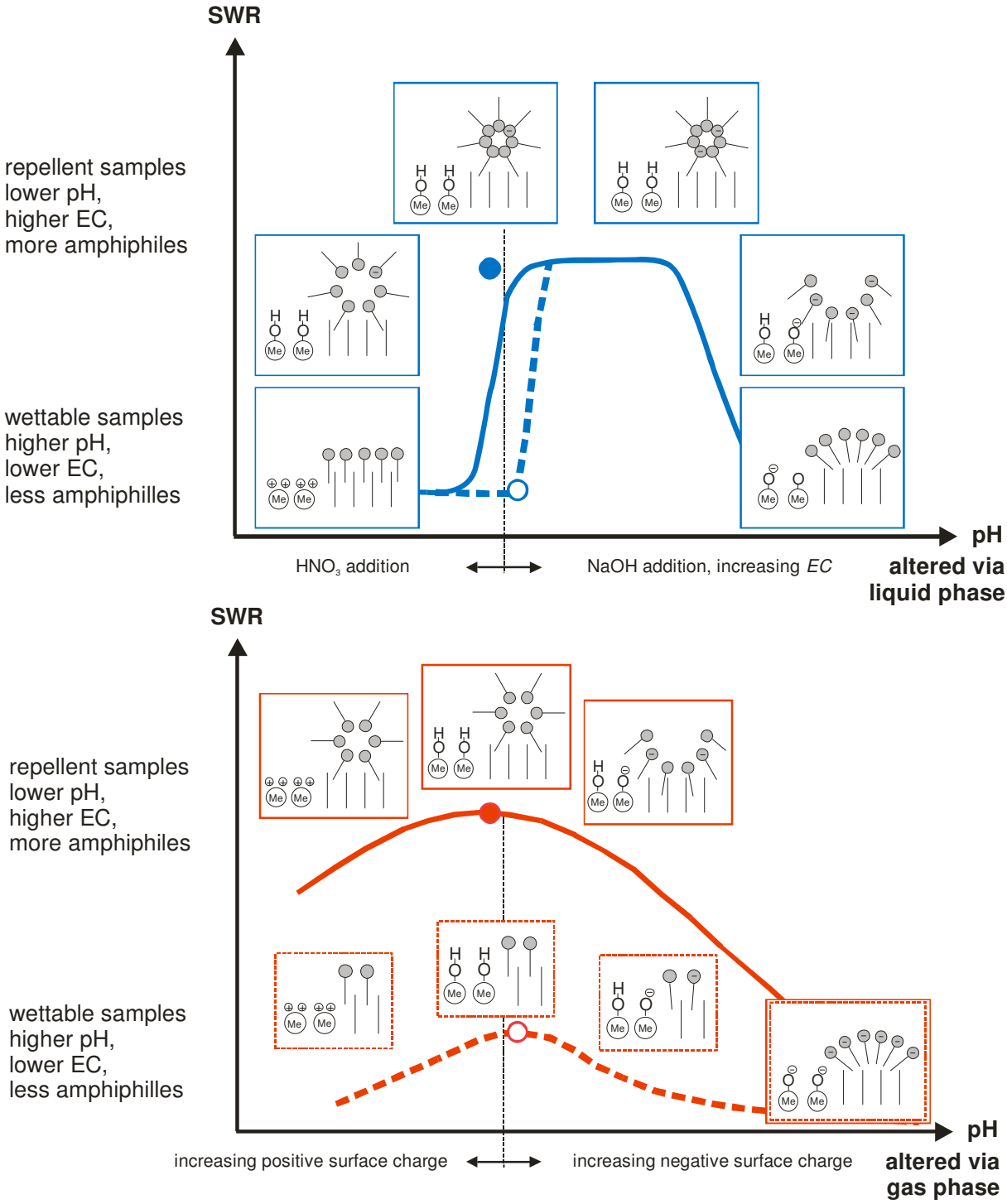

Figure 6-3 Schematic model of suggested mechanisms of changes in soil water repellency (SWR) in Tiergarten samples upon pH altering via liquid phase (top) and via gas phase in dried samples (bottom)

These spatial re-arrangements of amphiphilic molecules, which may transform wettable into repellent samples, probably require both a liquid environment and a high ionic strength as given by the addition of the liquid NaOH solutions. The liquid environment allows an effective re-arrangement and a water content driven orientation of

the amphiphilic molecules. High ionic strength weakens the repulsion forces between negatively charged functional groups and enables an aggregation of hydrophilic groups (Figure 6-2 c). Despite increasing *pH* and an increasing number of negatively charged groups, repellency persists within a certain *pH* range because the ionic strength also increases. At a higher *pH*, deprotonation overbalances the effects of ionic strength. Thus, in a *pH* range above 7, repulsion forces cannot be effectively weakened to lead to an aggregation of hydrophobic groups and surface exposition of hydrophilic groups (Figure 6-2 a).

Repellent Tiergarten samples tend to have a higher concentration or a higher efficiency of water soluble amphiphilic substances and a higher content of smaller-sized water soluble molecules than the respective wettable samples (Hurraß, 2006). This may favour the process of changes in spatial re-arrangements of amphiphilic molecules and the establishment of repellency. In contrast to this, lower concentration and larger molecule size of soluble amphiphiles and lower ionic strength in wettable samples inhibit the establishment of a stable repellent layer (compare curves and respective cartoons of molecular arrangements Figure 6-3, bottom). However, the addition of liquid NaOH solution increases ionic strength and thus enables a micelle-like aggregation of hydrophobic groups even in the originally wettable samples (compare curves and respective sketches of molecular arrangements in Figure 6-3, top).

The micelle-like aggregation and orientation of hydrophobic or hydrophilic molecule moieties toward the outside probably occurs only in the very outermost molecule layers of SOM and, most likely, mainly smaller water soluble molecules (Hurraß, 2006) are involved in this process. Deeper layers in SOM bulk phase are probably not affected by these mechanisms. This can explain why the correlation between *WDPT* and relative abundance of aliphatic groups (CH_N) detectable by DRIFT is significantly weaker in Tiergarten samples than in Buch samples since the penetration depth of radiation of DRIFT exceeds the surface-active molecular layer, and the signal from the surface is diluted by the contribution from deeper layers.

6.4 Site dependent causes for the nature of SWR

The nature of SWR in Buch and Tiergarten strongly differs between the sites. Although protonation, deprotonation and hydrolysis-condensation reactions as well as the arrangement of amphiphiles play a role for the appearance of SWR at both sites, different site-dependent conditions determine which process dominates the nature of SWR. The abovementioned conceptual models suggest water content and temperature dependent hydrolysis and condensation reactions in Buch and *pH* and ionic strength dependent changes in the arrangement of amphiphiles in Tiergarten as the dominant processes controlling SWR.

A cause for SWR in the former sewage disposal field at Buch is probably the high accumulation of organic matter derived from application of untreated mainly municipal waste water (including ~10 % industrial waste water) between 1905 and 1985. Under flooded conditions, organic matter could not be decomposed due to oxygen deficiency.

Once the site was no longer used as a sewage disposal field, the groundwater level sank and the initiated decomposition of organic matter resulted in acidification of the soil. The high input of organic matter from the municipal waste water most likely contained, among others, household chemicals and detergents as well as high loads of nitrogen- and phosphate-containing organic compounds which are highly reactive and therefore possible reactants for hydrolysis-condensation reactions. Since the sandy mineral soil part of the topsoil is likely completely coated by organic material, no free mineral surfaces are available to provide positive surface charges which would enhance wettability at this low *pH*. A high quantity of large pores and a low quantity of medium and fine pores in the sandy subsoil cause a very limited soil water storage capacity and fast drainage. The hydraulic conductivity of the sandy soil is extremely high under saturated conditions but reduced by three orders of magnitude under unsaturated conditions at pF 1.8 (Täumer, 2007). The physical properties of mineral soil (texture) and chemical properties of SOM together render this soil especially prone to preferential flow (Taumer *et al.*, 2006). Once dried, the repellent soil prevents an even infiltration of the precipitation, but the water collects in depressions, and infiltrates only at several points where hydraulic pressure sufficiently increased, root or animal channels facilitate penetration, or chemical reactions increase wettability of SOM. Short-term water saturated, the so-formed preferential flow paths drain the water very fast, whereas the adjacent soil zones remain dry, and a vicious cycle ensues.

In contrast to that, there is likely a higher salt content and a lower *pH* in repellent samples than in wettable samples at the Tiergarten site, which leads to the development of a stable amphiphilic layer with outward directed hydrophobic molecule moieties after drying. Remoistening of a repellent soil may slightly reduce repellency but does not change it into a wettable one. The Tiergarten soil is not grown naturally but rather an artificially backfilled topsoil with a clay content of ~5%. Therefore it has a higher water storage capacity than the Buch soil and not all mineral surfaces are covered with SOM, and thus free mineral surfaces are available to provide positive surface charge at low *pH*. A possible cause for SWR at this site is a mineral fertiliser for the lawn which is irregularly applied in form of salt grains. This leads to spots with higher salt concentrations. A low *pH* in these spots provide favourable conditions to SWR. A lower wettability in these spots consequently would lead to a reduced leaching of fertiliser and thus to an accumulation of salt that enhances the repellency effect.

Using the example of the two investigated sites, it can be shown that the nature of SWR and dominant processes which cause its appearance and dynamics are determined by the history of the respective site.

6.5 Final conclusion

The main conclusion of the present thesis is that SWR is subject to numerous antagonistically and synergistically interacting environmental factors. The degree of influence that a single factor exerts on SWR is site-specific, e.g., it depends on special characteristics of mineral constituents and SOM which underlies the influence of climate,

soil texture, topography, vegetation and the former and current use of the respective site. The investigation of two sites with exceptionally different natures of repellency leads to new insights in the variety of appearance of SWR since all investigations were carried out in parallel for both sites and are therefore directly comparable.

The previously debated assumption that changes in the arrangement of molecules and functional groups in the outer layer of SOM determine the degree of SWR (e.g., Tschapek, 1984; Horne & McIntosh, 2000; Doerr *et al.*, 2005b) can only explain the nature of repellency at the Tiergarten site. The spatial arrangement of these molecules upon drying is strongly influenced by properties of the soil solution, i.e., *pH, EC,* and quality and amount of dissolved organic matter (*DOM*). Both the macromolecular (e.g., Pignatello, 2003) and the supramolecular view of SOM (e.g., Schulten & Schnitzer, 1997) can explain changes in molecular arrangement. However, several observations suggest smaller water soluble substances are responsible for SWR. E.g., Arye *et al.* (Arye *et al.*, 2007) reported a decrease in soil hydrophobicity with increasing amount of *DOM* leached out by water. Hurraß & Schaumann (2006) found a higher quantity and a smaller size of amphiphiles in soil solutions of repellent samples than of wettable samples. Other authors made the observation that components accumulated in the soil solution serve to retard the wetting process (Krispil *et al.*, 2006; Graber *et al.*, 2007). These observations emphasize the role of smaller molecules for SWR and can thus be better explained by a more flexible supramolecular association of relatively small molecules at the SOM surface. The influence of ionic strength of soil solution on SWR has barely been investigated. Graber *et al.* (2009) varied salt concentration and *pH* in drop solution for penetration tests and found a higher influence of $CaCl_2$ than of NaCl concentration on drop penetration time and thus on repellency. They explained this influence with the complexation of fatty acid headgroups at positively charged surfaces or via divalent cation bridges at negatively charged surfaces. Since ionic strength of $CaCl_2$ is three times higher than that of NaCl at the same concentration, it cannot be excluded from their experiments that ionic strength may have a relevant influence on spatial arrangement of amphiphilic molecules at the SOM surface and thus on the penetration time. Unfortunately, drop penetration times were indicated as ratio of (salt solution) drop penetration time (*DPT*) to water drop penetration time (*WDPT*) and therefore does not allow for direct comparison with the results from the present investigations.

For the other site investigated in this study (Buch site), the results indicate that SOM can chemically bind water by hydrolysis reactions as suggested by Todoruk *et al.* (2003b). This mechanism is, however, dominant only in one of the two investigated sites. SOM, which was accumulated during the time when the site was used as a sewage disposal field, likely contains a high number of reactive functional groups and thus promotes *WC*-driven hydrolysis-condensation reactions as the mechanism controlling SWR. The high *WC* dependency of acidic hydrolysis-condensation equilibrium can also serve as an explanation for the concept of critical water content (WC_{crit}) for SWR (Dekker & Ritsema, 1994). Depending on SOM properties a *WC* is required that can provide an excess of water in the hydrolysis-condensation equilibrium and minimise

condensation. Below this *WC*, condensation increases with decreasing *WC,* and an increasing number of hydrophilic functional groups are bonded leading to reduced wettability. Hurraß (2006) reported no significant differences of the intrinsic SOM quality between wettable and repellent samples for the site with chemical nature of repellency. Together with the concept of *WC*-driven hydrolysis-condensation equilibrium, this can explain why Täumer et al. (2005) found a good correlation between SOM content and WC_{crit} for this site. Furthermore, according to this concept, increasing SWR with increasing drying temperature (Dekker *et al.*, 2001) can be explained by an increased reaction rate of condensation at an elevated temperature.

The two suggested mechanisms of chemical and physicochemical control of repellency are probably not restricted to one of the two sites but occur in some degree on both sites. Specific local soil characteristics determine which mechanism dominates and controls the nature of repellency. Furthermore, it cannot be excluded that additional mechanisms play an important role for repellency at other sites. However, the two suggested mechanisms together with the previous history of the sites allow identifying critical conditions which may favour SWR. Long hot and dry periods may enhance soil water repellency especially in soils with high organic accumulation. In these soils chemically bonded water can be released from organic matter by condensation reactions. Rewetting requires high activation energy, i.e. it is slow at ambient temperatures but can be accelerated by elevated temperature as long as the water does not evaporate. Special care is also needed in soils with a relatively high salt concentration, a low *pH*, and a SOM containing a relatively high amount of water soluble low molecular amphiphilic molecules. The combination of high ionic strength and low *pH* in the soil solution can favour the appearance of SWR after drying.

6.6 Outlook

Although the suggested conceptual models can explain most observations made in this study and many observations of other studies, they need to be verified further. New measurement techniques are required that enable the investigation of small scale variations in SOM or mineral surfaces.

IR radiation penetration depth of DRIFT spectroscopy exceeds the molecule layer relevant for surface characteristics and is disturbed by the high absorbance of water. Attenuated total reflectance (ATR) FTIR is a more promising method to identify functional groups in a surface layer of organic or mineral samples under natural conditions, i.e, with varying water content. Due to the small light penetration depth, the ATR technique is promising for highly absorbing samples and for surfaces and thin film measurements (Grdadolnik, 2002) and allows for measurements under various conditions, e.g., in solid or liquid state, at various *WCs*, *pHs*, salt and DOM concentrations, etc. In combination with the new methods developed in this study, ATR FTIR can help to test the hypothesis that water content driven SWR changes in the Buch samples are related to hydrolysis–condensation reactions. The time dependent sessile drop measurement (TISED) can be improved by the use of a video-based optical contact angle meter instead

of manual evaluation. Together with the artificial *pH* alteration via gas or liquid phase, wetting kinetics obtained by TISED dependent on *pH* will give further information about the nature of chemical reactions during the wetting process. ATR-FTIR measurements are expected to detect changes in the amount of functional groups upon drying and upon *pH* changes in the outer surface layer.

Another promising technology is atomic force microscopy (AFM) which can measure and image forces at surfaces at the nanometer level. Well established in material sciences, AFM has been used successfully in life sciences for characterisation of biochemical surfaces, e.g., proteins (Schuck, 2007), cell surfaces (Ahimou *et al.*, 2003), and organic self-assembled monolayers (SAM) on biological surfaces (Koch *et al.*, 2004). Its application in soil science has only just started (Ulery & Drees, 2008). A study of conformations and aggregate structures of sorbed natural organic on mineral surfaces (Namjesnik-Dejanovic & Maurice, 1997; Namjesnik-Dejanovic & Maurice, 2001) indicates a possible implication for investigations with respect to SWR. Currently, the first comprehensive AFM analysis of a natural soil system correlates to nano-scale observations with established soil science measurements regarding SWR (Cheng *et al.*, 2008). Thus, AFM measurements can help to verify the hypothesis that surface micelle formation induces repellency and investigate the relevance of this mechanism in dependence of *pH*, ionic strength and DOM content. Attractive or repulsive forces between chemically functionalized AFM tips and samples can give detailed information about surface-properties, e.g., hydrophobic or hydrophilic interactions, charge effects etc. Furthermore, by using AFM, the degree of mineral surfaces covered with organic coatings (Cheng *et al.*, 2008) can be compared between Buch and Tiergarten samples. To test the hypothesis that positive charge of mineral surfaces enhances wettability with decreasing *pH* in Tiergarten samples, the influence of artificially lowered *pH* on surface forces measured by AFM has to be investigated. Therefore, an important future challenge is the evaluation of specific nano-scale measures and respective methods which can be directly correlated with the degree of repellency.

Approaches in the described techniques will give new insights in the nature of SWR and can help in the better understanding of mechanisms leading to changes of SOM surface on a molecular scale. The knowledge about these mechanisms is closely connected to a general understanding of structure and behaviour of SOM which becomes increasingly important in the course of global climate change.

7 References

AG Boden, 2005. Bodenkundliche Kartieranleitung. Hannover. 5. Aufl. 438 pp.

Abadi Ghadim, A.K. 2000. Water repellency: a whole-farm bio-economic perspective. *Journal of Hydrology*, **231-232**, 396-405.

Adamson, A.W. & A. Petry. 1997. *Physical chemistry of surfaces*. John Wiley and Sons, New York.

Ahimou, F., A. Touhami & Y.F. Dufrêne. 2003. Real-time imaging of the surface topography of living yeast cells by atomic force microscopy. *Yeast*, **20**, 25-30.

Akim, L.G., G.W. Bailey & S.M. Shevchenko. 1998. A computational chemistry approach to study the interactions of humic substances with mineral surfaces. *Special Publication - Royal Society of Chemistry*, **228**, 133-145.

Arye, G., I. Nadav & Y. Chen. 2007. Short-term Reestablishment of Soil Water Repellency after Wetting: Effect on Capillary Pressure-Saturation Relationship. *Soil Science Society of America Journal*, **71**, 692-702.

Babejova, N. 2001. An influence of changing the humic acids content on soil water repellency and saturated hydraulic conductivity. *Journal of Hydrology and Hydromechanics*, **49**, 291-300.

Bachmann, J., G. Arye, M. Deurer, Susanne k. Woche, R. Horton, K.-H. Hartge & Y. Chen. 2006. Universality of a surface tension - contact-angle relation for hydrophobic soils of different texture. *Journal of Plant Nutrition and Soil Science*, **169**, 745-753.

Bachmann, J., A. Ellies & K.H. Hartge. 2000a. Development and application of a new sessile drop contact angle method to assess soil water repellency. *Journal of Hydrology*, **231-232**, 66-75.

Bachmann, J., R. Horton, S.A. Grant & R.R. Van Der Ploeg. 2002. Temperature Dependence of Water Retention Curves for Wettable and Water-Repellent Soils. *Soil Science Society of America Journal*, **66**, 44-52.

Bachmann, J., R. Horton, R.R. Van Der Ploeg & S. Woche. 2000b. Modified sessile drop method for assessing initial soil-water contact angle of sandy soil. *Soil Science Society of America Journal*, **64**, 564-567.

Bachmann, J. & G. Mchale. in press. Superhydrophobic surfaces: a model approach to predict contact angle and surface energy of soil particles. *European Journal of Soil Science*.

Baker, I., D. Furlong, F. Grieser & C. Drummond. 2000. Sugar fatty acid ester surfactants: Base-catalyzed hydrolysis. *Journal of Surfactants and Detergents*, **3**, 29-32.

Barrett, G. & O. Slaymaker. 1989. Identification, characterization, and hydrological implications of water repellency in mountain soils. *Catena*, **16**, 477-489.

Bashforth, S. & J.C. Adams. 1882. *An Attempt to Test the Theory of Capillary Action by Comparing the Theoretical and Measured Forms of Drops of Fluid* Bell and Co., London.

Bashforth, S. & J.C. Adams. 1883. *An Attempt to Test the Theory of Capillary Action by Comparing the Theoretical and Measured Forms of Drops of Fluid*. University Press Cambridge.

Baßmann, F. 2001. *Hydrophob modifizierte Polyacrylsäuren: Wechselwirkungen mit Bodenmineralen und organischen Schadstoffen*. PhD, Heinrich-Heine-Universität Düsseldorf.

Bayer, J.V. 2004. *Physikalische, chemische und biologische Einflussfaktoren für die Hydrophobizität auf urbanen Standorten (Physical, chemical and biological*

factors of influence for water repellency on urban sites). Diploma, TU Berlin, Berlin.

Bayer, J.V. & G.E. Schaumann. 2007. Development of soil water repellency in the course of isothermal drying and upon pH changes in two urban soils. *Hydrological Processes*, **21**, 2266 - 2275.

Berglund, K. & L. Persson. 1996. Water repellence of cultivated organic soils. *Acta agriculturae Scandinavica, Section B, Soil and plant science*, **46**, 145-152.

Beyer, H. & W. Walter. 1998. *Lehrbuch der Organischen Chemie*. S. Hirzel Verlag, Stuttgart; Leipzig.

Bisdom, E.B.A., L.W. Dekker & J.F.T. Schoute. 1993. Water repellency of sieve fractions from sandy soils and relationships with organic material on soil structure. *Geoderma*, **56**, 105-118.

Blackwell, P.S. 2000. Management of water repellency in Australia, and risks associated with preferential flow, pesticide concentration and leaching. *Journal of Hydrology*, **231-232**, 384-395.

Böckenhoff, K. & W.R. Fischer. 2001. Determination of electrokinetic charge with a particle-charge detector, and its relationship to the total charge. *Fresenius' Journal of Analytical Chemistry*, **371**, 670-674.

Buczko, U. & O. Bens. 2006. Assessing Soil Hydrophobicity and Its Variability through the Soil Profile Using Two Different Methods. *Soil Science Society of America Journal*, **70**, 718-727.

Buczko, U., O. Bens & W. Durner. 2006. Spatial and temporal variability of water repellency in a sandy soil contaminated with tar oil and heavy metals. *Journal of Contaminant Hydrology*, **88**, 249-268.

Cammeraat, L.H., S.J. Willott, S.G. Compton & L.D. Incoll. 2002. The effects of ants' nests on the physical, chemical and hydrological properties of a rangeland soil in semi-arid Spain. *Geoderma*, **105**, 1-20.

Capriel, P. 1997. Hydrophobicity of organic matter in arable soils: influence of management. *European Journal of Soil Science*, **48**, 457-462.

Capriel, P., T. Beck, H. Borchert, J. Gronholz & G. Zachmann. 1995. Hydrophobicity of the organic matter in arable soils. *Soil Biology and Biochemistry*, **27**, 1453-1458.

Celi, L., M. Schnitzer & M. Negre. 1997. Analysis of carboxyl groups in soil humic acids by a wet chemical method, Fourier-transform infrared spectroscopy, and solution-state carbon-13 nuclear magnetic resonance. A comparative study. *Soil Science*, **162**, 189-197.

Cerdà, A. & S.H. Doerr. 2007. Soil wettability, runoff and erodibility of major dry-Mediterranean land use types on calcareous soils. *Hydrological Processes*, **21**, 2325-2336.

Chatelier, R.C., A.M. Hodges, C.J. Drummond, D.Y.C. Chan & H.J. Griesser. 1997. Determination of the Intrinsic Acid-Base Dissociation Constant and Site Density of Ionizable Surface Groups by Capillary Rise Measurements. *Langmuir*, **13**, 3043-3046.

Chen, L.X.L. & J. Yu. 2005. Abiotic hydrolysis of poly[(R)-3-hydroxybutyrate] in acidic and alkaline media. *Macromolecular Symposia*, **224**, 35-46.

Chen, Y. & M. Schnitzer. 1978. The surface tension of aqueous solutions of soil humic substances. *Soil Science*, **125**, 7-15.

Cheng, S., R. Bryant, S.H. Doerr, P.R. Williams & C.J. Wright. 2008. Application of atomic force microscopy to the study of natural and model soil particles. *Journal of Microscopy*, **231**, 384-394.

Conte, P. & A. Piccolo. 1999. Conformational Arrangement of Dissolved Humic Substances. Influence of Solution Composition on Association of Humic Molecules. *Environmental Science and Technology*, **33**, 1682-1690.

De Jonge, L.W., O.H. Jacobsen & P. Moldrup. 1999. Soil Water Repellency: Effects of Water Content, Temperature, and Particle Size. *Soil Science Society of America Journal*, **63**, 437-442.

De Ruijter, M., P. Kolsch, M. Voue, J. De Coninck & J.P. Rabe. 1998. Effect of temperature on the dynamic contact angle. *Colloids and Surfaces, A: Physicochemical and Engineering Aspects*, **144**, 235-243.

Debano, L.F. 1969. Water repellent soils: A worldwide concern in management of soil and vegetation. *Agricultural Science Review*, **7**, 11-18.

Debano, L.F. 1981. Water repellent soils: a state-of-the-art. p. 20pp. Pacific Southwest Forest and Range Experiment Station, Berkeley, California.

Debano, L.F. 1992. The effect of fire to soil properties. pp. 151-156. USDA Forest Service General Technical Report, Portland.

Debano, L.F. 2000. Water repellency in soils: a historical overview. *Journal of Hydrology*, **231-232**, 4-32.

Dekker, L.W., S.H. Doerr, K. Oostindie, A.K. Ziogas & C.J. Ritsema. 2001. Water repellency and critical soil water content in a dune sand. *Soil Science Society of America Journal*, **65**, 1667-1674.

Dekker, L.W. & P.D. Jungerius. 1990. Water repellency in the dunes with special reference to the Netherlands. In: *Dunes of the European coasts* (ed. Bakker, T.W.), pp. 173-183. Catena-Verlag, Cremlingen-Destedt.

Dekker, L.W. & C.J. Ritsema. 1994. How water moves in a water repellent sandy soil: 1. Potential and actual water repellency. *Water Resources Research*, **30**, 2507-2517.

Deo, P., N. Deo, P. Somasundaran, S. Jockusch & N.J. Turro. 2005. Conformational Changes of Pyrene-Labeled Polyelectrolytes with pH: Effect of Hydrophobic Modifications. *Journal of Physical Chemistry B*, **109**, 20714-20718.

Derjaguin, B.V. & N.V. Churaev. 1986. Properties of Water Layers Adjacent to Interfaces. In: *Fluid Interfacial Phenomena* (ed. Croxton, C.A.), pp. 663-738. Wiley.

Diehl, D., R.H. Ellerbrock & G.E. Schaumann. 2009. DRIFT-Spectroscopy of untreated and dried soil samples of different wettability. *European Journal of Soil Science*, **60**, 557-566.

Diehl, D. & G.E. Schaumann. 2007. Wetting mechanism assessed from time dependent sessile drop shape. *Hydrological Processes*, **21**, 2255 - 2265.

Doerr, S.H. 1997. *Soil Hydrophobicity in Wet Mediterranean Pine and Eucalyptus Forests, Águeda Basin, North-Central Portugal*. Doctoral, University of Wales Swansea.

Doerr, S.H., L.W. Dekker, C.J. Ritsema, R.A. Shakesby & R. Bryant. 2002. Water repellency of soils: The influence of ambient relative humidity. *Soil Science Society of America Journal*, **66**, 401-405.

Doerr, S.H., P. Douglas, R.C. Evans, C.P. Morley, N.J. Mullinger, R. Bryant & R.A. Shakesby. 2005a. Effects of heating and post-heating equilibration times on soil water repellency. *Australian Journal of Soil Research*, **43**, 261–267.

Doerr, S.H., C.T. Llewellyn, P. Douglas, C.P. Morley, K.A. Mainwaring, C. Haskins, L. Johnsey, C.J. Ritsema, F. Stagnitti, G. Allison, A.J.D. Ferreira, J.J. Keizer, A.K. Ziogas & J. Diamantis. 2005b. Extraction of compounds associated with water repellency in sandy soils of different origin. *Australian Journal of Soil Research*, **43**, 225–237.

Doerr, S.H. & C.J. Ritsema. 2005. Water movement in hydrophobic soils. In: *Encyclopedia of Hydrological Sciences* (eds. Anderson, M.G. & McDonnell, J.). John Wiley & Sons.

Doerr, S.H., C.J. Ritsema, L.W. Dekker, D.F. Scott & D. Carter. 2007. Water repellence of soils: new insights and emerging research needs. *Hydrological Processes*, **21**, 2223-2228.

Doerr, S.H., R.A. Shakesby, L.W. Dekker & C.J. Ritsema. 2006. Occurrence, prediction and hydrological effects of water repellency amongst major soil and land-use types in a humid temperate climate. *European Journal of Soil Science*, **57**, 741-754.

Doerr, S.H., S.H. Shakesby & R.P.D. Walsh. 2000. Soil water repellency: its causes, characteristics and hydro-geomorphological significance. *Earth-Science Reviews*, **51**, 33-65.

Doerr, S.H. & A.D. Thomas. 2000. The role of soil moisture in controlling water repellency: new evidence from forest soils in Portugal. *Journal of Hydrology*, **231-232**, 134-147.

Douglas, P., K.A. Mainwaring, C.P. Morley & S.H. Doerr. 2007. The kinetics and energetics of transitions between water repellent and wettable soil conditions: a linear free energy analysis of the relationship between WDPT and MED/CST. *Hydrological Processes*, **21**, 2248-2254.

Dupré, A. 1869. *Théorie Mecanique de la Chaleur*. Gauthier-Villars, Paris.

Duval, J.F.L., K.J. Wilkinson, H.P. Van Leeuwen & J. Buffle. 2005. Humic substances are soft and permeable: Evidence from their electrophoretic mobilities. *Environmental Science & Technology*, **39**, 6435-6445.

Ellerbrock, R.H., H.H. Gerke, J. Bachmann & M.O. Goebel. 2005. Composition of organic matter fractions for explaining wettability of three forest soils. *Soil Science Society of America Journal*, **69**, 57-66.

Ellerbrock, R.H., A. Höhn & J. Rogasik. 1999. Functional Analysis of soil organic matter as affected by long-term manurial treatment. *European Journal of Soil Science*, **50**, 65-71.

Ellerbrock, R.H. & M. Kaiser. 2005. Stability and composition of different soluble soil organic matter fractions-evidence from d13C and FTIR signatures. *Geoderma*, **128**, 28-37.

Engebretson, R.R. & R. Van Wandruszka. 1994. Microorganization in dissolved Humic Acids. *Environmental Science and Technology*, **28**, 1934-1941.

Essington, M.E. 2003. *Soil and water chemistry*. CRC Press.

Ferreira, A.J.D., C.O.A. Coelho, R.P.D. Walsh, R.A. Shakesby, A. Ceballos & S.H. Doerr. 2000. Hydrological implications of soil water-repellency in *Eucalyptus globulus* forests, north-central Portugal. *Journal of Hydrology*, **231-232**, 165-177.

Fink, D.H. 1970. Water-repellency and infiltration-resistance of organic-film-coated soils. *Soil Science Society of America Proceedings*, **34**, 189-194.

Fleer, G.J., M.A.C. Stuart, M.H.M. Scheutjens, T. Cosgrove & B. Vincent. 1993. *Polymers at interfaces*. Chapmann & Hall, London.

Franco, C.M.M., P.J. Clarke, M.E. Tate & J.M. Oades. 2000. Hydrophobic properties and chemical characterisation of natural water repellent materials in Australian sands. *Journal of Hydrology*, **231-232**, 47-58.

Franks, F. 2000. *Water-A Matrix of Life*. Royal Society of Chemistry, 2nd Edition.

Goebel, M.-O., J. Bachmann, S.K. Woche & W.R. Fischer. 2005. Soil wettability, aggregate stability, and the decomposition of soil organic matter. *Geoderma*, **128**, 80-93.

Goebel, M.-O., J. Bachmann, S.K. Woche, W.R. Fischer & R. Horton. 2004. Water potential and aggregate size effects on contact angle and surface energy. *Soil Science Society of America Journal*, **68**, 383-393.

Gottwald, W. & G. Wachter. 1997. *IR-Spektroskopie für Anwender*. Wiley-VCH, Weinheim.

Graber, E.R. & M.D. Borisover. 1998. Evaluation of the Glassy/Rubbery Model for Soil Organic Matter. *Environmental Science and Technology*, **32**, 3286-3292.

Graber, E.R. & A.R.W. S. Taggera. 2009. Role of Divalent Fatty Acid Salts in Soil Water Repellency. *Soil Science Society of America Journal*, **73**, 541-549.

Graber, E.R., S. Tagger & R. Wallach. 2007. Do surface active substances from water repellent soils aid wetting? *European Journal of Soil Science*, **58**, 1393-1399.

Grasset, L. & A. Amblès. 1998. Structure of humin and humic acid from an acid soil as revealed by phase transfer catalyzed hydrolysis. *ORGANIC GEOCHEMISTRY*, **29**, 881-891.

Grdadolnik, J. 2002. ATR-FTIR Spectroscopy: Its Advantages and Limitations *Acta Chimica Slovenica*, **49**, 631-642.

Hallett, P.D. & I.M. Young. 1999. Changes to water repellence of soil aggregates caused by substrate-induced microbial activity. *European Journal of Soil Science*, **50**, 35-40.

Hoffmann, C. 2002. Schwermetallmobilität und Risikopotential der Rieselfelder Berlin Buch. *Bodenökologie und Bodengenese*, **35**, 226 pp.

Holmes-Farley, S.R., R.H. Reamey, T.J. Mccarthy, J. Deutch & G.M. Whitesides. 1985. Acid-base behavior of carboxylic acid groups covalently attached at the surface of polyethylene: The usefulness of contact angle in following the ionization of surface functionality. *Langmuir*, **1**, 725-740.

Holzhey, C.S. 1968. Water-repellent soils in southern California. In: *Symposium on water repellent soils*, pp. 31-41, Riverside, California.

Horne, D.J. & J.C. Mcintosh. 2000. Hydrophobic compounds in sands in New Zealand—extraction, characterisation and proposed mechanisms for repellency expression. *Journal of Hydrology*, **231-232**, 35-46.

Hudson, R.A., S.J. Traina & W.W. Shane. 1994. Organic matter comparison of wettable and nonwettable soils from bentgrass sand greens. *Soil Science Society of America Journal*, **58**, 361-367.

Hurraß, J. 2006. *Interactios between Soil Organic Matter and Water with special respect to the Glass Transition Behavior*. PhD, TU Berlin, Berlin.

Hurraß, J. & G.E. Schaumann. 2006. Properties of soil organic matter and aqueous extracts of actually water repellent and wettable soil samples. *Geoderma*, **132**, 222-239.

Imeson, A.C., J.M. Verstraten, E.J. Van Mullingen & J. Sevink. 1992. The effects of fire and water repellency on infiltration and runoff under Mediterranean type forest. *Catena*, **19**, 345-361.

Jaeger, F., S. Bowe & G.E. Schaumann. under revision. Evaluation of 1H NMR relaxometry for the assessment of pore size distribution in soil samples. *European Journal of Soil Science*.

Jaramillo, D.F., L.W. Dekker, C.J. Ritsema & J.M.H. Hendrickx. 2000. Occurrence of soil water repellency in arid and humid climates. *Journal of Hydrology*, **231-232**, 105-111.

Jex, G.W., B.H. Bleakley, D.H. Hubbell & L.L. Munro. 1985. High humidity-induced increase in water repellency in some sandy soils. *Soil Science Society of America Journal*, **49**, 1177-1182.

Karnok, K.A., E.J. Rowland & K.H. Tan. 1993. High pH treatments and the alleviation of soil hydrophobicity on golf greens. *Agronomy Journal*, **85**, 983-986.

King, P.M. 1981. Comparison of methods for measuring severity of water repellence of sandy soils and assessment of some factors that affect its measurement. *Australian Journal of Soil Research*, **19**, 275-285.

Kleber, M., P. Sollins & R. Sutton. 2007. A conceptual model of organo-mineral interactions in soils: self-assembly of organic molecular fragments into zonal structures on mineral surfaces. *Biogeochemistry*, **85**, 9-24.

Klitzke, S. & F. Lang. 2007. Hydrophobicity of soil colloids and heavy metal mobilization: Effects of drying. *Journal of Environmental Quality*, **36**, 1187-1193.

Koch, K., C. Neinhuis, H.-J. Ensikat & W. Barthlott. 2004. Self assembly of epicuticular waxes on living plant surfaces imaged by atomic force microscopy (AFM). *Journal of Experimental Botany*, **55**, 711-718.

Kostka, S.J. 2000. Amelioration of water repellency in highly managed soils and the enhancement of turfgrass performance through the systematic application of surfactants. *Journal of Hydrology*, **231-232**, 359-368.

Krispil, S.R., R. Wallach & E.R. Graber. 2006. Do surface active substances released from the soil contribute to repellency and wetting dynamics? In: *1st International Conference BIOHYDROLOGY 2006 - Impact of biological factors on soil hydrology*, Prague, Czech Republic.

Leboeuf, E.J. & W.J. Weber. 2000. Macromolecular characteristics of natural organic matter. 1. Insights from glass transition and enthalpic relaxation behavior. *Environmental Science and Technology*, **34**, 3623-3631.

Letey, J. 1969. Measurement of contact angle, water drop penetration time, and critical surface tension. In: *Water repellent soils - Proceedings of the symposium on water repellent soils*, p. 4347, University of California, Riverside, May 6-10, 1968.

Lichner, L., N. Babejova & L.W. Dekker. 2002. Effects of kaolinite and drying temperature on the persistence of soil water repellency induced by humic acids. *Rostlinná Výroba*, **48**, 203-207.

Lin, C.Y., W.C. Chou, J.S. Tsai & W.T. Lin. 2006. Water repellency of Casuarina windbreaks (Casuarina equisetifolia Forst.) caused by fungi in central Taiwan. *Ecological Engineering*, **26**, 283-292.

Lin, S.-Y., H.-C. Chang, L.-W. Lin & P.-Y. Huang. 1996. Measurement of dynamic/advancing/receding contact angle by video-enhanced sessile drop tensiometry. *Review of Scientific Instruments*, **67**, 2852-2858.

Llewellyn, C.T. 2004. *Studies of the molecular basis of soil water repellency*. Univerisity of Wales, Swansea.

Ma'shum, M. & V.C. Farmer. 1985. Origin and assessment of water repellency of a sandy South Australian Soil. *Australian Journal of Soil Research*, **23**, 623-626.

Ma'shum, M., M.E. Tate, G.P. Jones & J.M. Oades. 1988. Extraction and characterization of water-repellent material from Australian soils. *European Journal of Soil Science*, **39**, 99-110.

Maccarthy, P., M.J. Peterson, R.L. Malcolm & E.M. Thurman. 1979. Separation of humic substances by pH gradient desorption from a hydrophobic resin. *Analytical Chemistry*, **51**, 2041-2043.

Mainwaring, K.A. 2004. *Chemical characterisation and repellency-inducing effects of organic compounds isolated from sandy soils. Department of Chemistry*. University of Wales, Swansea.

Mainwaring, K.A., C.P. Morley, S.H. Doerr, P. Douglas, C.T. Llewellyn, G. Llewellyn, I. Matthews & B.K. Stein. 2004. Role of heavy polar organic compounds for water repellency of sandy soils. *Environmental Chemistry Letters*, **2**, 35-39.

Marmur, A. 1992. Penetration and displacement in capillary systems of limited size. *Advances in Colloid and Interface Science*, **39**, 13-33.

Mataix-Solera, J., V. Arcenegui, C. Guerrero, A.M. Mayoral, J. Morales, J. González, F. García-Orenes & I. Gómez. 2007. Water repellency under different plant species in a calcareous forest soil in a semiarid Mediterranean environment. *Hydrological Processes*, **21**, 2300-2309.

Mataix-Solera, J. & S.H. Doerr. 2004. Hydrophobicity and aggregate stability in calcareous topsoils from fire-affected pine forests in south-eastern Spain. *Geoderma*, **118**, 77-88.

Mcghie, D.A. & A.M. Posner. 1980. Water repellence of heavy textured Western australian surface soil. *Australian Journal of Soil Research*, **18**, 309-323.

Mcghie, D.A. & A.M. Posner. 1981. The effect of plant top material on the water repellence of fired sands and water repellent soils. *Australian Journal of Agricultural Research*, **32**, 609-620.

Mchale, G., H.Y. Erbil, M.I. Newton & S. Natterer. 2001. Analysis of Shape Distortions in Sessile Drops. *Langmuir*, **17**, 6995-6998.

Mchale, G., M.I. Newton & N.J. Shirtcliffe. 2005. Water repellent soils and its relationship to granularity, surface roughness and hydrophobicity: a material science view. *European Journal of Soil Science*, **56**, 445-452.

Mchale, G., N.J. Shirtcliffe, M.I. Newton & F.B. Pyatt. 2007. Implications of ideas on super-hydrophobicity for water repellent soil. *Hydrological Processes*, **21**, 2229-2238.

Mckissock, I., R.J. Gilkes, R.J. Harper & D. Carter, J. 1998. Relationships of water repellence to soil properties for different spatial scales of study. *Australian Journal of Soil Research*, **36**, 495-507.

Mckissock, I., R.J. Gilkes & W. Van Bronswijk. 2003. The relationship of soil water repellency to aliphatic C and kaolin measured using DRIFT. *Australian Journal of Soil Research*, **41**, 851-265.

Mehlich, A. 1984. Mehlich 3 soil test extractant: A modification of Mehlich 2 extractant. *Communications in Soil Science and Plant Analysis*, **15**, 1409 - 1416.

Michel, J.-C., L.M. Rivière & M.N. Bellon-Fontaine. 2001. Measurement of the wettability of organic materials in relation to water content by the capillary rise method. *European Journal of Soil Science*, **52**, 459-467.

Morley, C.P., K.A. Mainwaring, S.H. Doerr, P. Douglas, C.T. Llewellyn & L.W. Dekker. 2005. Organic compounds at different depths in a sandy soil and their role in water repellency. *Australian Journal of Soil Research*, **43**, 239-249.

Namjesnik-Dejanovic, K. & P.A. Maurice. 1997. Atomic force microscopy of soil and stream fulvic acids. *Colloids and Surfaces A: Physicochemical and Engineering Aspects*, **120**, 77-86.

Namjesnik-Dejanovic, K. & P.A. Maurice. 2001. Conformations and aggregate structures of sorbed natural organic matter on muscovite and hematite. *Geochimica Et Cosmochimica Acta*, **65**, 1047-1057.

Nguyen, H.V., J.L. Nieber, C.J. Ritsema, L.W. Dekker & T.S. Steenhuis. 1999. Modeling gravity driven unstable flow in a water repellent soil. *Journal of Hydrology*, **215**, 202-214.

Nguyen, T.T., L.J. Janik & M. Raupach. 1991. Diffuse Reflectance Infrared Fourier-Transform (Drift) Spectroscopy in Soil Studies. *Australian Journal of Soil Research*, **29**, 49-67.

Ohashi, H. & H. Nakazawa. 1996. The microstructure of Humic Acid-Montmorillonite composites. *Clay Minerals*, **31**, 347-354.

Pantze, A., O. Karlsson & U. Westermark. 2008. Esterification of carboxylic acids on cellulosic material: Solidstate reactions. *Holzforschung*, **62**, 136–141.

Piccolo, A. 2002. The supramolecular structure of humic substances: A novel understanding of humus chemistry and implications in soil science. *Advances in Agronomy*, **75**, 57-134.

Piccolo, A. & J.S.C. Mbagwu. 1999. Role of Hydrophobic Components of Soil Organic Matter in Soil Aggregate Stability. *Soil Science Society of America Journal*, **63**, 1801-1810.

Piccolo, A., R. Spaccini, G. Haberhauer & M.H. Gerzabek. 1999. Increased Sequestration of Organic Carbon by Hydrophobic Protection. *Naturwissenschaften*, **86**, 496-499.

Pignatello, J.J. 2003. Polymer sorption theory applied to macromolecular forms of natural organic matter. In: *Preprints of Extended Abstracts presented at the ACS National Meeting, American Chemical Society, Division of Environmental Chemistry*, pp. 883-888.

Richardson, J.L. 1984. Field Observation and measurement of water repellency for soil surveyors. *Soil Survey Horizons*, **25**, 32-36.

Ritsema, C.J. & L.W. Dekker. 1994. Soil moisture and dry bulk density patterns in bare dune sands. *Journal of Hydrology*, **154**, 107-131.

Ritsema, C.J. & L.W. Dekker. 2000. Preferential flow in water repellent sandy soils: principles and modeling implications. *Journal of Hydrology*, **231-232**, 308-319.

Roberts, F.J. & B.A. Carbon. 1971. Water repellence in sandy soils of south-western Australia. I. Some studies related to field occurence. *Field station record*, **10**, 13-20.

Roberts, F.J. & B.A. Carbon. 1972. Water repellence in sandy soils of southwestern Australia. II. Some chemical characteristics of the hydrophobic skins. *Australian Journal of Soil Research*, **10**, 35-42.

Robichaud, P.R. 2000. Fire effects on infiltration rates after prescribed fire in Northern Rocky Mountain forests, USA. *Journal of Hydrology*, **231-232**, 220-229.

Roper, M.M. 2005. Managing soils to enhance the potential for bioremediation of water repellency. *Australian Journal of Soil research*, **43**, 803-810.

Roy, J.L., B. Mcgill & P. Rawluk. 1999. Petroleum residues as water-repellent substances in weathered nonwettable oil-contaminated soils. *Canadian Journal of Soil Science*, **79**, 367-380.

Roy, J.L. & W.B. Mcgill. 2002. Assessing soil water repellency using the molarity of ethanol droplet (MED) test. *Soil Science*, **167**, 83-97.

Savage, S.M. 1974. Mechanism of fire-induced water repellency in soil. *Soil Science Society of America Proceedings*, **38**, 652-657.

Savage, S.M., J.P. Martin & J. Letey. 1969. Contribution of some soil fungi to natural and heat-induced water repellency in sand. *Soil Science Society of America Proceedings*, **33**, 405-409.

Savage, S.M., J. Osborn, J. Letey & C. Heaton. 1972. Substances contributing to fire-induced water repellency in soils. *Soil Science Society of America Proceedings*, **36**, 674-678.

Schaumann, G.E. 2006. Soil organic matter beyond molecular structure. 1. Macromolecular and supramolecular characteristics. *Journal of Plant Nutrition and Soil Science*, **169**, 145-156.

Schaumann, G.E. & M. Bertmer. 2008. Do water molecules bridge soil organic matter molecule segments? *European Journal of Soil Science*, **59**, 423-429.

Schaumann, G.E., E. Hobley, J. Hurraß & W. Rotard. 2005. H-NMR Relaxometry to monitor wetting and swelling kinetics in high organic matter soils. *Plant and Soil*, **275**, 1-20.

Schaumann, G.E., C. Siewert & B. Marschner. 2000. Kinetics of the release of dissolved organic matter (DOM) from air-dried and pre-moistened soil material. *Journal of Plant Nutrition and Soil Science*, **163**, 1-5.

Schlenther, L.M., B.; Hoffmann, C.; Renger, M. 1996. Ursachen mangelnder Anwuchserfolge bei der Aufforstung der Rieselfelder in Berlin-Buch. *Verhandlungen der Gesellschaft für Ökologie*, **25**, 349-359.

Schmeer, G., S. Riembauer & J. Barthel. 1990. The influence of hydrophobic solvation on the alkaline hydrolysis of ethyl esters of polar substituted 2-methylpropionic acids in water. *Journal of Solution Chemistry*, **19**, 1175-1189.

Scholl, D.G. 1975. Soil Wettability and Fire in Arizona Chaparral. *Soil Science Society of America Journal*, **39**, 356-361.

Schuck, P. 2007. *Protein interactions: biophysical approaches for the study of complex reversible systems*. Springer.

Schulten, H.-R. & M. Schnitzer. 1997. Chemical model structures for soil organic matter and soils. *Soil Science*, **162**, 115-130.

Schwuger, M.J. 1996. *Lehrbuch der Grenzflächenchemie*. Georg Thieme Verlag, Struttgart-New York.

Shakesby, R.A., C.J. Chafer, S.H. Doerr, W.H. Blake, P. Wallbrink, G.S. Humphreys & B.A. Harrington. 2003. Fire severity, water repellency characteristics and hydrogeomorphical changes following the Christmas 2001 Sydney forest fires. *Australian Geographer*.

Shakesby, R.A., S.H. Doerr & R.P.D. Walsh. 2000. The erosional impact of soil hydrophobicity: current problems and future research directions. *Journal of Hydrology*, **231-232**, 178-191.

Siebold, A., M. Nardin, J. Schultz, A. Walliser & M. Oppliger. 2000. Effect of dynamic contact angle on capillary rise phenomena. *Colloids and Surfaces A: Physicochemical and Engineering Aspects*, **161**, 81-87.

Siebold, A., A. Walliser, M. Nardin, M. Oppliger & J. Schultz. 1997. Capillary Rise for Thermodynamic Characterization of Solid Particle Surface. *Journal of Colloid and Interface Science*, **186**, 60-70.

Spaccini, R., A. Piccolo, P. Conte, G. Haberhauer & M.H. Gerzabek. 2002. Increased soil organic carbon sequestration through hydrophobic protection by humic substances. *Soil Biology and Biochemistry*, **34**, 1839-1851.

Sparks, D.L. 1985. Kinetics of ionic reactions in clay minerals and soils. *Adv. Agron.*, **38**, 231-266.

Spiros, H.A. & G.H. Savvas. 1998. The work of adhesion of polymer/wall interfaces and its association with the onset of wall slip. *Journal of Rheology (New York)*, **42**, 795-812.

Steenhuis, T.S., J.C. Rivera, C.J.M. Hernández, M.T. Walter, R.B. Bryant & P. Nektarios. 2001. Water Repellency in New York State Soils.

Stenius, P. 1994. Theory of the ring and Wilhelmy plate methods. *Helsinki University of Technology, Laboratory of Forest Products Chemistry, Reports, Series C*, **2**, 22pp.

Stevenson, F.J. 1985. Geochemistry. In: *Humic substances in soil, sediment, and water: geochemistry, isolation and characterization.* (ed. Aiken, G.R., McKnight, D. M., Wershaw, R. L., MacCarthy, P.), pp. 13-52. John Wiley & Sons, New York.

Stevenson, F.J. 1994. *Humus Chemistry : Genesis, Composition, Reactions*. Wiley, New York.

Swift, R.S. 1989. Molecular weight, size, shape and charge characterisitcs of humic substances: Some basic considerations. In: *Humic substances II: In search of structure* (eds. Hayes, M.H.B., MacCarthy, P., Malcolm, R.L. & Swift, R.S.), pp. 449-465. John Wiley & Sons, New York.

Swift, R.S. 1999. Macromolecular properties of soil humic substances: fact, fiction, and opinion. *Soil Science*, **164**, 790-802.

Täumer, K. 2007. *Analyzing soil water repellency phenomena*. PhD, TU Berlin, Berlin.

Taumer, K., H. Stoffregen & G. Wessolek. 2006. Seasonal dynamics of preferential flow in a water repellent soil. *Vadose Zone Journal*, **5**, 405-411.

Täumer, K., H. Stoffregen & G. Wessolek. 2005. Determination of repellency distribution using soil organic matter and water content. *Geoderma*, **125**, 107-115.

Teramura, A.H. 1980. Relationships between Stand Age and Water Repellency of Chaparral Soils. *Bulletin of the Torrey Botanical Club*, **107**, 42-46.

Terashima, M., M. Fukushima & S. Tanaka. 2004. Influence of pH on the surface activity of humic acid. Micelle-like aggregate formation and interfacial adsorption. *Colloids and Surfaces, A: Physicochemical and Engineering Aspects*, **247**, 77-83.

Todoruk, T.R., C.H. Langford & A. Kantzas. 2003a. Pore-Scale Redistribution of Water during Wetting of Air-Dried Soils As Studied by Low-Field NMR Relaxometry. *Environmental Science and Technology*, **37**, 2707-2713.

Todoruk, T.R., M. Litvina, A. Kantzas & C.H. Langford. 2003b. Low-Field NMR Relaxometry: A Study of Interactions of Water with Water-Repellant Soils. *Environmental Science and Technology*, **37**, 2878-2882.

Tremblay, L. & J.P. Gagne. 2002. Fast quantification of humic substances and organic matter by direct analysis of sediments using DRIFT spectroscopy. *Analytical Chemistry*, **74**, 2985-2993.

Tschapek, M. 1984. Criteria for determining the hydrophilicity - hydrophobicity of soils. *Zeitschrift für Pflanzenernährung und Bodenkunde*, **147**, 137-149.

Ulery, A.L. & L.R. Drees. 2008. *Methods of Soil Analysis: Part 5 - Mineralogical Methods*. American Society of Agronomy.

Valat, B., C. Jouany & L.M. Rivière. 1991. Characterization of the wetting properties of air-dried peats and composts. *Soil Science*, **152**, 100-107.

Van't Woudt, B.D. 1959. Particle coatings affecting the wettability of soils. *Journal of Geophysical Research*, **64**, 263-267.

Varela, M.E., E. Benito & E. De Blas. 2005. Impact of wildfires on surface water repellency in soils of northwest Spain. *Hydrological Processes*, **19**, 3649-3657.

Waksman, S.A. & H.W. Reuszer. 1932. On the origin of the uronic acids in the humus of soil, peat, and composts. *Soil Science*, **33**, 135.

Wallach, R. & E.R. Graber. 2007. Infiltration into effluent irrigation-induced repellent soils and the dependence of repellency on ambient relative humidity. *Hydrological Processes*, **21**, 2346-2355.

Wallis, M.G. & D.J. Horne. 1992. Soil water repellency. *Advances in Soil Science*, **20**, 91-146.

Wallis, M.G., D.J. Horne & A.S. Palmer. 1993. Water-repellency in a New Zealand development sequence of yellow-brown sands. *Australian Journal of Soil Research*, **31**, 641-654.

Wander, I.W. 1949. An interpretation of the cause of restistance to wetting in Florida Soils. *Florida State Horticultural Society*, **11**, 92-94.

Washburn, E.W. 1921. The dynamics of capillary flow. *The Physical Review Letters* **17**, 273–283.

Wedler, G. 1987. *Lehrbuch der physikalischen Chemie*. VCH Verlagsgesellschaft mbH, Weinheim.

Wendland, F. 1993. *Der Große Tiergarten in Berlin : seine Geschichte und Entwicklung in fünf Jahrhunderten*. Mann, Berlin.

Wenzel, R.N. 1949. Surface roughness and contact angle. *Journal of Physical and Colloid Chemistry*, **53**, 1466-1467.

Wershaw, R.L. 1986. A new model for humic materials and their interactions with hydrophobic organic chemicals in soil-water or sediment-water systems. *Journal of Contaminant Hydrology*, **1**, 29-45.

Wershaw, R.L. 1999. Molecular aggregation of humic substances. *Soil Science*, **164**, 803-813.

Wessel, A.T. 1988. On using the effective contact angle and water drop penetration time for classification of water repellency in dune soils. *Earth Surface Processes and Landforms*, **13**, 555-562.

Wilhelmy, L. 1863. Ueber die Abhängigkeit der Capillaritäts - Constante des Alkohols von Substanz und Gestalt des benetzten festen Körpers. *Annalen der Physik und Chemie*, **119**, 177.

Yang, B., P.S. Blackwell & D.F. Nicholson. 1996. A numerical model of heat and water movement in furrow-sown water repellent sandy soils. *Water Resources Research*, **32**, 3051-3061.

Young, T. 1855. *Miscellaneous Works of the Late Thomas Young*. Murray, London.

Zhan, C.-G., D.W. Landry & R.L. Ornstein. 2000. Reaction Pathways and Energy Barriers for Alkaline Hydrolysis of Carboxylic Acid Esters in Water Studied by a Hybrid Supermolecule-Polarizable Continuum Approach. *Journal of American Chemical Society*, **122**, 2621-2627.

Ziogas, A.K., L.W. Dekker, K. Oostindie & C.J. Ritsema. 2003. Soil water repellency in northeastern Greece. In: *Soil Water Repellency: Occurence, Consequences and Amelioration* (eds. Ritsema, C.J. & Dekker, L.W.), p. 325pp. Elsevier, Amsterdam.

Ziogas, A.K., L.W. Dekker, K. Oostindie & C.J. Ritsema. 2005. Soil water repellency in north-eastern Greece with adverse effects of drying on the persistence. *Australian Journal of Soil Research*, **43**, 281–289.

8 Annex

8.1 List of abreviations

Latin symbols

a	semi-major axis of an ellipse	[m]
A_{act}	actual contact area	[m^2]
A_{geo}	geometric area, i.e., the planar projection of A_{act}	[m^2]
$A_{geo,s}$	geometric water covered solid area	[m^2]
A_i	area of the material i	[m^2]
A_p	cross sectional area of the plate	[m^2]
A_s	surface area	[m^2]
A_{tot}	total area	[m^2]
b	semi-minor axis of an ellipse	[m]
B_1; B_2	weighting factors of the subprocesses at the whole process	[-]
C	geometrical factor	[m]
c	weight concentration	[mg kg^{-1} SOM]
C/N	C to N ratio	[-]
CEC_{pot}	potential cation exchange capacity	[$cmol_c$ kg^{-1}]
CH	combined integral area under the peaks at 2930 and 2850 cm^{-1} for intensity of asymmetric and symmetric C-H-stretching vibrations of aliphatic CH_3 and CH_2 groups	[K.-M. unit cm^{-1}]
CH_N; OH_N	normalized CH and OH by dividing the respective areas by the Ref area	[-]
E	energy	[J = kg m^2 s^{-2}]
E_A	activation energy	[kJ mol^{-1}]
EC	electrical conductivity	[µS cm^{-1}]
F	force, gravitational force F_g, buoyancy F_b and surface force F_s	[N = kg m s^{-2}]
g	gravitational acceleration (9.80665)	[m s^{-2}]
h	height	[m]
k	rate constant	[µL h^{-1}]
k_1; k_2	rate constants of the subprocesses	[µL h^{-1}]
LoI	Loss on ignition	[weight %]
l_s	perimeter	[m]
L_w	wetted length	[m]
OH	integral area under the O-H band of DRIFT spectra (3800 and 2500 cm^{-1})	[K.-M. unit cm^{-1}]
p	hydrostatical pressure	[N m^{-2}]
pH	negative decimal logarithm of the hydroxonium ion activity in an aqueous solution	[-]
$pH_{(max Repel)}$	pH of maximum repellency	[-]
pH_{pzc}	pH of point of zero charge	[-]
pK_a	deprotonation constant	[-]
$pK_{1, mineral}$ $pK_{2, mineral}$	deprotonation and the protonation constants of mineral surfaces	[-]
pK_{SOM}	deprotonation constant of SOM surfaces	[-]
q	charge of the titrant	[mol_c L^{-1}]
Q	charge	[$cmol_c$ kg^{-1}]
$Q_{(max Repell)}$	charge of maximum repellency	[$cmol_c$ kg^{-1}]
Q_{ek}	electrokinetic charge	[$cmol_c$ kg^{-1}]
$Q_{max, mineral}$	maximum negative or positive charge from deprotonation or protonation of mineral compounds	[$cmol_c$ kg^{-1}]
$Q_{max, SOM}$	maximum negative charge from deprotonation of organic functional groups	[$cmol_c$ kg^{-1}]
$Q_{mineral}$	charge caused by protonation and deprotonation of mineral compounds	[$cmol_c$ kg^{-1}]
Q_{perm}	permanent charge	[$cmol_c$ kg^{-1}]
Q_{SOM}	charge caused by deprotonation of organic functional groups	[$cmol_c$ kg^{-1}]
R	universal gas constant (8.32441)	[J K^{-1} mol^{-1}]
r_0	radius of curvature at the drop apex	[m]

r_1; r_2	radii of curvature at (x_0, y_0)	[m]
Ref	integral area under DRIFT spectra (4000 and 400 cm^{-1})	[K.-M. unit cm^{-1}]
RH	relative air humidity	[%]
t	time	[h; min; s]
T	temperature	[°C]
TOC	total organic carbon content	[g kg^{-1}]
U_p	perimeter of the plate	[m]
V	volume: V_l of the displaced liquid, V_p of the plate	[m^3]
w	weight	[kg]
W_{adh}	work of adhesion	[J = kg m^2 s^{-2}]
W_{app}	apparent work of adhesion	[J = kg m^2 s^{-2}]
W_{app}^{0}	initial work of adhesion for t = 0	[J = kg m^2 s^{-2}]
WC	water content	[weight %]
WC_{crit}	critical water content for soil water repellency	[weight %]
WDPT	water drop penetration time	[h = 60 min = 3600 s]
z	immersion depth	[m]

Greek symbols

α, β, γ	parameters of linear regression	[-]
ε	model parameter for distance between spherical particles	[-]
$\gamma^{\alpha\beta}$	interfacial tension between the phases a and b with v for vapour, l for liquid and s for solid phase	[N m^{-1}= J m^{-2}]
η	viscosity	[kg m^{-1} s^{-1}]
κ^{-1}	capillary length	[mm]
Θ	contact angle	[°]
Θ_{adv}	advancing contact angle	[°]
Θ_{app}	apparent contact angle	[°]
Θ_{eff}	effective contact angle	[°]
Θ_r	contact angle of a rough chemically homogenous surface	[°]
Θ_{rec}	receding contact angle	[°]
Θ_{sess}	sessile drop contact angle	[°]
Θ_{sm}	contact angle of a smooth chemically heterogeneous surface	[°]
Θ_{WPM}	Wilhelmy plate contact angle	[°]
Θ_Y	Young´s law contact angle	[°]
ρ	density	[kg m^{-3}]

Statistical measures

n	number	[-]
R	correlation coefficient	[-]
P	probability of error	[-]

Methods

^{1}H-NMR	proton nuclear magnetic resonance spectroscopy
AFM	atomic force microscopy
ATR FTIR	attenuated total reflectance infrared fourier transform spectroscopy
BET	method of determination of the inner surface using the BET theory developed by S. Brunauer, P. Emmett, and E. Teller and called after the initials in their last names
CRM	capillary rise method
DRIFT	diffuse reflectance infrared fourier transform spectroscopy
PCD	particle charge detection
TISED	time dependent sessile drop measurement
WPM	Wilhelmy plate method

Sample names

NLW	originally wettable samples from Ouddorp, Netherlands
NLR	originally repellent samples from Ouddorp, Netherlands
UKW	originally wettable samples from Pennard Golf Course, United Kingdom
UKR	originally repellent samples from Nicholaston Dunes, United Kingdom
AUW	originally wettable samples from Myome, Australia
AUR	originally repellent samples from Pine Views, Australia

Others

DOC	dissolved organic carbon
DOM	dissolved organic matter
SOM	soil organic matter
SWR	soil water repellency
HS	humic substances
FA	fulvic acids
HA	humic acids
HU	humins
PHA	peat humic acid

8.2 List of Figures

Figure 1-1 Sample site Berlin-Tiergarten (photo: K. Täumer, Department of Soil Protection, TU-Berlin) 13

Figure 1-2 Sample site Berlin-Buch: result of an attempt of afforrestation (left), small-scale differences in *WC* visible in dark wettable and light repellent patches at a depth of 5 cm during sampling in Berlin-Buch (Hurraß & Schaumann, 2006); (right); (photos: K. Täumer, Department of Soil Protection, TU-Berlin) 14

Figure 2-1 Interfacial tensions at the three phase line (TPL) of the adjacent liquid, solid and vapour phase for various contact angles Θ. 17

Figure 2-2 Schematic drawing of hydrogen bonds between water molecules 17

Figure 2-3 Gravitational force F_g, buoyancy F_b and surface force F_s acting at the three phase line of a Wilhelmy plate immersed into a liquid with liquid-solid contact angle below and above 90°. 20

Figure 2-4 A sessile drop fitted as ellipsoidal cap showing the vectors of interfacial tensions, γ, at the drop edge, the observable contact angle Θ_{app} and elliptical parameters a, b, h necessary to calculate Θ_{app} and drop volume V according to Equation (2-20) and (2-21). 21

Figure 2-5 (a): Sessile drop on rough surface with decreasing apparent contact angle, Θ_{app}, and increasing total geometric contact area, A_{tot}, by *spreading* from time t_0 to t_2. (b – d): *sinking* of drop water into air filled gaps in a zoomed intersection of the water-solid contact area beneeth the drop. Side views: hemispheric particles partly covered by water in dark grey, entrapped air (white) between dry parts of particles (black) and from t_0 to t_2 sinking water level (light grey). Plan views: from t_0 to t_2 increasing geometric area, A_{geo}, (grey) of water covered particles and decreasing water-air interface (white) 27

Figure 3-1 (a) Volume of sessile drops on the dried sample B2 at 5°C in different measurement conditions: I on soil body, at ca. 50% *RH*, II on a thin soil layer, at ca. 50% *RH* and III on a thin soil layer, at >99,9% *RH, (b)* Curve III: Figure 3-1 (a) in a smaller scale with deviation range and exponential and initial linear fitting curve 34

Figure 3-2 Apparent work of adhesion, W_{app}, according to Eq 3 as a function of contact time of one representative sessile drop on all investigated samples at 5°C, 20°C and 30°C and the respective double exponential fitting curves (standard deviation ± 5 mN m^{-1}) 36

Figure 3-3 A model visualising different re-wetting behaviour of the investigated samples. *Buch*: Hydrophilic functional groups (black circles) are linked chemically towards the interior of SOM in the air-dried sample. Re-wetting requires high activation energy, E_A, to disrupt linkages. Tiergarten: Surface characteristics do change only slightly during drying and re-wetting. Probably, *pH*-differences result in differing percentage of charged functional

groups (uncharged groups as white circles) and persist drying and re-wetting. Re-wetting requires medium E_A at repellent samples for conformational re-orientation of some hydrophilic functional groups (physico-chemical process) and low E_A at wettable samples for changes in water coverage (physical process). 40

Figure 4-1 (I) DRIFT spectra of initially wettable Buch samples (BW) and repellent Buch samples (BR) and initially wettable Tiergarten samples (TW) and repellent Tiergarten samples (TR) dried at 105°C and (II) expanded spectral region showing peaks, associated with selected C-H bands and a typical baseline for evaluation of peak area..... 46

Figure 4-2 Effect of drying conditions on water drop penetration time (*WDPT*), water content (*WC*) and normalized C-H band intensity (CH_N) of initially wettable and repellent samples from Buch (BW □ and BR ▲) and the Tiergarten (TW □ and TR ▲, respectively) for field moist and dried samples. Lines connect the data points of subsamples drawn from the same soil sample. Error bars are *WC* ± 15% and estimates of the standard deviation from triplicate measurements of *WDPT* and DRIFT peak areas. 48

Figure 4-3 Water drop penetration time (*WDPT*) as a function of water content (*WC*), and as a function of normalized C-H band intensity (CH_N) of initially wettable (BW, $n = 32$, open symbols) and repellent Buch samples (BR, $n = 10$, solid symbols) and wettable and repellent Tiergarten samples (TW, $n = 18$; and TR, $n = 10$, respectively) in field moist state (□■) and after drying at 35°C (○●), 65°C (△▲), 105°C (▽ ▼) and at 31% *RH* (◇◆). Error bars are *WC* ± 15% and estimates of the standard deviation from triplicate measurements of *WDPT* and DRIFT peak areas..... 51

Figure 4-4 Water drop penetration time (*WDPT*) calculated using Equation (1) and the values of α, β and γ shown for BT in Table 4-4 as a function of the experimentally determined *WDPT*s of wettable (○, $n = 32$) and repellent (●, $n = 10$) Buch samples and wettable (△, $n = 18$) and repellent (▲, $n = 10$) Tiergarten samples, respectively..... 53

Figure 4-5 Plane of wettability (water drop penetration time, *WDPT*) as a function of water content (*WC*) and surface hydrophobicity (normalized peak height of C-H band intensity, CH_N) of Buch (B) and the Tiergarten (T) soils as calculated by Equation 1 in combination with the schematic model of three dimensional arrangement of outer organic molecules and the average thickness of a water film for homogeneous moisture distribution suggested by Bayer & Schaumann (2007)..... 54

Figure 5-1: Experimental design of modification of soil-*pH*. **A** Exposition of soil to gaseous ammonia enriched atmosphere. **B** Exposition of soil to HCl enriched atmosphere. 65

Figure 5-2: **A** *pH*, **B** electrical conductivity (*EC*), **C** Soil C/N ratio, and **D** "Mehlich"-extractable iron measured in wettable and repellent soil samples from

Tiergarten (TW, TR) and from Buch (BW, BR, respectively) from a study of seasonally sampling between spring 2002 and spring 2004. 66
Figure 5-3: Artificially induced soil-*pH* as a function of the added volume of HCl- and NH_3-enriched air for **D** samples from Germany, **NL** samples from Netherlands, **UK** samples from the UK, and **AU** samples from Australia. 68
Figure 5-4: Water drop penetration time (*WDPT*) as a function of artificially induced *pH* of repellent samples and wettable control samples: **D** from two sites in Germany, **NL** from a profile in the Netherlands, **UK** from two sites in UK, and **AU** from two sites in Australia. 70
Figure 5-5: Wettability of the German Tiergarten (TW, TR) and Buch (BW, BR) samples as a function of artificial induced soil *pH*: **A** as contact angle measured by Wilhelmy Plate Method (Θ_{WPM}), **B** as contact angle measured by sessile drop method (Θ_{sess}), and **C** measured as water drop penetration time (*WDPT*). **D** *WDPT* and Θ_{WPM} as a function of the respective Θ_{sess}..... 71
Figure 5-6: Particle surface charge (Q) of soil fraction < 63 µm of selected *pH*-treated sub-samples with highest, lowest and medium artificially induced *pH* from the wettable and repellent Buch samples (BW, BR) and Tiergarten samples (TW, TR, respectively). 72
Figure 5-7: Wettability of the German Tiergarten (TW, TR) and Buch (BW, BR) samples as contact angle measured by sessile drop method depicted as a function of particle surface charge (Q) of soil fraction < 63 µm. Particle surface charge data are measured at four data points for each sample (indicated by double symbol frame) and linearly interpolated between these four points by their *pH* dependency (Figure 5-6). 73
Figure 5-8: Simplified schematic *pH* dependent interplay of negative and positive surface charge provided by SOM surfaces (Q_{SOM}), by mineral surfaces ($Q_{mineral}$), and by permanent surface charge ($Q_{perm.}$) using equation 4 and 5 with parameters (Table 5-4) chosen to create a scenario with minimum $\Sigma\sqrt{Q_i^2}$ at $pH_{(max\ Repell)}$ and a ΣQ-curve crossing the data points of measured net surface charge of the respective German samples. 76
Figure 6-1 Schematic model of suggested mechanisms of changes in soil water repellency (SWR) upon altering pH via liquid phase and via gas phase in dried samples from Buch. 83
Figure 6-2 Suggested model of orientation of amphiphilic organic molecules at the SOM surface during drying in dependence of pH and ionic strength of the soil solution..... 85
Figure 6-3 Schematic model of suggested mechanisms of changes in soil water repellency (SWR) in Tiergarten samples upon pH altering via liquid phase (top) and via gas phase in dried samples (bottom) 86

8.3 List of Tables

Table 1-1 Water content (*WC*), loss on ignition (*LoI*), *pH*, electrical conductivity, C to N ratio (*C/N*) and water drop penetration time in field moist state ($WDPT_{fm}$) and in air dried state ($WDPT_{ad}$) of wettable and repellent samples from Tiergarten TW and TR, respectively. 13

Table 1-2 Water content (*WC*), loss on ignition (*LoI*), *pH*, electrical conductivity, C to N ratio (*C/N*) and water drop penetration time in field moist state ($WDPT_{fm}$) and in air dried state ($WDPT_{ad}$) of wettable and repellent samples from Buch BW and BR, respectively..... 14

Table 2-1 Repellency classes according to (Dekker & Jungerius, 1990). 18

Table 3-1 Characteristics of the field moist and air-dried initially water repellent (B1, T1) and initially wettable samples (B2, T2) from Buch and Tiergarten (a - by Wilhelmy Plate Method, b - by Capillary Rise Method) 30

Table 3-2 Means of linear rate of apparent volume decrease, *k*, during observation of sessile drops on all samples at all temperatures in different measurement conditions: I on soil body, at ca. 50% *RH*, II on a thin soil layer, at ca. 50% *RH* and III on a thin soil layer, at >99,9% *RH* (standard errors of fitting in brackets) 34

Table 3-3 Activation energy, E_A, of the apparent decrease of drop volume during the spreading under 3 different conditions on the initially repellent samples B1 and T1 and the initially wettable samples B2 and T2 from Buch (B) and Tiergarten (T), (standard errors of fitting in brackets; n.d. - not determined; a - Infiltration was too fast to monitor.) 35

Table 3-4 Parameters of double exponential fitting according to Eq 19 and of linear fitting of the initial increase for W_{app} as a function of time in course of wetting of sessile drops on all investigated samples at all temperatures, (standard errors of fitting in brackets) 37

Table 3-5 Activation energy, E_A, obtained by double exponential and initial linear fitting of wetting by sessile drops on all investigated samples, (standard errors of fitting in brackets) 38

Table 4-1 Number (*n*) of individual samples, water content (*WC*), soil organic matter content (*SOM*), *pH* and water drop penetration time (*WDPT*) of field moist wettable samples (BW) and repellent samples (BR) from Buch and from the Tiergarten (TW, TR, respectively). Estimates of errors, *WC* ± 15% and of *SOM*, *pH* and *WDPT* (from triplicate measurements) are shown in parentheses. 45

Table 4-2 Correlation coefficient (*R*), number (*n*), and probability of error (*P*) for the integral area under the DRIFT spectra from 4000 to 400 cm^{-1} (*Ref*) against soil organic matter (*SOM*) and water content (*WC*) and the areas under the *OH* and *CH* peaks against *WC* and, similarly, for the normalized peak areas OH_N and CH_N..... 47

Table 4-3 Probabilities (P) in support of the alternative hypothesis (H_A) and rejection of the null hypothesis for normalized C-H peak areas (CH_N) obtained for sample pairs dried using two different procedures obtained from sample paired t-tests. 49
Table 4-4 Correlation coefficients (R) for linear regression of log$WDPT$ against water content (WC) and normalized C-H peak area (CH_N), and of WC against CH_N for all samples of both soils (BT) and the various sample subsets (see text). 52
Table 4-5 Multiple regression parameters α, β and γ, their standard errors and correlation coefficients (R) of log$WDPT$ against water content (WC) and normalized C-H peak area (CH_N) for all samples (BT) and those from Buch (B) and those from Tiergarten (T). 53
Table 5-1: Sample characteristics..... 61
Table 5-2: Water content (WC) and wettability as water drop penetration time ($WDPT$), as contact angle measured by Wilhelmy Plate method (Θ_{WPM}), and by sessile drop method (Θ_{sess}) in field moist state and dried at 19°C at a constant relative humidity of 31%RH, and soil organic matter content (SOM) and potential cation exchange capacity (CEC_{pot}) of the 4 German samples. 62
Table 5-3: Point of zero charge, pH_{pzc} (PCD) suggested by PCD measurement, pH of maximum repellency ($pH_{(max\ Repell}$) and particle charge of maximum repellency ($Q_{(max\ Repell}$). 72
Table 5-4: Parameters chosen in order to create a scenario with minimum $\Sigma\sqrt{Q_i^2}$ at $pH_{(max\ Repell)}$ and a ΣQ-curve crossing the data points of measured net surface charge of the respective German samples (Figure 5-6) using equation 4 and 5: permanent charge ($Q_{perm.}$), maximum negative surface charge obtainable by deprotonation of SOM ($Q_{max,\ SOM}$) and the respective deprotonation constant (pK_{SOM}), maximum negative and positive surface charge obtainable by deprotonation / protonation of mineral surfaces ($Q_{max,\ mineral}$) and the respective deprotonation and protonation constants ($pK_{1,\ mineral}$ / $pK_{2,\ mineral}$).77
Table 6-1 Overview of the main observations of differences in soil characteristics and in responses on changes in environmental conditions between wettable and repellent samples from Buch and Tiergarten..... 81

8.4 Curriculum vitae

Contact

Name:	Dörte Diehl
Adress:	Universität Koblenz-Landau
Email:	diehl@uni-landau.de
Telephone:	0049 6341 280 567

Personal information

Date of Birth:	30.08.1969
Place of Birth	Rostock, Germany
Nationality:	German

Education

Date:	1995-2003
Qualification:	Graduated engineer for environmental technology
Principle subject:	Environmental technology
University:	Technische Universität Berlin, Institut of Environmental Technology
Date:	1988-1990
Qualification:	Abitur (general qualification for university entrance)
Highschool:	Volkshochschule Berlin-Mitte Volkshochschule Rostock (adult evening classes)
Date:	1986-1988
Qualification:	Certificate of apprenticeship as a photographer

Employment history

Date:	since October 2008
Occupation:	scientific assistant
Employer:	University Koblenz-Landau, Institute of Environmental Sciences, Department of Environmental and Soil Chemistry
Date:	September 2006 - September 2008
Occupation:	scientific assistant
Employer:	University Koblenz-Landau, Institute of Natural Sciences, Department of Organic and Environmental Chemistry
Date:	May 2004 - July 2006
Occupation:	scientific assistant
Activity:	DFG research project Interurban II: subproject Humus
Employer:	TU-Berlin, Institut of Environmental Technology, Department of Environmental Chemistry
Date:	June - July 2003
Occupation:	Internship
Employer:	Leibnitz-Institute of Freshwater Ecology and Inland Fisheries
Date:	June 1999 - September 2003
Occupation:	student research assistant
Employer:	TU-Berlin, Institute of Ecology, Department of Soil Science

8.5 Publications

Peer-reviewed:

Diehl, D., J.V. Bayer, S.K. Woche, R. Bryant, S.H. Doerr & G.E. Schaumann. (subm.). Reaction of soil water repellency on artificially induced changes in soil pH. Geoderma.

Diehl, D., R.H. Ellerbrock & G.E. Schaumann. (2009). Influence of drying conditions on wettability and DRIFT spectroscopic C-H band of soil samples. European Journal of Soil Science. 60, 557-566.

Diehl, D. & G.E. Schaumann. (2007). Wetting mechanism assessed from time dependent sessile drop shape. Hydrological Processes, 21, 2255 - 2265.

Oral presentations

Diehl, D., G.E. Schaumann, R.H. Ellerbrock. 2008. Drying state and wettability of soil samples assessed by DRIFT-Spectroscopy. Eurosoil Congress. August 2008 in Vienna, Austria.

Diehl, D., G.E. Schaumann, R.H. Ellerbrock. 2007a. Trocknungsmethoden und DRIFT-Spektroskopie in hydrophoben und benetzbaren Bodenproben urbaner Standorte. Jahrestagung der Deutschen Bodenkundlichen Gesellschaft. September 2007 in Dresden, Germany.

Langbein, J., D. Diehl, G.E. Schaumann. 2007b. Characterization of amphiphilic substances in wettable and non-wettable soil samples. Soil Science Society of America Bouyoucos Conference: On the Origin of Water Repellency in Soils. 29th April – 3rd May 2007, Sanibel Island, Florida, USA.

Diehl, D. & G.E. Schaumann. 2006a. Wetting mechanisms assessed from time dependent sessile drop shape. International Conference Biohydrology 2006: "Impact of biological factors on soil hydrology" September 2006 in Prague, Czech Republic.

Diehl, D. & G.E. Schaumann. 2006b. The nature of wetting by sessile drops on urban soil samples. Interurban II: „Water and Organic Matter in Anthropogenic soils: Dynamics and processes“: March 2006 in Berlin, Germany.

Poster presentations

Diehl, D. & G.E. Schaumann. 2006a. Zeitliche Änderung des Boden-Wasser-Kontaktwinkels im Verlaufe der Benetzung. 11. Annual Meeting of the Society of Environmental Toxicology and Chemistry - German-Language-Branch e.V. (SETAC-GLB). September 2006 in Landau (Pfalz), Germany.

Diehl, D. & G.E. Schaumann. 2006b. Water repellency, kinetics and nature of wetting in urban soil samples. IV International Conference Interfaces Against Pollution, IAP'2006, June 2006 in Granada, Spain.

Diehl, D. & G.E. Schaumann. 2005a. Zeitliche Änderung des Boden-Wasser-Kontaktwinkels im Verlaufe der Benetzung. DBG-Jahrestagung. September 2005 in Marburg, Germany.

Diehl, D. & G.E. Schaumann. 2005b. Wetting kinetics determined from contact angle measurement. EGU 2005 – Annual Meeting of the European Geophysical Union. April 2005 in Vienna, Austria.